Determinants and evolution of metabolic interactions in synthetic microbial communities

Dissertation

zur Erlangung des Grades eines
Doktor der Naturwissenschaften
(Dr. rer.nat.)
des Fachbereichs Biologie der Philipps-Universität Marburg

vorgelegt von

Giovanni Scarinci

aus Catania, Italien

Marburg an der Lahn, März 2023

Die vorliegende Dissertation wurde von Oktober 2018 bis Februar 2023 am Max-Planck-Institut für terrestrische Mikrobiologie in Marburg unter Leitung von Prof. Dr. Victor Sourjik angefertigt.

Vom Fachbereich Biologie der Philipps-Universität Marburg
(Hochschulkennziffer 1180) als Dissertation angenommen am 20.03.2023

Erstgutachter(in): **Prof. Dr. Victor Sourjik**

Zweitgutachter(in): **Prof. Dr. Hans-Ulrich Mösch**

Weitere Mitglieder der Prüfungskommission:

Prof. Dr. Robert Junker

Prof. Dr. Martin Thanbichler

Tag der Disputation: 30.03.2023

Die während der Promotion erzielten Ergebnisse wurden in folgend Originalpublikation veröffentlicht:

Scarinci, G., Sourjik, V. Impact of direct physical association and motility on fitness of a synthetic interkingdom microbial community. ISME J (2022). https://doi.org/10.1038/s41396-022-01352-2

Table of Contents

Abbreviations

CSM Complete supplement mixture

OD optical density measured at λ=600

MES 2-(N-morpholino)ethanesulfonic acid

NGS Next generation sequencing

YNB Yeast nitrogen base

IPTG Isopropyl-thiogalactopyranoside

KO knockout

ddH2O Double-distilled water

Zusammenfassung

Im Gegensatz zu Laborbedingung teilen sich Mikroorganismen Raum und Ressourcen in ihrer natürlichen Umgebung. Dies führt dazu, dass eine Reihe von Interaktionen verschiedenster Art und mit unterschiedlichem Einfluss auf die Fitness der einzelnen Organismen etabliert werden. Eine Unterkategorie dieser Interaktionen ist der obligatorisch-mutualistische Austausch von Metaboliten. Diese Form von metabolischer Verschränkung führt zu einer notwendigen kooperativen Koexistenz zwischen den jeweiligen Metaboliten austauschenden Organismen. Ein Beispiel, um ihre Relevanz zu verdeutlichen, ist, dass derartiger Interaktionen vermutlich eine entscheidende Rolle in der frühen Evolution von eukaryotischen Zellen gespielt haben. Ein adäquates Verständnis dieser evolutionären Dynamik, welche dazu führte, dass zwei ursprünglich autonome Organismen in ein Verhältnis der wechselseitigen und obligatorischen Abhängigkeit eintreten, ist bislang nicht gegeben. Derartige Gemeinschaften sehen sich mit diversen Herausforderungen konfrontiert. Zu nennen sind hier beispielweise die unkontrollierte Zerstreuung von Metaboliten oder die Infiltrierung der Gemeinschaft durch nicht-kooperative Organismen. Um ein tiefgehenderes Verständnis dieser Gemeinschaften zu entwickeln, ist es erforderlich, die Strategien zu untersuchen, mit denen sie den zuvor genannten Herausforderungen begegnen. In der vorliegenden Arbeit gingen wir diesen Fragen nach, indem eine zweiteilige synthetische Gemeinschaft von auxotrophen *E. coli* und *S. cerevisiae* Stämmen etabliert wurde, welche notwendigerweise bidirektionalen Metaboliten-Austausch (´cross-feeding‘) betreiben muss. Darauffolgend wurde das Wachstum von einer der getesteten Gemeinschaften durch einen iterativen Zyklus von Wachstum und Verdünnung stark verbessert. Eine derartige Verbesserung konnte zu großen Teilen durch die Präsenz von vier hochfrequentierten Mutationen erläutert werden. Es ist hervorzuheben, dass diese Mutationen ihren Vorteil lediglich unter Cross-Feeding-Bedingungen entfalten, was das Vorhandensein einer weiteren Reihe von vorteilhaften Mutationen nahelegt, welche nur unter *cross-feeding* Bedingungen auftreten. Interessanterweise führte eine Gruppe von Mutationen zu der Reduktion der Fähigkeit zur Ammonium-Assimilation in den Hefe-Partnern, was potentiell zu einer höheren Abhängigkeit von dem Bakterium führt. Sofern weitere Experimente diese Beobachtung wiederholen, kann dies als eine Bestätigung dafür angesehen werden, dass obligatorisch-mutualistische Gemeinschaften den Grad ihrer Verschränkung weiter verstärken können.

Unter Verwendung eines weiteren *cross-feeding* Paars konnten wir den Einfluss von Aggregation, Motilität und Chemotaxis für obligatorisch-mutualistische Gemeinschaften unter turbulenten

Umweltbedingungen untersuchen. Konkurrenz-Experimente ermöglichten es uns zu demonstrieren, dass Zell-Zell-Adhäsion und daraus folgende Aggregation einen Fitness-Vorteil für die bakteriellen Partner darstellen. Dieser Vorteil wird durch den Effekt von Motilität verstärkt. Im Gegensatz dazu konnte unter selbigen Bedingungen kein Vorteil durch Chemotaxis festgestellt werden. Durch die Einführung eines manipulierten ´Cheater-Stamms` konnte die Relevanz von Aggregation und Motilität als Schutz gegen nicht kooperative Organismen in Form der Reduktion des Eindringens letzterer in die Gemeinschaft nachgewiesen werden.

Summary

Conversely to laboratory conditions, microorganisms often share space and resources with other organisms in their natural environments. This can result in the emergence of a plethora of interactions of different natures and diverse outcomes on fitness. Obligate mutualistic exchanges of metabolites represent a subset of these possible interactions. These lead to a strong entanglement between partners, resulting in the inevitable coexistence of the two trading organisms. The relevance of these interactions is exemplified by the fact that these trades might have played a crucial role in the early step of the evolution of eukaryotic cells. Nonetheless, a complete understanding of the evolutionary dynamics leading two originally autonomous organisms to become interdependent remains mostly elusive. Furthermore, since communities relying on metabolic mutualism face several challenges, including metabolite dispersal and the potential exploitation of the shared building blocks by non-cooperators, a deep investigation of the strategies adopted by these organisms to cope with such detrimental factors is required to have a complete overview of these systems and their evolution. In this work, we aimed to address these questions by engineering a mutualistic bipartite system obtained via the co-culture of *E. coli* and *S. cerevisiae* auxotrophic strains, which thus relies on a bidirectional and obligate cross-feeding of metabolites. We further proceed with iterative growth-dilution cycles resulting in a dramatic improvement in growth for one of the tested communities. Such improvement could be recapitulated to a good extent by the presence of four highly frequent mutations. Notably, these mutations seem to provide an advantage exclusively under cross-feeding, thus suggesting the existence of a different pool of beneficial mutations which emerge in the presence of partner interactions. Interestingly, some of these mutations caused a reduction in the ammonium assimilation ability by the yeast partner, potentially resulting in a higher degree of dependency on the bacterium. Even though additional experiments are required, if confirmed, this would prove that partners connected by obligate metabolic dependencies can increase their entanglement.

Using another cross-feeding pair, we were able to investigate the role of aggregation, motility, and chemotaxis on obligate mutualistic communities grown under turbulence. Through competition experiments, we were able to demonstrate that cell-cell adhesion, and the ensuing aggregation, provide a fitness advantage to the bacterial partner. This advantage is further increased by the joint effect of motility. On the contrary, under our conditions, chemotaxis does not play a role. By introducing an engineer cheater strain, we were also able to prove the role of both aggregation and

motility also as protective factors against a cheater by reducing its invasion success and thus delaying community collapse.

1. Introduction

1.1. Microbial communities, a network of interactions

One of the most common procedures in microbiology is represented by the isolation from their natural habitats of specific microorganisms or even individual strains, followed by their investigation as a single line. This might be essential in medicine to demonstrate the presence of distinct pathogens and thus adopt the appropriate therapy or, for research purposes, in order to simplify the system under investigation. However, the artificial constraints obtained under these experimental environments create growth conditions which are completely different from those experienced by microorganisms in their original habitats. Indeed, in natural environments, microorganisms often coexist both with other small entities such as bacteria, unicellular fungi and viruses, but also with (or even in) multicellular organisms, like plants and animals. This results in sharing the same space and resources, thus leading to the emergence of interactions which might generate conflicts and exploitative behaviours but also potentially guide cooperation and mutualism[1–3]. Examples of these co-occurrences are quite widespread and diverse, as exemplified by the gut microbiome[4], soil communities associated with plant roots and leaves[5] or microbial communities colonizing degrading organic matter in pelagic environments[6]. Additionally, the emergent properties displayed by these consortia made such systems appealing and suitable for several biotechnological applications[7]: production of milk-derived products, wastewater treatments and biogas production are some of the most widespread. Furthermore, engineered consortia showed enhanced production of value-added compounds compared to simple monocultures[8], suggesting the applicability of such communities as an alternative approach compared to the classical monospecies metabolic engineering strategies. Eventually, recent studies on the gut microbiome, especially those connected to dysbiosis and inflammatory bowel disease, inspired and guided the production of novel drugs and therapeutics constituted by microbial communities[9]. Therefore, the interest in microbial consortia and the rules guiding their emergence, stability, evolution and collapse is increasing. Nonetheless, despite all these considerations, several features of microbial communities remain elusive. Predictions on community dynamics and compositions are so far limited, factors stabilizing these communities are not well known and ecological and evolutionary rules guiding their assembly and strengthening remain poorly explored. The main reason for this lack of knowledge is due to the inherent difficulty of investigating such systems, caused by the broad intricacy between their interactions. Several works

attempted to reduce this complexity by engineering artificial communities. This can be achieved using two different approaches. On the one hand, it is possible to co-culture several organisms isolated from the same or alternative natural environments (top-down approach)[10]. This strategy allows a defined initial composition of the system and can be used to select and evolve communities with a specific function[11] while retaining a significant fraction of the complexity of natural microbial networks. Consequently, this implies that such intricacy remains mostly undefined in such communities. On the other hand, with a bottom-up approach, it is possible to generate consortia displaying a specific property or performing a desired task by selecting or engineering the members in a rational fashion, hence making such engineered systems the preferred choice when studying specific community features or functions[12]. However, the main drawback of such a strategy is that while the investigation of these *de-novo* communities is relatively easy and their outcome somehow predictable, their level of complexity is relatively low, thus far from those displayed by natural communities.

While these artificial systems simplified the investigation of communities and allowed researchers to successfully shed light on some of the key ecological features of microbial communities[13], a lot of work still awaits, and studies aimed to decipher potential stabilizing factors and to reveal eco-evolutionary forces and dynamics leading to community assembly are sorely needed. During my PhD, I tried to contribute in this direction, mainly focusing on the latter points.

1.2. Mutualistic cross-feeding, a case study on microbial trade of metabolites

As mentioned above, organisms present in microbial consortia can display different types of interactions, which might confer fitness benefits to the interacting community members. For example, physical adhesion between motile and non-motile microorganisms can favour the spread of the non-motile microorganism by exploiting the motile ability of the partner [14], which might result in the emergence of new taxis[15]. Additionally, digestion of high molecular weight substrates is favoured, or sometimes only possible, by microbial consortia[16]. Furthermore, these communities can display emergent biosynthetic capabilities[17], such as the production of complex chemical entities which a single organism cannot synthesize.

Another notable feature of these communities, implying a high degree of interaction and connectivity between organisms, is represented by the exchange of essential building blocks

between community members. In fact, according to bioinformatic analysis[18], more than 90% of natural bacterial isolates carry at least one auxotrophy, thus making metabolic dependencies a common trait in natural environments. Accordingly, different exchanges of metabolites between partners have been reported within the bacterial kingdom but also between bacteria and higher organisms[19]. Furthermore, the fact that most of the isolated microorganisms fail to grow in isolation under laboratory conditions and that, on the other hand, co-cultivation allows the successful growth and propagation of these organisms remark the fact that such metabolic interactions might be vital in natural environments[20,21]. While these "trades" can occur in a unidirectional fashion (e.g. a prototroph feeding an auxotroph), a subset of these interactions involves an obligate reciprocation of exchanges between partners, thus making these exchanges bidirectional. Therefore, in such communities, each organism relies on the growth and metabolite production of the other interacting members to survive, thus displaying an obligate mutualistic cross-feeding behaviour. Such strong inter-organisms dependence is common in symbiotic communities[22] but can also be found between free-living bacteria[23,24]. Notably, the presence of beneficial endosymbionts seems to be primarily derived from the acquisition of free mutualists by the host[25], confirming that the physical sequestration of the partner observed in endosymbiotic relationships between cooperators might be favoured, but it is not a necessary parameter required to establish and maintain cooperation. Eventually, such strong inter-organisms dependence obtained via mutualism has even been proposed to be a crucial step towards the establishment of more complex symbiotic relationships and, for example, speculated to be the starting point for the evolution of eukaryotic cells[26], thus making such systems, and the forces leading to their emergence and stability, quite interesting.

Consequently, one of the main questions raised about such mutualistic behaviours in microbial communities concerns the evolutionary force driving the emergence and fixation of such traits and the path leading two metabolically self-sufficient organisms towards a loss of autonomy and the establishment of obligate mutualism. According to the classical Darwinian definition of natural selection, the fittest should prevail. The transposition of this concept into the microbial world should result in the selection of organisms able to be self-sustained, and partnerships based on cooperative behaviours, which favour the growth of other non-related microorganisms, should be discouraged. Therefore, selfishness, accounted as metabolic autonomy, should be preferred over mutualism. However, as mentioned before, auxotrophies are common in the microbial world, and

cross-feeding seems to be widespread[20], suggesting the existence of potential fitness advantages derived from such behaviour.

A possible explanation reconciling the fixation of dependency even without a direct fitness benefit might derive from genetic drifts, such as a dramatic event abruptly decreasing the population size. As a result of these selectively random events, even non-beneficial traits might result in an enrichment. However, while such a bottleneck effect might have played a role in endosymbiotic communities, where the population of endosymbionts is relatively small, a similar effect could not explain the high occurrence of these traits also in dispersed communities, which are generally constituted by large numbers of free-living organisms that can also migrate[25].

Therefore, the occurrence of mutualistic cross-feeding suggests that the presence of such exchanges, under specific conditions, must represent a maximum in the fitness landscape and consequently is evolutionarily favoured, thus implying that physiological, metabolic and/or energetic benefits should play a relevant role behind this phenomenon. But which are these forces leading the evolution of mutualism?

One of the first hypotheses relates to a reduction in genome size. As mentioned before, metabolic mutualism is widespread among symbiotic communities. Here, bacterial partners depend on their host for a large part of their metabolism and often carry a small genome[27]. Indeed, a shortening in genome size, known as genome streamlining[28], might account for a reduction in cost for the cell both due to the lower metabolic burden caused by protein synthesis and also because of the energetic "savings" obtained via a reduced anabolic activity.

Furthermore, the fact that the production of specific metabolites can present cost differences between organisms can also determine a difference in fitness, thus favouring cooperation over autonomy. In fact, the biosynthesis of every cellular building block represents a cost for the cell that derives from a combination of two factors: the intrinsic energetic cost necessary to convert a specific precursor into the desired product (e.g. reducing energy) and the cost due to the biosynthetic pathway used by the cell (e.g. enzyme synthesis)[29–31]. Different organisms can have different pathways performing the same metabolic functions[32], but the cost of running these alternative pathways might be different[33]. Therefore, some organisms might produce a particular compound "in a cheaper way" compared to another organism and *vice versa*. Consequently, the energetic burden derived from the overproduction of a specific metabolite invested in metabolic trades in exchange for another building block might be lower than the total cost derived from the autonomous production of both the shared and the received compound. Furthermore, the

generation of different metabolites might result in a competition between pathways for precursors and energy but also might require different biochemical conditions, which can be incompatible with other pathways or for the survival of the cell itself. Examples of these incompatibilities are the fixation of CO_2 or nitrogen, which are hampered by the presence of oxygen that, on the other hand, might be essential for other biosynthetic pathways[34,35]. Therefore, since both these reactions are necessary, organisms require to find a specific trade-off between different metabolic networks and biochemical conditions, resulting in suboptimal production. Some strategies found by nature to overcome these problematics are temporal or spatial segregation between conflicting reactions/conditions within the same organism, such as performing these reactions in organelles[36,37]. However, another alternative might be represented by the spatial isolation of these incompatible pathways between different cells. This could result in Pareto-optimal resource allocation, leading to an overall enhanced production/growth. Thus, from an energetic point of view, the trade of metabolites between cells could provide a better resource allocation strategy resulting in higher fitness [38].

Additionally, from a more physiological perspective, it has been shown that auxotrophic organisms engaged in metabolite exchange display an increased resistance to antimicrobial drugs due to an enhanced efflux ability[39]. Metabolic trades can also generate, by the secretion of protective agents, an extracellular environment able to extend the lifespan of the community members[40], thus guaranteeing another fitness advantage.

Therefore, all these shreds of evidence suggest that, under some conditions, mutualistic behaviours, specifically those relying on metabolite exchange, can provide fitness benefits and might therefore be selected during evolution.

1.3. Evolution of mutualistic microbial communities

The presence of factors promoting the emergence and fixation of a specific trait is a necessary condition underlying evolutionary processes. However, while these may indicate the presence of a fitness maximum, they cannot explain which were the evolutionary steps leading the transition towards this maximum and what guided it. In other words, how did the evolutionary transition from fully autonomous organisms to mutualists occur? Trying to address that, J. Morris introduced the concept of leakiness and leaky functions as potential guides for this transition[41,42]. Several cellular functions, which are vital for cell survival, take place outside the cellular envelope. These tasks are often performed by molecular entities (enzymes or siderophores) actively released outside of the cell and recruited for the digestion of complex carbon sources[43], degradation of antibiotics[44], and micronutrient scavenging[45]. Interestingly, exchanges between the cytoplasm and the extracellular environment are not limited to these macromolecules but also to small metabolites, as demonstrated by experimental works[46]. A classic example of these releases is represented by the overflow metabolism caused by glucose under oxygen-limiting conditions, resulting in acetate secretion in the extracellular milieu[47]. These compounds are considered "waste products" from the cell, which proceed with their removal from the cytosol. However, this release is not limited to undesired or "toxic" products but also to other, and more expensive, building blocks such as vitamins[48], organic acids and amino acids[49]. All of these contribute to the generation, in the extracellular environment, of a pool of freely available metabolites and metabolic functions available to all the community members. This ensemble of cellular and metabolic functions in the extracellular matrix, including the presence of metabolites, is often referred to as public goods. Since performing such functions and producing such metabolites has an energetic cost for the producing cells and generates a metabolic burden, when public goods are available in sufficient amounts, losing the ability to carry such tasks and acquire the needed metabolite directly from the environment, or exploit the specific function performed by others, could provide a fitness advantage and might be fixed by mutations silencing and removing the gene/s encoding for the protein involved in the costly task. During the early phases of community assembly, if several organisms perform the leaky function, all of them would start a "race", leading to the loss of the function, until the slowest will be "stuck" as the member of the community performing the task abandoned by all the other members. This model is known as "the black queen" hypothesis. Since several tasks can be leaky, the same process might lead to the appearance of other dependencies, thus driving the emergence of mutualism. A model based on these assumptions was proposed by

Pande and Kost[19] and reconstituted the potential evolutionary steps required by two initially metabolically autonomous organisms in order to establish an obligate mutualistic cross-feeding relationship (Fig. 1). Specifically, they define specific keystone steps: The first one is represented by the generation of an "exometabolome" [46] obtained via the natural tendency of cells to release metabolites into the environment. Under these circumstances, if the concentration of a specifically released metabolite is abundant enough, the loss of the ability to self-produce such building block might be favoured, for example, by the derived absence of production costs[50], allowing the emergence of autotrophies[51]. This would result in a unidirectional cross-feeding between the two organisms, and, as stated before, this type of dependency seems to be quite common in nature. At this point, the donor organism might acquire a reliance on metabolites produced and released by the recipient, thus generating an interaction loop between the two partners [52].

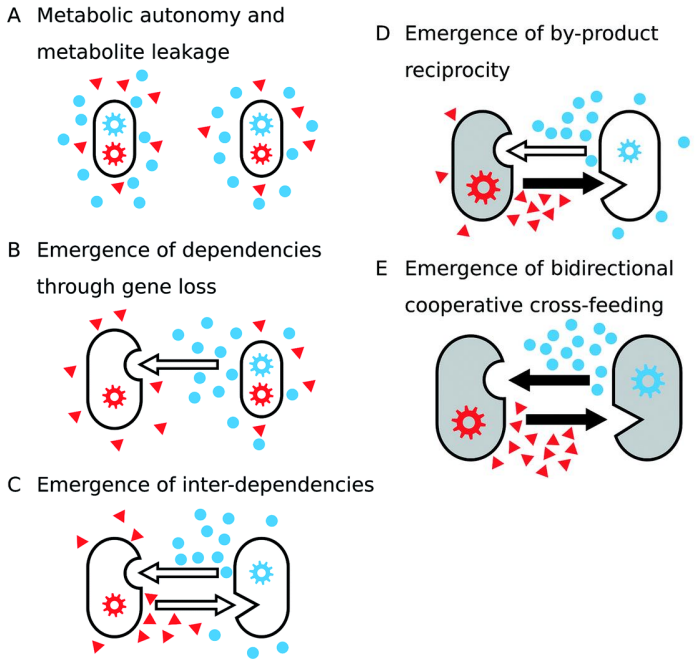

Figure 1 Evolutionary transitions required to generate an obligate mutualistic community
A Autonomous organisms living together releases internal metabolites into the environment, thus creating a pool of freely available metabolites.
B The acquisition of an auxotrophy for one of the environmentally abundant metabolites might be favored, thus generating a unidirectional cross-feeding
C A similar dependence might also arise in the other partner, thus closing the loop and generating an inter-dependence between the partners.
D,E Active investment in production of the traded metabolite might result, through a feedback loop, in an overproduction of the required metabolite. Therefore, an enhancement of the trading fluxes could provide fitness benefits and therefore be favored.
Modified from D'Souza *et al* 2018

At this stage, these interactions are still passive since they are based on the presence of certain compounds already released into the environment, and the producers require no additional metabolic investment to generate them. Such an active investment would then be acquired in the last step of the evolutionary process. Indeed, the emergence of these traits would generate positive feedback on growth, thus reinforcing the interaction itself and favouring partners committed to metabolite exchange. However, the fixation of this behaviour requires stabilizing factors (e.g. spatial structuring) that allow an increased exchange when partners are trading and reduces or even prevent it in the presence of non-cooperators. Since some of these strategies have been investigated in this work, these will be discussed more thoroughly in the next chapter. Experimental data providing evidence for such a model have been obtained with synthetic communities. Indeed, not only has it been observed that auxotrophies can emerge when organisms are grown in supplemented media[50] and that prototrophic organisms can sustain, via their exometabolome, the growth of auxotrophs[53], but also that a transition from a unidirectional to bidirectional cross-feeding is possible[52] and that such closed loop can be reinforced by mutations increasing the production of the traded metabolites[54]. This model, therefore, in its simplicity, can explain the initial phases determining the emergence of cross-feeding. A simple question, however, arises. What would happen next? According to the black queen hypothesis, a race to lose all the leaky functions should occur, thus resulting in a community able to carry, as a whole, the same functions performed by the ancestral autonomous organisms but without redundancy between partners, and therefore resulting in an optimal division of labour. However, while a reinforcement of the existing or engineered interactions have been observed, an increase in metabolic dependencies has not been reported. Nonetheless, proofs that such strengthening of metabolic entanglement between partners must have been occurred in nature are represented by the overwhelming presence of mutualistic symbiotic interactions, which in the vast majority of the cases rely on several metabolite exchanges and it is unrealistic to imagine that all these interactions might have emerged all at the same time. Furthermore, an example of this transition from weak to strong entanglement has been hypothesized to be the driving force leading to the evolution of eukaryotic cells.

As exemplified above, natural evolution is undoubtedly one of the main driving forces of complexity in ecological systems. Therefore, protocols inspired by evolutionary principles have been used under laboratory conditions both at organism level[11,55] and below[56] to increase the performances of these systems in achieving a desired task or function with astonishing results. However, adaptive laboratory evolution can be used not only for biotechnological applications but

also as a learning tool aimed at testing evolutionary hypotheses and following evolutionary dynamics. In this regard, as described previously, several groups used adaptive laboratory evolution on synthetic consortia and were able to successfully reproduce the initial steps leading to the emergence, and initial stabilization, of a mutualistic cross/feeding community. Here we adopted a similar approach to investigate the later steps of mutualistic community assembly and, at the same time, follow the molecular and metabolic dynamics resulting from the forced co-evolution between *E. coli* and *S. cerevisiae*.

1.4. Factors stabilizing mutualistic communities

Mutualistic cross-feeding communities face several challenges that might hinder their growth, stability and evolution. One major problem is the rapid dispersal and subsequent loss of the exchanged compounds as they are released into the environment[57]. Another challenge is the exploitation of shared metabolites by non-cooperating ("cheating") organisms, which can reduce community growth and even lead to its collapse [58–60]. A common strategy that might be used by mutualistic communities to counteract these negative effects is the spatial assortment of partners[61,62]. As predicted by theory and confirmed by experimental studies of model synthetic communities grown on an agar surface or in a microfluidic chamber, the stability of cross-feeding communities can benefit from positive spatial assortment between partners that facilitates short-

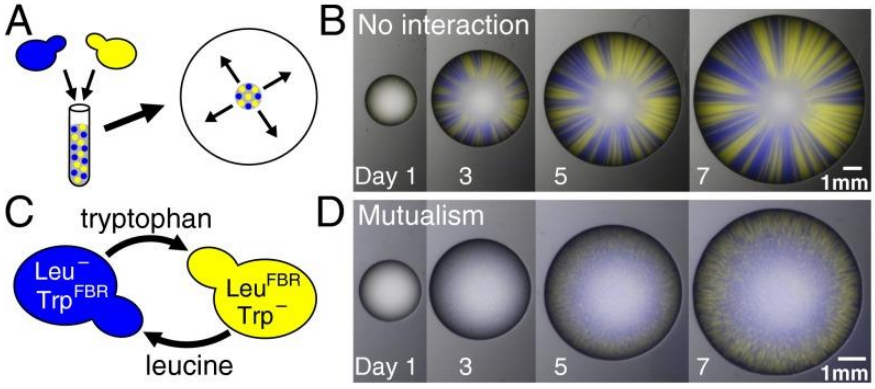

Figure 2 Examples of structuring emerging in communities grown on solid surfaces
A-D Two yeast strains, labelled with two alterative fluorescent markers, are mixed together and a drop is seeded on an agarose plate and the colony growth is followed (A). When there is no interaction between the two strains (B), the strains grow without mixing, and distinct sectors are clearly visible. On the contrary, when a metabolic mutualistic interaction (e.g. cross-feeding) is established (C) between the two organisms, the radial patterns disappear and the colony display a higher degree of mixing between the strains (D). Figure from Müller *et al.* 2014

range metabolic interactions and prevents exploitation by cheaters[63–68]. Consistently, spatial structuring spontaneously emerges in cross-feeding communities grown on agar surfaces (Fig. 2)[66,68–72]. Moreover, structuring might favour the evolution of bacterial cross-feeding[54] and be itself enhanced by such evolution[73]. An extreme example of assortment is the direct channelling of metabolites between two cooperating partners, as occurs in endosymbiosis[22,74,75] but also in cross-feeding bacterial communities[54,76,77].

Although partner proximity in natural sessile communities can similarly result from passive spatial assortment during growth on a surface[78], it can be alternatively achieved through direct physical interactions between partners at both intra- and interkingdom levels[79,80]. Such adhesion may be especially important for suspended aggregates[81,82] as well as for epibionts[15,83–85], communities in which one of the partners, usually smaller, adheres and grows on the surface of the other partner. Even for such closely associated communities, it typically remains unknown whether the physical interaction can enhance metabolite exchange on its own or rather stabilize specific structures involved in direct metabolite transfer[19,57].

Since non-surface attached communities are typically found in open aquatic environments [24], additional parameters might play a role in guiding community association and might confer further protection from the potential challenges previously discussed. In this sense, the presence of chemical gradient formed by degrading organic matter in aquatic environments has been reported to drive the establishment of ecological interactions through the differential chemotactic response of the different microorganisms present in such environments[86]. Therefore, the ability of motile planktonic microorganisms to swim, possibly led by a chemical gradient (chemotaxis), might similarly be beneficial in the search for partners[87–89]. But despite their assumed importance, the joint impact of physical association, motility and chemotaxis remains little studied because of the inherent complexity of microbial interactions in natural communities[90]. Therefore, one of the tasks of my work was to characterize their impact on a bi-partite cross-feeding community.

1.5. Aims of this work

Microbial communities represent a complex system that is often difficult to study. In order to facilitate the investigation of specific features of these consortia and parameters affecting their stability and survival, artificial communities could be used as a proxy. In this work, we adopted this strategy to study the impact of some key parameters on mutualistic communities and follow the

evolutionary transition from individuality to mutualism. Specifically, we decided to proceed by building a bipartite system between *E. coli* and *S. cerevisiae* auxotrophs. These two organisms were chosen for several reasons. First of all, the resulting consortia would be represented by two organisms belonging to two different kingdoms. This would render the system quite unique since, with few exceptions, most of the studies adopting a bottom-up approach present in literature are based on monospecies consortia. Such a feature is important because, even though the emergence of different subpopulations from an original monoculture has been observed[91], the most widespread form of microbial consortia is represented by organisms belonging to different species and kingdoms[19]. Therefore, this would render our system more similar to natural conditions, where a trade-off between different preferences and lifestyles might be necessary to allow coexistence. Furthermore, the establishment of communities adopting a bottom-up approach requires not only a deep knowledge of the physiological and biochemical features of the organisms but also molecular tools allowing a feasible and straightforward genetic manipulation. This is quite a key feature of these two model organisms that have been extensively studied, thus allowing a rapid and precise rational engineering via both a plethora of genetics and molecular tools and a deep knowledge of their physiology and metabolism.

Additionally, since we are interested in exploring the evolutionary path leading from weak-cooperators to strong-cooperating communities, the use of organisms derived from different natural niches, and therefore with no previous co-evolutionary experience, might represent an excellent starting point for our evolutionary experiment. Eventually, these two organisms can co-aggregate [92], thus allowing the investigation of the joint role of motility and chemotaxis performed by *E. coli* with cell-cell adhesion.

Therefore, all these features are indeed perfectly matched by a bipartite *E. coli*-*S. cerevisiae* consortium.

In short, the goals of this work are the following:

1) Engineer a bipartite mutualistic system consisting of *S. cerevisiae* and *E. coli* auxotrophs
2) Perform laboratory evolution on some of these pairs to follow the evolutionary dynamics leading to community optimization.
3) Assessing the joint role of aggregation, motility and chemotaxis a stabilization factors on mutualistic communities grown in turbulent environments.

2. Results

2.1. Engineering of synthetic interkingdom microbial communities

In order to generate a viable bipartite consortium between *S. cerevisiae* and *E. coli* relying on metabolic mutualism, one of the first tasks that needed to be performed was the definition and optimization of a minimal media suitable for the co-culture of these two organisms. This step was done together with a bachelor student I was supervising.

Firstly, the ability of the bacteria and the yeast to grow in the minimal media commonly used for their respective monoculture was tested. While in the minimal media optimized for bacteria (M9), *E. coli* displays robust growth, *S. cerevisiae* is unable to grow (Fig. 3, *left panel*). Almost symmetrically, while *S. cerevisiae* thrives in the minimal media optimized for yeast (YNB), the bacterium is partially able to grow but does not reach high OD values (Fig. 3, *right panel*). These results are, *per se,* not surprising considering that the two organisms have different life styles and preferences, and such discrepancies are mirrored by the composition of their respective minimal media. In this regard, pH represents one of these differences. While M9 is buffered at a neutral pH (7.1) through the balancing between mono- and di-basic sodium phosphate salts, YNB has a pH of 5.7 and contains sulphate-based salts as the main component, thus providing no buffering power in this pH range.

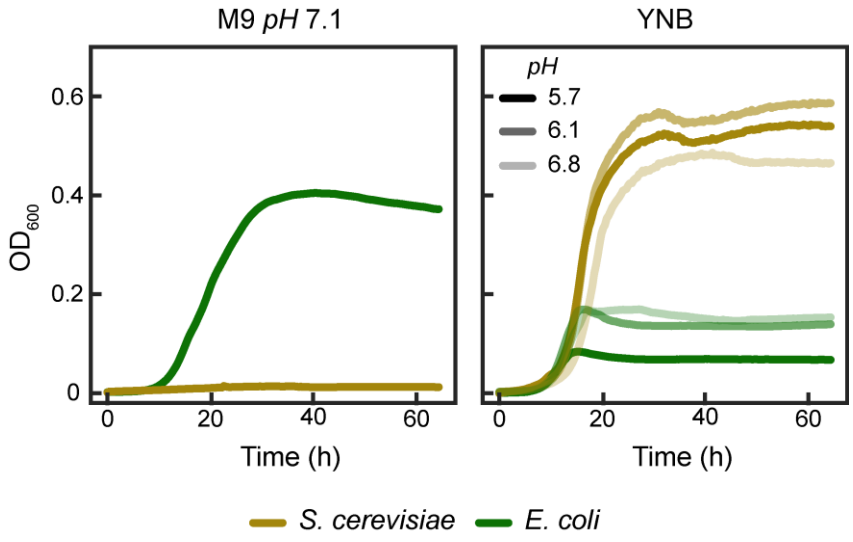

Figure 3 Bacterial and yeast growth in different minimal media
Curves representing the growth of the wt strains of *E. coli* (green) and *S. cerevisiae* (yellow) grown respectively in M9 (left panel) and YNB (right). In the right plot, the different shades indicate different pH at which the YNB media was adjusted.

Considering that, and also that both organisms were able to grow (at least partially) in YNB, we proceed by assessing the effects of variations of media pH on *E. coli* and *S. cerevisiae* growth. Interestingly, a small increase in pH from 5.7 to 6.1 resulted in the doubling of the final OD reached by *E. coli,* and this reduced acidity of the media appeared to be slightly beneficial also for *S. cerevisiae* (Fig. 3, *right panel*). However, an additional increase in pH not only did not boost further the bacterial growth but also resulted in marked salt precipitation in the medium and reduced *S. cerevisiae* growth (Fig. 3, *right panel*).

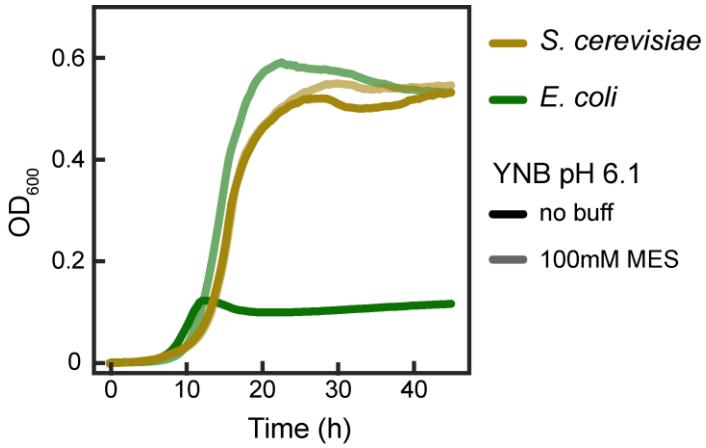

Figure 4 Effects of media buffering on E. coli and S. cerevisiae growth
Curves representing the growth of either *S. cerevisiae* (yellow) or *E. coli* (green) in YNB adjusted to pH 6.1 respectively buffered with MES (opaque) or without buffer.

Remarkably, the addition of MES (2-(N-morpholino) ethanesulfonic acid) into the media (a buffering component) provided a strong benefit to *E. coli*, resulting in a comparable growth behaviour between *E. coli* and *S. cerevisiae* (Fig. 4). Notably MES is compatible with cellular cultures and has a p*Ka* of 6.15[93], thus perfect for our desired pH range. Consistently, its addition had no effect on *S. cerevisiae* growth.

Once the minimal media was optimized (referred to as YNB from now on), we proceeded by defining the most suitable strategy to engineer a mutualistic cross-feeding behaviour between the two organisms. Ideally, these communities would be composed of organisms whose growth in minimal media is exclusively present in co-cultures and absent in monocultures. A common strategy adopted to achieve this is through the co-cultivation of auxotrophs [94], which, by definition, are unable to grow in minimal media without the required supplements. A similar approach was used in this work. Specifically, we proceed by performing yeast-bacteria pairwise co-cultures using eighteen auxotrophic strains of *E. coli* directly obtained from a collection of *E. coli* strains, each carrying a different gene deletion [95] and fourteen auxotrophs of *S. cerevisiae,* selected from the yeast

knockout collection[96] and engineered to express a fluorescent marker constitutively. This resulted in 252 unique co-cultures displaying various degrees of growth performances (Fig. 5).

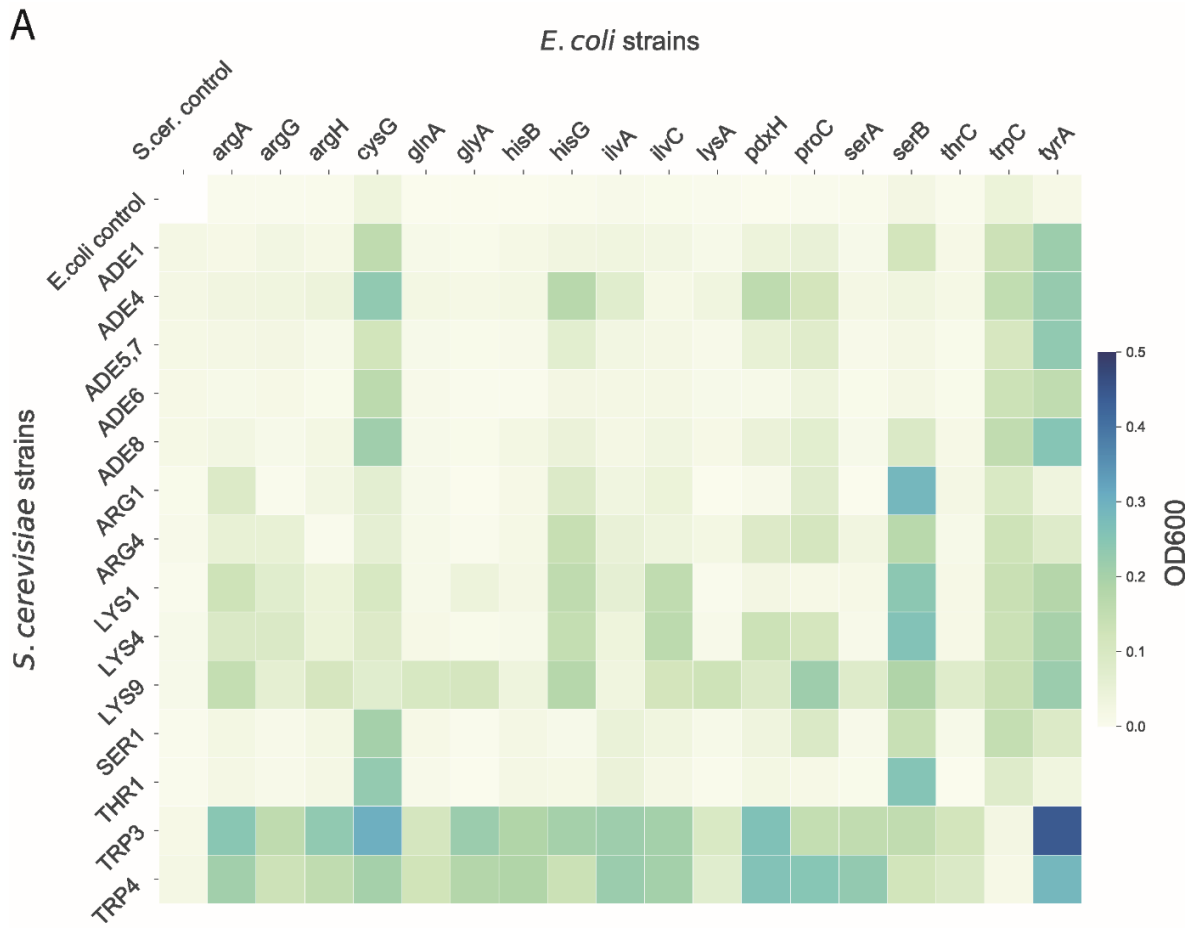

Figure 5. Cross-feeding between E. coli and S. cerevisiae auxotrophs
Heatmap representing the OD600 reached after seven days of co-culture in YNB minimal media by all the communities resulting from the cultivation of all the possible pairwise combinations between *E. coli* and *S. cerevisiae* auxotrophic strains inoculated in equal amounts (OD= 0.05 each). The names of the genes reported indicate the mutation (knockout) carried by that strain. The first row and the first column (defined as control) represent the growth of each strain as monoculture in the minimal media to assess for any basal growth.

While some strains display a broader ability to establish mutualistic exchanges of metabolites (e.g. both *E. coli* and *S. cerevisiae* tryptophan auxotroph strains), thus being able to establish mutualistic interactions with different strains with interruptions in different biosynthetic pathways, others have reduced tendency in establishing these interactions (e.g. *S. cerevisiae Δthr1*). This might result from differences in metabolic fluxes rewiring and/or metabolite release.

2.2. Evolution of mutualistic interkingdom communities

In order to follow the evolutionary dynamics arising during the emergence of mutualism, we proceed by selecting from the previous table eight co-cultures reaching different final cell densities, and for those, we performed a laboratory evolution experiment (Table 1).

Table 1 Co-cultures used for the evolutionary experiment
Per each co-culture evolved, the yeast strain is indicated in the first column, while the bacterial in the second for a total of eight communities. Similar to Fig. 5, each member was inoculated in equal amounts (OD 0.05).

#	*S. cerevisiae* auxotroph	*E. coli* auxotroph
1	*Δtrp3*	*ΔtyrA*
2	*Δtrp3*	*ΔserA*
3	*Δade4*	*ΔhisG*
4	*Δarg1*	*ΔhisG*
5	*Δlys1*	*ΔargA*
6	*Δlys1*	*ΔargG*
7	*Δlys4*	*ΔargA*
8	*Δlys4*	*ΔargG*

This was done by iterating the transfer of the co-culture into fresh minimal media after a specified amount of time (Fig. 6).

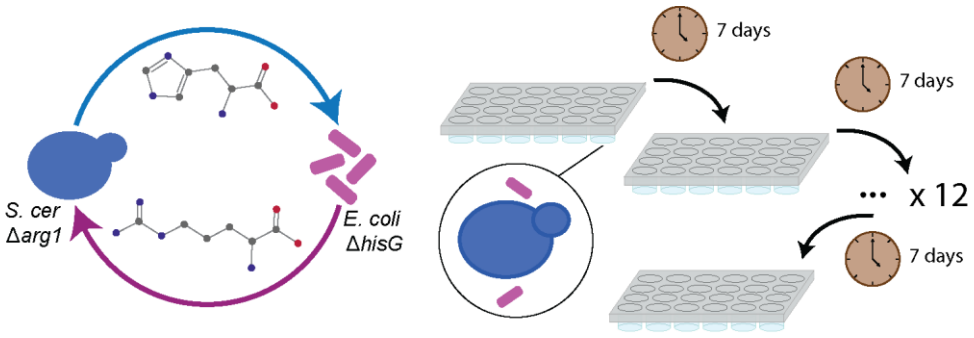

Figure 6 Experimental procedure followed for the evolutionary experiment
Schematic representation of the experimental setup. Both organisms were inoculated in equal amounts in 24 wells plates containing YNB minimal media. After seven days of growth, an inoculum from these co-cultures was transferred to a new plate containing fresh media. This transfer-growth cycle was repeated for 15 transfers. The ratio between inoculum and fresh media was set to 1:9.

Previous studies report the yeast and the bacterium can co-aggregate via type I fimbriae[97], a bacterial appendage (Fig. 7A) and also that partner adhesion might favour the evolution of mutualistic traits[54]. Indeed, we observed an association between bacteria and yeast cells and their ensuing co-aggregation in co-cultures (Fig. 7B). These interactions were abolished in *E. coli* mutants lacking either the major subunit of fimbriae FimA (**Fig. 7**C) or the mannose-binding fimbrial tip FimH (Fig. 7D) or when mannose was added to the culture medium (Fig. 7E).

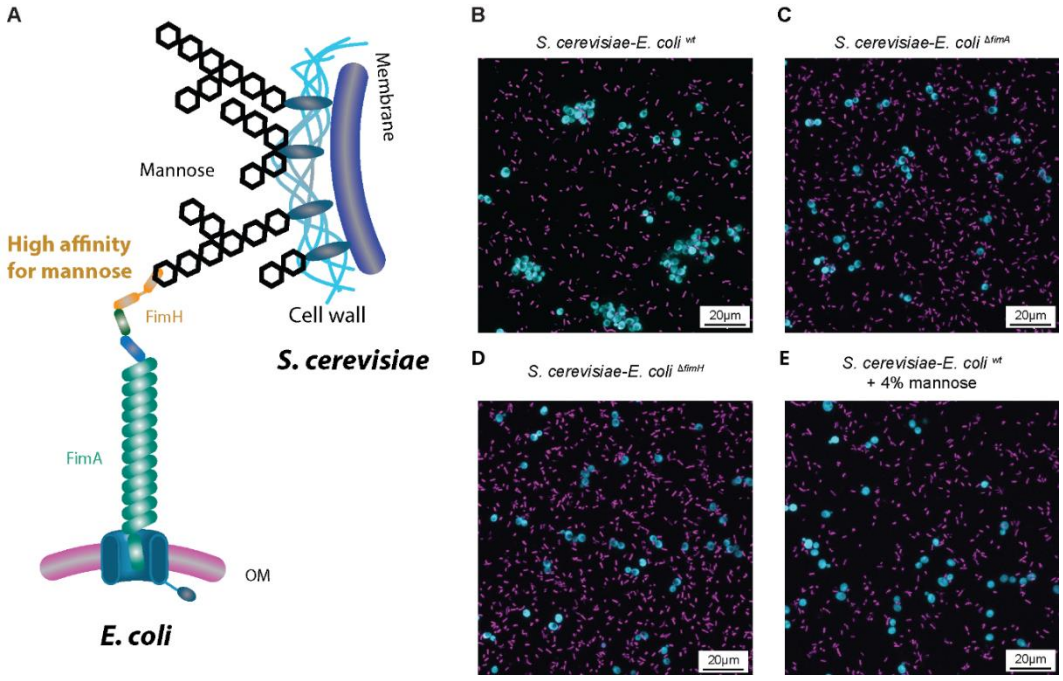

Figure 7 Fimbriae mediated yeast-bacteria adhesion

A Schematic representation of the binding between the tip of type I fimbriae (FimH) and the mannose moieties present on the surface of *S. cerevisiae*.
B-E Confocal microscopy images of *S. cerevisiae* expressing mTurquoise2 (blue) mixed with either wt (B), *ΔfimA* (C), *ΔfimH* (D) or wt in presence of mannose (E) *E. coli* expressing mCherry (magenta). Scale bar = 20 µm.

We therefore proceed by assembling co-cultures with the same auxotrophic pairs either with a fimbriated or a fimbrialess (*ΔfimA*) *E. coli* partner (6 lines per auxotroph pairs with three lines per fimbriation state).

Notably, the final cell densities reached by ancestral communities inoculated with the fimbrialess partner generally showed a higher cell density compared to the cultures containing the fimbriated *E. coli* (Appendix table 1 *day 7*). This might be due to the reduced growth of the yeast partner under clumping conditions (Fig. 8).

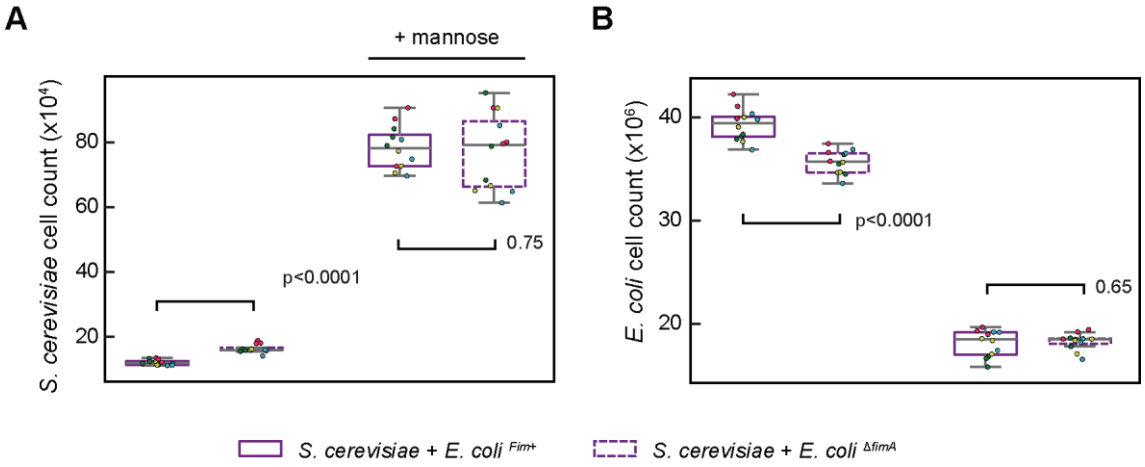

Figure 8 Effects of yeast-bacteria adhesion on growth

A,B Numbers of (A) *S. cerevisiae* and (B) *E. coli* cells measured by flow cytometry in co-cultures grown for 72 h in YNB-glucose supplemented with CSM either in absence or presence of 4% mannose, as indicated. Boxes represent the second and third quartile of the distribution and whiskers extends to show the rest of the distribution of four biological replicates (indicated by dots, different colors represent technical replicates for the same biological replica). p values from two-tailed *t*-tests assuming equal variances of the data sets.

At the end of the experiment, almost all the lines from communities #8 and #3 were fully extinct *(*Appendix Table 1*)*. By isolating the community partners from the rest of the evolved co-cultures through selective plates, we found that some communities had all their lines constituted by only one organism, suggesting a regain in prototrophy for the required metabolite (community 5-7 from Table1, Appendix Table 1*)*. This regain might have resulted in the relaxation from the metabolic dependency between members, thus leading to the extinction of the other auxotrophic partner. Since mutualism between members is lost in these communities, we excluded them from further experiments. Evolved community members from the remaining co-cultures were subsequently grown as monocultures in YNB minimal media without supplementation to assess whether their auxotrophy was maintained. In two cases (community 1 and 2 from Table 1), the *E. coli* partner isolated from all the lines was able to grow in monoculture in minimal media (data not shown). However, seen that from the same communities the auxotroph *S. cerevisiae* was also isolated, this suggests the presence of an underlying unidirectional cross-feeding between the evolved *E. coli* prototroph and the auxotroph *S. cerevisiae*. Nonetheless, since also in this case mutualism was lost, these communities were excluded from further analysis.

Conversely to the other communities, both partners isolated from all the lines of community #4 maintained auxotrophy (Appendix Fig. S1).

From this community, while the evolved lines containing a fimbriated partner generally reached higher final OD compared to their ancestral counterpart, lines containing a fimbrialess *E. coli* partner did not outperform their respective ancestral co-culture (Fig. 9). Since aggregation seems to hamper growth, this might suggest that the evolved yeast co-cultures with a fimbriated partner might have acquired traits enabling it to better cope with aggregation-induced stress, even though not at a sufficient level to achieve the same growth performances reached by the community with a fimbrialess partner.

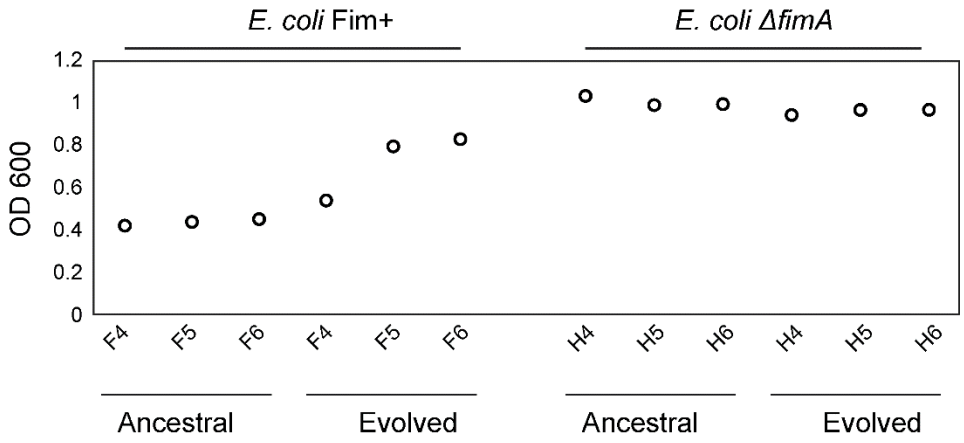

Figure 9 Assessing for improvement in final OD600 of evolved communities
Final OD600 measured for all the lines from the community retaining mutualism (#4) at the end of the first growth cycle (ancestral) and at the end of the fifteenth growth cycle (evolved) for either containing the fimbriated (Fim+) or the fimbrialess (*ΔfimA*) *E. coli* partner

To further assess for differences in growth dynamics between evolved and ancestral communities, plate reader experiments measuring the cell density of the communities over time were performed. Notably, even though we inoculated the partners in equal amounts, the initial ratio between partners did not have a big impact on the doubling time nor on the final yeast abundance in the community (Appendix Fig. S2). Since the presence of aggregates prevents a reliable measurement of OD, only communities having a fimbrialess partner were tested. Evolved communities were reconstituted by mixing organisms isolated from the respective lines by streaking communities on selective plates either for *E. coli* or *S. cerevisiae*. Notably, these isolated lines potentially retain most of the genetic variability present in the respective co-culture since each of them was derived from a pooled culture of all the colonies present in the respective selective plate.

These reconstituted evolved communities showed a strong reduction in lag phase and doubling time compared to the ancestral community, and in two cases, a slight increase in final OD (Fig. 10).

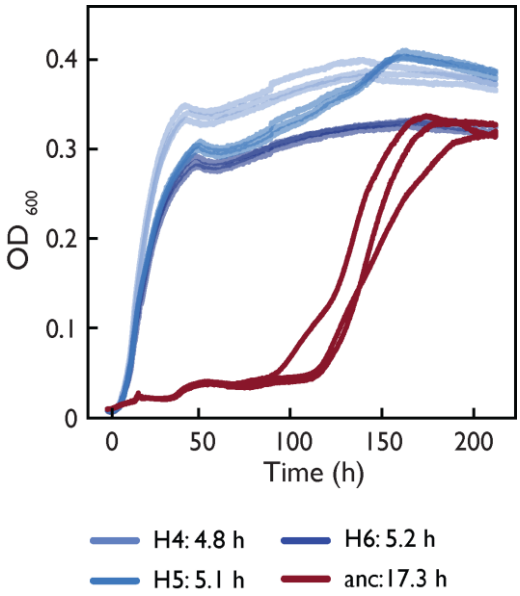

Figure 10 Growth performance comparison between evolved and ancestral co-cultures
Curves representing the growth of the ancestral co-culture (red) and three independent lines from the evolved communities (lines H4, H5, H6). Partners were inoculated in equal amount and with an initial total OD 600 (cuvettes) of 0.1. Average doubling times from three biological replicates, shown as individual lines, are reported in the legend.

However, when the same isolated evolved organisms were grown in monocultures in YNB minimal media supplemented with the required amino acid, their growth performance was strongly reduced compared to the ancestral ones (Fig. 11A,B). Competition experiments between ancestral and evolved communities under cross-feeding conditions or between ancestral and isolated evolved organisms in supplemented media confirmed a higher fitness of evolved community members under cross-feeding and, at the same time, a reduced fitness under supplementation, suggesting that the mutations fixed by the evolved strains are linked to cross-feeding behaviour and possibly favoured by it (Fig. 11C), and not derived from an adaptation to the media.

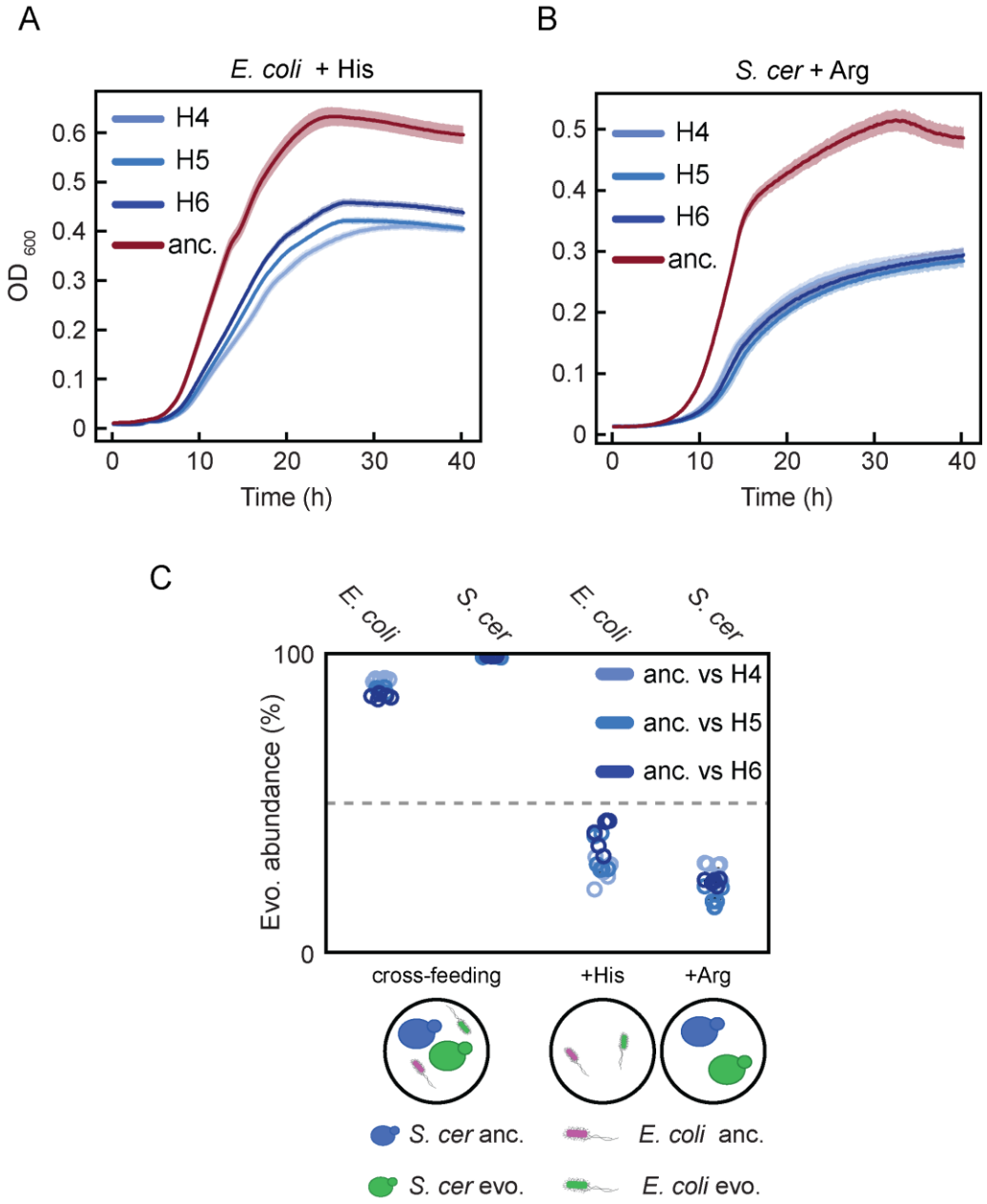

Figure 11 Assessing specificity of acquired mutations to cross-feeding conditions

A, B Curves showing the growth of either *E. coli* (A) or *S. cerevisiae* (B) strains isolated from the evolved lines and their respective ancestral strain both grown as monocultures in media supplemented either with 20 mg/l of histidine or 100 mg/l of arginine. Shades indicate standard deviation from three biological replicates.

C Abundance of the evolved organisms at the end of the growth either both in co-culture with the whole ancestral community under cross-feeding conditions in YNB minimal media, or in direct competition with only the respective ancestral strain in YNB minimal media supplemented with the required amino acid. Competing strains were expressing different fluorescent markers, thus allowing their individual quantification through flow cytometry.

To detect these mutations, we proceed by sequencing each member of the evolved communities. NGS sequencing revealed that a small set of mutations in the two organisms were recurrent among different (or all) lines and present at high frequency in each individual population (>40%). For what concerns *E. coli* (Appendix Table 2), interruptions in *argR* mediated by the insertion of IS sequences (transposons) were quite recurrent. ArgR is a transcription factor primarily involved in the downregulation of those genes involved in the biosynthesis and transport of arginine[98] but also reported to have a broad repressive activity among several metabolic pathways[99]. Other common mutations were localized in the promoter region of the *hisJQMP* operon, a gene cluster encoding for an ABC transporter responsible for histidine and arginine uptake.

Transcriptional quantifications of these evolved versions of the promoter showed an increase in activity compared to the wt promoter, and when their activity was measured in an *E. coli ΔargR* strain, this resulted in a further boost of transcription (Fig. 12). This is consistent with previous observations reporting the repression activity of ArgR on this promoter[100].

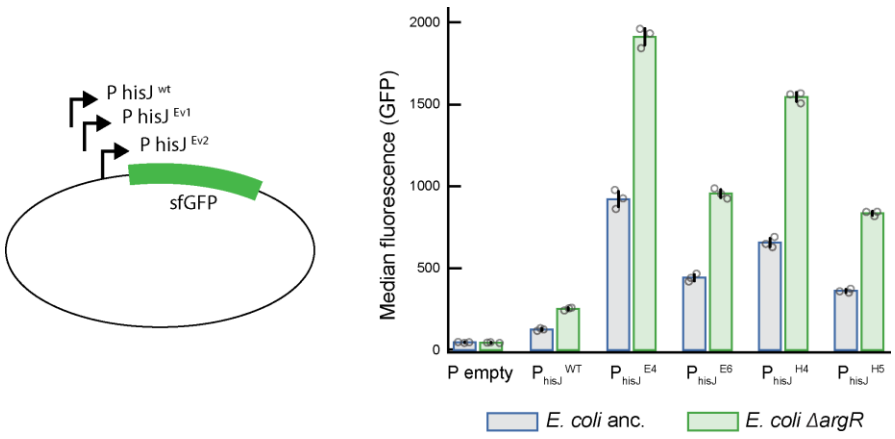

Figure 12 Transcriptional characterization of the effect of mutations on the *hisJQMP* promoter
Schematic representation of the plasmid used. The reporter plasmid (pU66A backbone) carries the super-folder GFP (sfGFP) under the transcriptional regulation of either the wt or the mutated versions of the promoter of *hisJQMP*. These plasmids were then introduced either in the ancestral *E. coli* strain (blue), or in the *ΔargR* mutant (green) and the resulting fluorescence was quantified via flow cytometry. Error bars represent the average of the median fluorescence intensity measured per each plasmid in the two different strains. Bars represent the standard deviation measured from three biological replicates represented as circles.

While in *E. coli* the number of genes carrying mutations, even with a low threshold for mutation call (0.15), was limited, for *S. cerevisiae* this was not the case. To find potentially relevant mutations, we proceed in a stepwise manner consisting of a first analysis with a high threshold (80%) to call for a mutation (Appendix Table 3), aimed to spot genes and regions mutagenized at high frequency among the different lines and potentially involved in potentially related metabolic pathways. Subsequently, we performed an additional analysis with more relaxed parameters (threshold 5%) on specific target regions aimed to reveal low-frequency mutations (Appendix Table 4). This allowed the identification of two genes recurrently mutated in all the yeast lines. One of these is *ecm21* (also known as *art2*), encoding for an adaptor of a ubiquitin ligase guiding the internalization and degradation of several amino acid transporters under nitrogen starvation[103]. This includes Can1p, a known arginine transporter[104]. Since most of the mutations detected on this gene among the different lines are mainly nonsense or frameshift, the inactivation of this gene in these lines is consequently expected.

A second group of mutations was found in *gdh1*. This gene encodes for one of the two glutamate dehydrogenases present in *S. cerevisiae* and leads glutamate biosynthesis from nitrogen ad α-ketoglutarate. Conversely to the *gdh3* isoform, *gdh1* is not repressed by glucose and therefore shows high activity under fermentation and in the presence of fermentable carbon sources, including glucose itself. Also in this case, frameshift and nonsense mutations suggest the inactivation of this gene. Notably, the presence of these four mutations detected in the two organisms was common

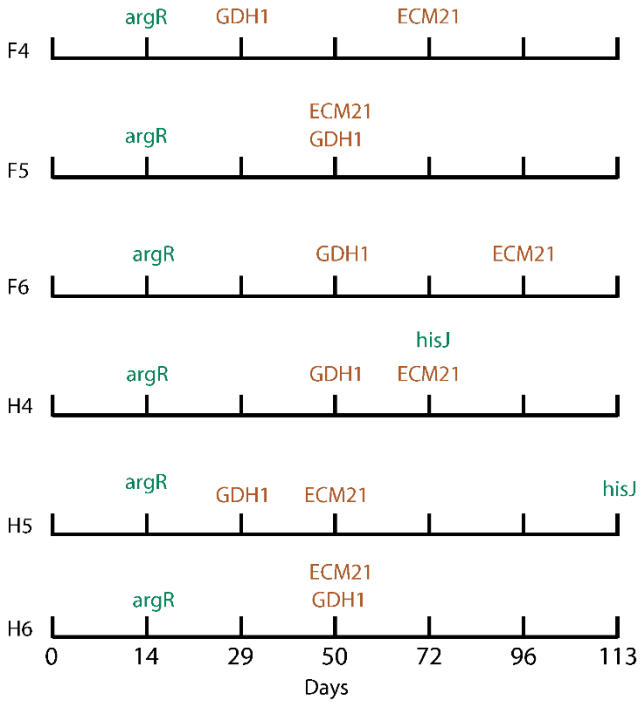

Figure 13 Order of appearance of individual mutations

Representation of a schematic timeline showing the first appearance of each individual mutation (indicated with the name of the gene) for six of the evolved community (individual lines) at the respective day from the initial inoculation. Appearance of mutations were detected via by Sanger sequencing on PCR amplicons of each genetic region obtained from each individual line at the indicated time.

for both fimbriated and fimbrialess lines (see mutation tables), thus excluding any role of aggregation in their fixation. Furthermore, when tracked over the evolution time, these four mutations seemed to follow a well-defined pattern and emerged in a highly consistent order among all the analyzed lines (Fig. 13), which might be explained by either a dramatic difference in their impact on fitness or by the possible presence of epistatic interactions between them imposing a determined order of appearance.

To assess this, and to determine the impact on growth caused by each mutation, both individually and in combination with the others, we generated a set of mutant strains from both organisms, each carrying respectively one or both of the highly frequent mutations. Notably, the *E. coli* fimbrialess strain was used to facilitate OD measurements. Subsequently, we proceeded by

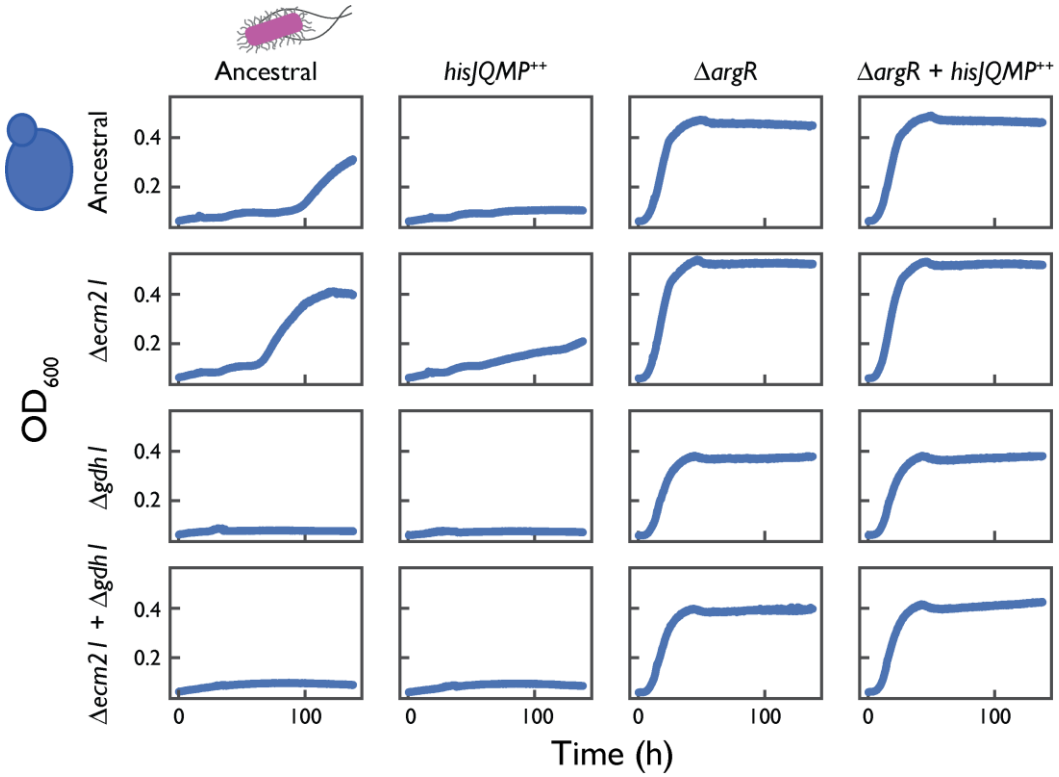

Figure 14 Dissecting the impact of highly frequent mutations on community growth.
Each subplot of the matrix shows the growth from the co-cultivation of a specific pair of the ancestral or the mutant strains of *S. cerevisiae* and *E. coli*. Growth curves from the same row results from the co-culture between the same yeast strain in combination with a different *E. coli* strains while similarly, curves from each column show growth of co-cultures having the same *E. coli* strain and different *S. cerevisiae* strains. The strain genotype is indicated respectively on top of the rows for *E. coli* and on the left of the columns for *S. cerevisiae*. Mutations were introduced into the respective ancestral backgrounds both as single or double mutations. For what concerns the mutation on the promoter of the *hisJQMP* (*hisJQMP*$^{++}$) the mutation carried by the *E. coli* from line E4 was introduced since it was observed to display the strongest overexpression.

assembling all the possible pairwise communities between the resulting strains (Fig. 14). This revealed that while some individual mutations enhance community growth (KO of *argR* on *E. coli* and *ecm21* on *S. cerevisiae*), others had a general detrimental and, in some cases, dramatic impact on growth (*hisJ, gdh1*), derived from a general decrease in both final yeast and *E. coli* cell count (Appendix, Fig. S3).

Since the order of appearance of each mutation is known (Fig. 13), we can use these data to track back the effect that each mutation had on the community when it appeared (Fig. 15). Initially, the transition from the ancestral *E. coli* strain to the Δ*argR* mutant caused the most dramatic growth

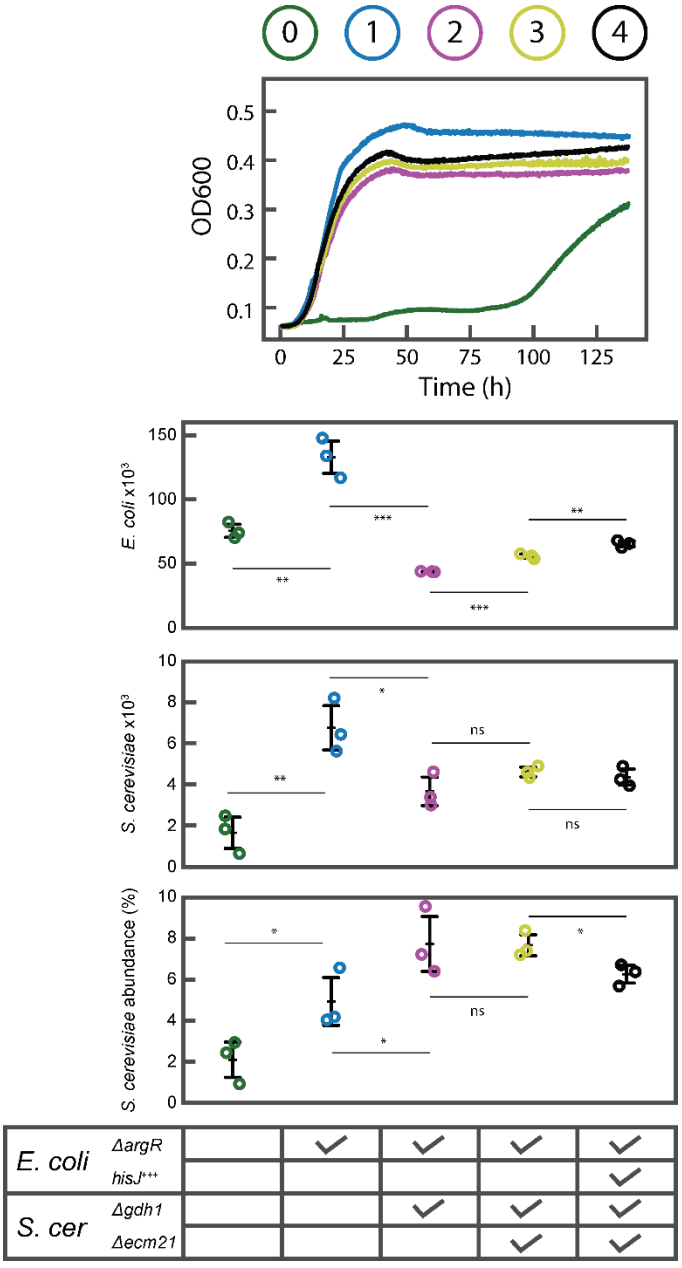

Figure 15 Growth and composition changes in the community throughout evolution

Growth curves, *E. coli* and *S. cerevisiae* cell count and yeast cell fraction from co-cultures recapitulating the evolution of the community. While the original community (green) is composed by ancestral strains, the other communities are assembled with pairwise combination of strains mimicking the progressive appearance of each mutation as observed over evolution and reported in Fig. 11. The genotype of each of the two community members is indicated in the table below the other plots. Therefore, each co-culture represents a specific time point of evolution (number in the upper part of the figure) and are distinguished by different colors. *p* values were obtained from a one tailed *t*-test for three biological replicates indicated as circles.

changes, thus explaining its quick appearance. Specifically, the growth lag phase was strongly reduced and the cell counts for both organisms increased, even though at different rates, resulting in an overall increase in yeast fraction in the community. This fraction was further increased by the inactivation of *gdh1* on yeast. Such an effect, however, was caused by an uneven reduction in cell count for both organisms reflected by a decrease in the final OD, thus suggesting that its emergence promotes selfish behaviour. Such reduction was partially rescued by the interruption of *ecm21* on yeast, whose fixation led to an increase in *E. coli* cell count but not in *S. cerevisiae*, thus, conversely to the inactivation of *gdh1*, indicating its role as a pure altruistic trait. Eventually, the overexpression of *hisJQMP* resulted in a small but significant increase in *E. coli* cell count, causing a slight increase in OD and a reduction of the yeast fraction. Interestingly, while this mutation in isolation was showing a detrimental effect on OD and both on bacterial and yeast cell count (Appendix, Fig. S3), when appearing in later phases provides a beneficial effect on *E. coli* growth and a neutral one on yeast cell count. This suggests an underlying epistatic interaction with the interruption in *argR* which appear to be independent of the yeast genotype (Appendix Fig. S3).

To assess to which extent communities composed of mutant members reproduced the evolved ones, a competition experiment between these two was performed by inoculating both evolved and

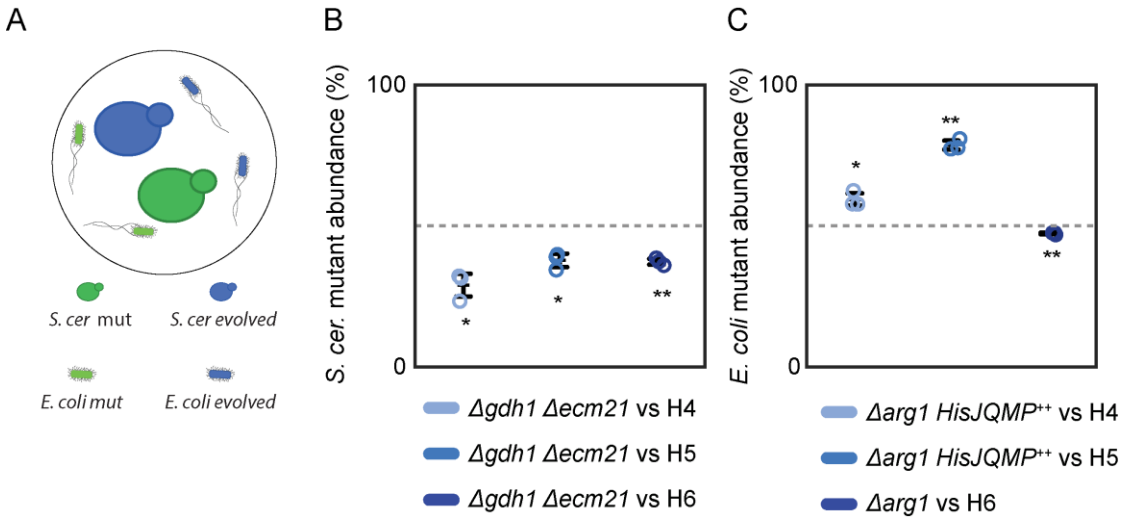

Figure 16 Relative growth performance of the mutated strains compared to the evolved ones.
A Schematic representation of the experimental setup. Mutant (green) and evolved (blue) community members were inoculated in equal amounts (OD600=0.025 each) in YNB minimal media. Difference in scattering properties between *E. coli* and *S. cerevisiae* (see Materials and Methods) and the different fluorescent marker expressed by each strain allowed the measurement of the abundance of all the individual community members.
B,C Final *S. cerevisiae Δecm21 Δgdh1* mutant (B) or either *E. coli ΔargR* or *E. coli ΔargR HisJQMP*$^{++}$ mutant (C) abundances from competition experiment performed with strains isolated from different evolved lines (H4, H5, H6). *p* values from a one sample t-test assessing for differences compared to a 50% average.

mutant strains in equal amounts in YNB. Under these conditions, the *S. cerevisiae* mutant was outcompeted by all the evolved partners (Fig. 16), thus suggesting the presence of additional beneficial mutations on the evolved yeast providing a further fitness benefit under cross-feeding conditions. Conversely, the mutant *E. coli* was able to outcompete some of the evolved counterparts. This might be explained by the fact that the mutant strain used in this experiment carries a version of the *hisJQMP* promoter having an enhanced transcriptional activity (line E4, Fig. 12) compared to the one observed from the evolved promoters present in the tested lines (H4, H5), thus potentially guaranteeing a higher uptake of histidine resulting in an enhanced fitness. This also correlates with the observation that the highest abundance of the *E. coli* mutant strain is observed when it competes with the evolved *E. coli* strain from line H5, which contains a version of the *hisJQMP* promoter less active compared to the *E. coli* strain from H4 (Fig. 12), and additionally that the evolved promoter is present in only 40% of its population (Appendix Table 2).

Impact of evolution on ammonium assimilation

While for three of the highly frequent mutations, the potential beneficial effect on cross-feeding, both at the organism or community level, can be hypothesized from the molecular function of the protein encoded by the respective gene (*argR, hisJQMP* for *E. coli* and *ecm21* for *S. cerevisiae*), and could be all reconciled with general reinforcement of the preexisting interaction, such a conclusion could not be easily made for *gdh1*, since the protein encoded by this gene is neither directly related to histidine metabolism nor to the arginine one.

To reveal the role of its interruption, since Gdh1 is a key enzyme in ammonia metabolism, we proceed by assessing for any difference in the ability to directly assimilate ammonium between the evolved yeast partners and the ancestral one. This was done by comparing their growth performances in YNB minimal media supplemented with arginine and either in the presence or absence of ammonium.

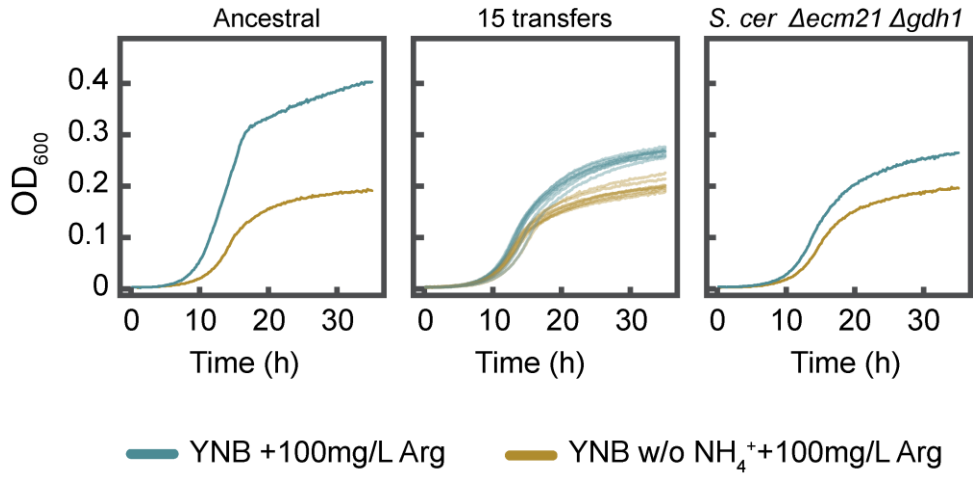

Figure 17 Assimilation of ammonia by different yeast lines
Curves representing the growth of the ancestral *S. cerevisiae* partner, the isolated yeast partners from all the evolved lines after 15 transfers and the yeast double mutant strain (*Δgdh1 Δecm21)* in either the minimal media used for the evolution of the co-culture supplemented with arginine (turquoise) or the minimal media supplemented with arginine but without ammonium (gold).

Remarkably, all the yeast strains isolated from the evolved co-cultures displayed reduced growth in the presence of ammonium compared to the ancestral strain, and the same phenotype is displayed by a mutant obtained through the deletion of both *gdh1* and *ecm21* from the ancestral strain (Fig. 17).

Since that in the absence of ammonium, all the lines grew similarly to the ancestral (Fig. 17, Appendix Fig. S4), a general reduction in the growth of these isolates can be excluded, suggesting instead that the evolved lines are affected in their ability to directly assimilate ammonia.

The fixation of this trait was even more surprising, considering that the minimal media used for the evolutionary experiment was YNB minimal media containing ammonium as the main nitrogen source. To assess whether this reduction represented a maximum point of the fitness landscape or, conversely, was a transient trait, we prolonged the evolutionary experiment for one of the lines (H6) for 20 additional transfers (84 h of growth between transfers). Isolated strains from these newly evolved communities showed a further decrease in their ammonium assimilation ability while still maintaining a similar growth profile and doubling times compared to the ancestral grown in the media lacking ammonium (Fig. 18, Appendix Fig. S4).

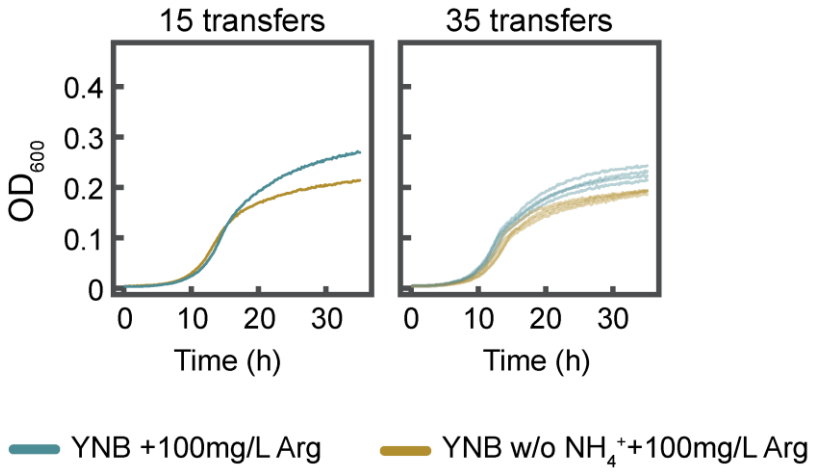

Figure 18 Test the ammonia assimilation ability of further evolved lines
Curves representing the growth of the *S. cerevisiae* partner isolated from line H6 after 15 transfers and after transferring it for 20 additional transfers (4 lines) in either the minimal media used for the evolution of the co-culture supplemented with arginine (turquoise) or the minimal media supplemented with arginine but without ammonium (gold).

Aiming to reveal the genetic changes underlying this further reduction, and considering that direct ammonia assimilation in yeast occurs mainly via two pathways (Fig. 19), we went back to our mutation table from the first round of evolution, and searched for the presence of other mutations in genes coding for enzymes relevant for these pathways.

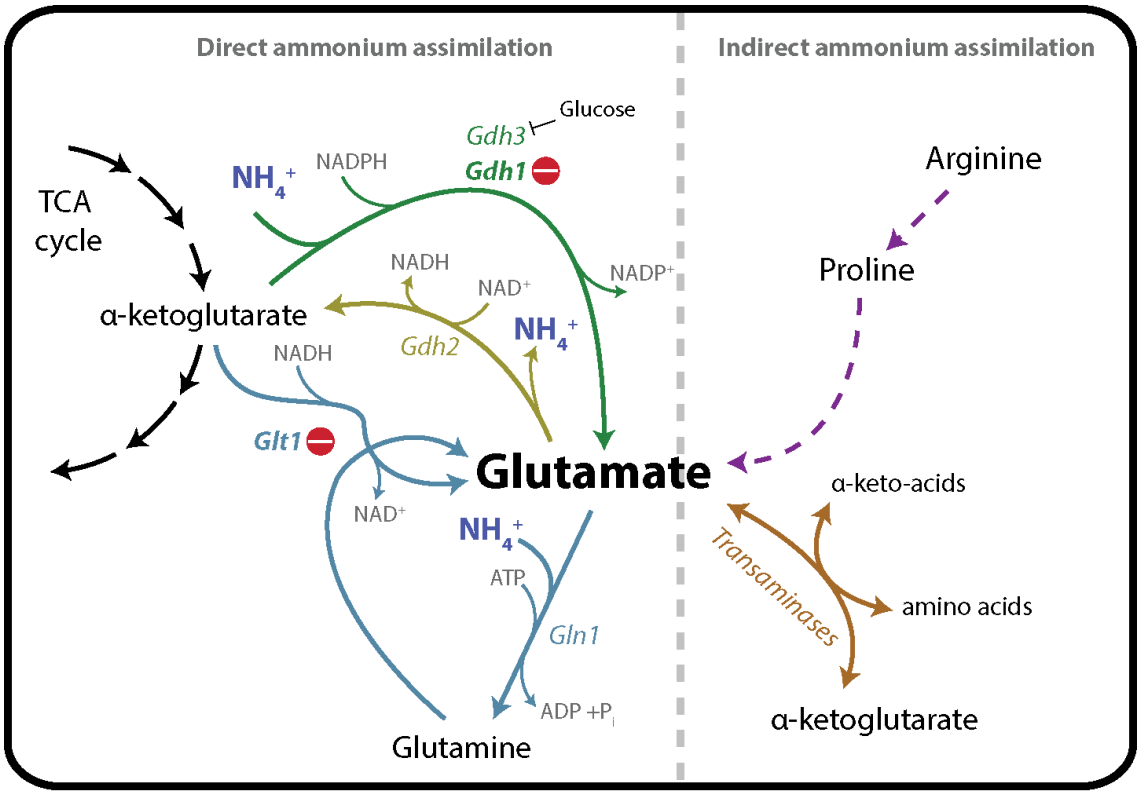

Figure 19 Nitrogen assimilation pathways in *S. cerevisiae*
Schematic representation of the pathways involved in nitrogen assimilation. Ammonium can be directly included into an organic molecule (alpha ketoglutarate) by either gdh1 (80 % of ammonium is assimilated via this pathway) or via a combination of two reactions carried out by enzymes encoded respectively from *gln1* and *glt1*. These two pathways, while give the advantage of assimilating an inorganic compound into an organic backbone, are energetically quite demanding. Notably, gdh1 and glt1 are interrupted in the evolved yeast lines. A direct transfer of ammonia from another amino acid via a transaminase represents an alternative pathway to synthetize glutamate, and is costless. Furthermore, yeast can alternatively transform arginine and proline into glutamate. These two pathways do not allow direct ammonium assimilation.

This revealed the presence of a set of mutations, both at intermediate and low frequencies (Appendix Table 4), on *glt1*, a gene encoding for a glutamate synthetase that belongs to the *gdh1* alternative route for direct ammonium assimilation (Fig.19). Considering that the line we used as a starting community for the second round of evolution contained a small fraction of *S. cerevisiae* carrying one of these mutations (non-sense) on *glt1* (Appendix Table 3), we proceed by assessing via sequencing whether the frequency of this mutation on the yeast population (initially approx. 25%) was increased in those lines that underwent additional passages. Qualitative analysis via Sanger sequencing confirmed an increase in frequencies in all of these lines (Fig. 20), supporting the phenotype observed from the growth curves (Fig. 18). Therefore, both the interruption of *gdh1* and *glt1* and the phenotypic confirmation of a marked reduction in direct ammonia assimilation,

suggest that such trait is evolutionarily favoured under the cross-feeding condition experienced by the yeast partner. However, while the fixation of such a trait was confirmed, the underlying physiological reasons behind the beneficial effect of this trait were not clear.

Figure 20 Frequency of the *glt1*-interrupted mutants in the population of the further evolved lines
Electropherogram from Sanger sequencing showing the mutated locus (position 617) of *glt1* in the four lines evolved for additional 20 transfers (derived from line H6). The top lane shows the amino acid sequence, from a.a 608 until a.a. 630 of glt1. Nucleotides are represented with peaks of different colours. A=green, T=red, G=blue and C= black. In position 617, the peaks from the mutated version (AA, two green peaks) appear more pronounced compared to those from the wt version (CC, two black peaks).

Considering that nitrogen is an essential macronutrient, and therefore its presence must be guaranteed by the cell, a plausible explanation accounting for the strong reduction in its direct assimilation in the mutant might involve the use of alternative sources, such as amino acids or other compounds containing nitrogen. These can be either directly converted into glutamate (e.g. proline) or can alternatively transfer their amino group to an α-ketoglutarate molecule through a transaminase, thus generating glutamate (Fig. 19). Since the assimilation of these alternative nitrogen sources and their conversion into glutamate requires a reduced energetic investment, their use could provide an advantage by reducing the cellular energetic burden. Furthermore, due to the natural "leakiness" of *E. coli*[49], these could be provided by the bacterial partner either by an overproduction of arginine or by the potential release of additional amino acids. In this regard, it was proven that selective pressure could favour the emergence of new auxtotrophies when the required metabolites are provided externally[50,66]

Following this hypothesis, we proceed by measuring the ability of the yeast double mutant *Δgdh1 Δecm21* strain to outcompete the ancestral one in the presence of alternative nitrogen sources in the media. This strain was chosen since its growth behaviour well recapitulates the one from the evolved yeast strains isolated from the first round of evolution (Fig. 17), thus allowing the targeted investigation of these two specific interruptions and the specific conditions favouring their appearance without any potential interference from other additional mutations.

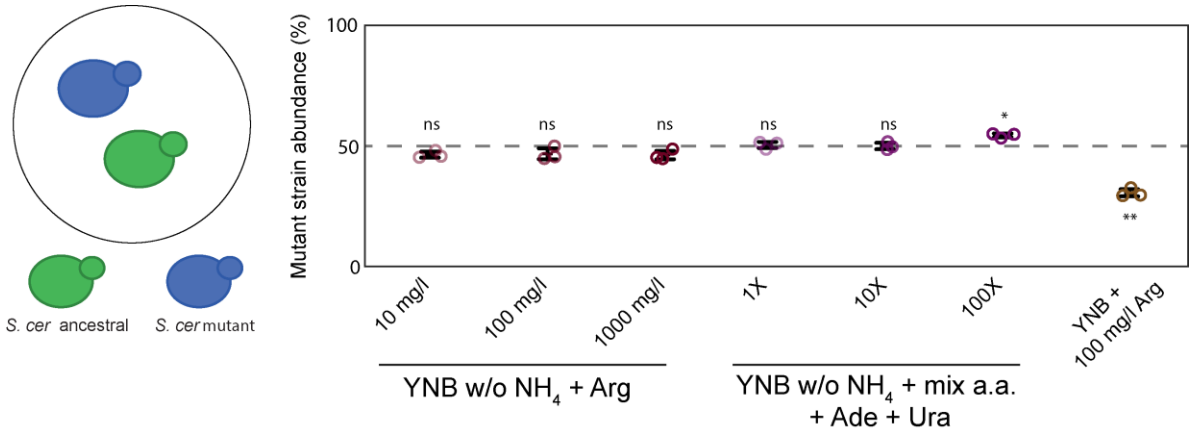

Figure 21 Influence of concentration and type of nitrogen source on fitness
Schematic representation of the experimental setup. *S. cerevisiae* ancestral and double mutant *Δgdh1 Δecm21* strains were inoculated in equal amounts in YNB minimal media containing either arginine or a mix of all the amino acids and two nucleotides at different concentrations. For the amino acid and nucleotide mix, 1x indicates a mix containing 1 mg/l of each amino acid, 0.2 mg/l of adenine and 0.2 mg/l of uracil. One sample *t*-test assessing for difference from a 50% abundance for three biological replicates.

Consistent to what observed for the evolved yeast lines, the double mutant was outperformed by the ancestral in the YNB minimal media supplemented with arginine (Fig. 9, Fig. 21). However, when ammonium was fully replaced by arginine as a nitrogen source, no difference in abundance between mutant and ancestral yeast was detectable, independently from the arginine concentration initially supplied in the media (Fig. 21). Even when a more complex mix of nitrogen source was provided, the yeast mutant slightly outcompeted the ancestral strain exclusively under very high supplement concentrations, while such enhanced performance of the double mutant was lost under moderate and low concentrations of this mix of alternative nitrogen sources (Fig. 21). Notably, the concentration under which the double mutant is slightly fitter compared to the ancestral yeast would be equivalent to approximately 2.2 g/l of nitrogen source, thus a concentration that is unlikely to be generated by the overflow metabolism of the *E. coli* partner. Overall, these results indicate that, under these experimental conditions, there is no major difference in arginine, or alternative nitrogen sources, utilization abilities between double mutant and ancestral yeast.

However, since the concentrations of arginine might be different compared to the one experienced by the yeast under cross-feeding, and also considering the presence of potential regulatory processes guiding alternative assimilation of nitrogen under slow growth regimes, we proceed by comparing the growth of both ancestral and mutant yeast in YNB with ammonium and supplemented with different concentrations of arginine. Furthermore, to assess for direct competition, both ancestral and double mutant yeast strains were inoculated in equal amounts under the same media conditions. Independently from the concentration of arginine, the ancestral yeast reached higher final OD and had lower doubling times compared to the double mutant yeast grown under equal concentrations of arginine (Fig. 22A). This indicates not only that *gdh1* seems to play a crucial role in direct ammonium assimilation under all the tested condition, but also that alternative fixation pathways are not induced under nitrogen starvation and slow growth. However, when the relative fitness of the mutant over the ancestral yeast was calculated from the direct competition experiment between the two yeast, a gradual increase in the relative fitness of the mutant was observed when the supplementation from arginine was decreased (Fig. 22 B).

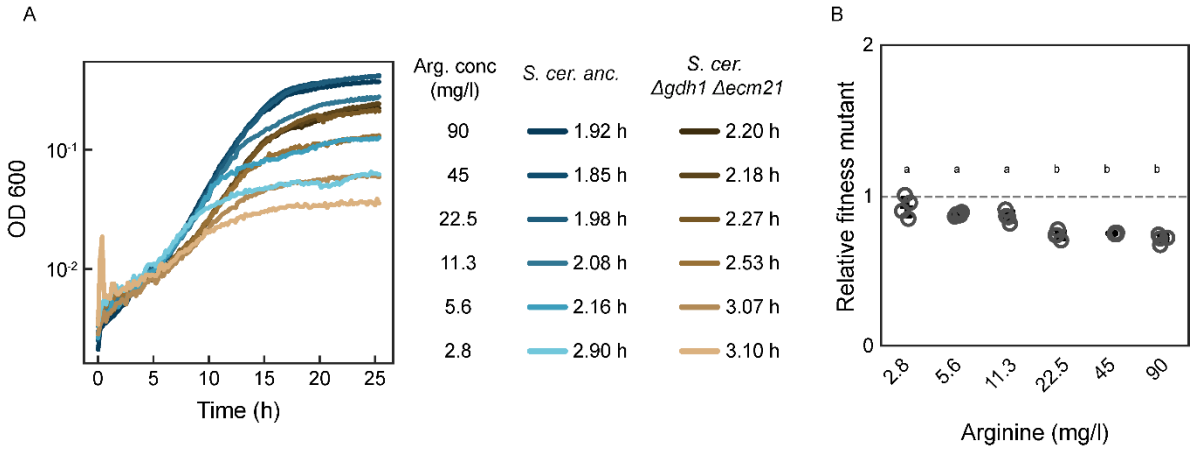

Figure 22 Effects of arginine abundance on nitrogen assimilation and fitness in the yeast partner
A Growth of ancestral and mutant *Δgdh1 Δecm21* yeast grown independently in YNB minimal medium containing ammonium and supplemented with different concentrations of arginine. Minimum doubling times reached by the two organisms under the different arginine concentrations are indicated. B Relative fitness abundance of the double mutant strain when co-inoculated in equal amounts with the ancestral in YNB minimal medium containing ammonium and supplemented with different concentrations of arginine. Letters represent within-group differences calculated from a Tukey test following a one-way ANOVA.

Notably, no difference in fitness was observed at the lowest arginine concentration ($p = 0.11$ from a one-sample *t*-test assessing for the difference from an average of 1), implying a comparable growth between ancestral and mutant. While this result appears contradictory with the growth rates and final OD reported from monocultures (Fig. 22A), a possible explanation might reside in a differential arginine uptake and consumption rate between the two organisms. In fact, while the

ancestral strain requires arginine potentially only as a building block, a lower arginine uptake rate would not compromise its growth under high concentrations of arginine, thus allowing it to outcompete the evolved strain. On the contrary, at low arginine concentrations, since the mutant carries a mutation potentially increasing arginine uptake (interruption of *ecm21*), this might confer enhanced scavenging abilities, which could compensate for the reduced ability to directly assimilate ammonium, thus increasing the relative fitness of the mutant strain compared to the ancestral one. Despite that, the fact that the relative fitness of the mutant never exceeded the value of one implies that, at least in this range of concentrations, the mutant is still not fitter compared to the ancestral. It must be noted that the two lowest concentrations of arginine used for these experiments are in the same range of metabolites concentrations measured previously from *E. coli* supernatant [49], thus potentially well mimicking the concentrations of arginine experienced by yeast under co-culture conditions with *E. coli*.

A possible factor resulting in a higher fitness of the mutant compared to the ancestral might be related to the presence of *E. coli* and, for example, a specific metabolite released by it. Therefore, we performed a competition assay between the double mutant and ancestral yeast in the presence of the *E. coli* partner while imposing different levels of metabolic dependencies between *E. coli* and the two competing *S. cerevisiae* strains. This was done by supplementing the minimal media with both arginine and histidine at different concentrations but with a constant ratio between them. The presence of *E. coli* was not sufficient by itself to boost the fitness of the double mutant since this strain outcompeted the ancestral yeast exclusively at low supplement concentrations or when no supplements were added (Fig. 23). Conversely, the appearance of a higher abundance of the double mutant seems to be related to an increased dependency between partners (Fig. 23, low supplements), thus implying the strong interplay between obligate mutualism and the advantage derived from a reduction in direct ammonium assimilation.

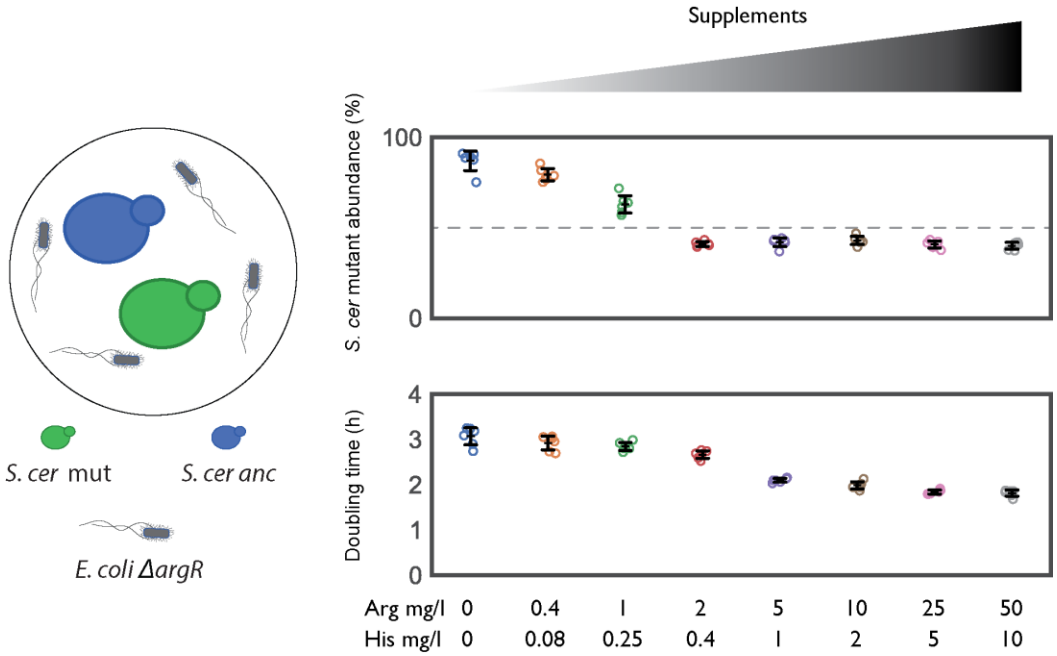

Figure 23 Impact of supplementation on the yeast mutant fitness under a cross-feeding regime
Schematic representation of the experimental setup. Both ancestral and mutant yeast strains were inoculated in equal amounts (OD=0.025 each) together with *the E. coli ΔargR* partner (OD=0.05) in YNB minimal media with ammonium supplemented with different concentrations of arginine and histidine. Plots report both the yeast mutant fraction over the total yeast cell count and the minimum doubling time reached by each co-culture in YNB with increasing concentrations of supplements.

2.3. Importance of direct physical association and motility on fitness for a planktonic interkingdom microbial community

Physical interaction with yeast provides a selective advantage to bacteria in a cross-feeding community

In order to investigate the effects of physical association and motility on our engineered communities under planktonic conditions, we exploited the natural ability of *E. coli* to bind to surface mannoproteins of *S. cerevisiae* via type I fimbriae (Fig. 7)[97], which was quantitatively confirmed by correlation analysis on microscopy (Appendix Fig. S5).

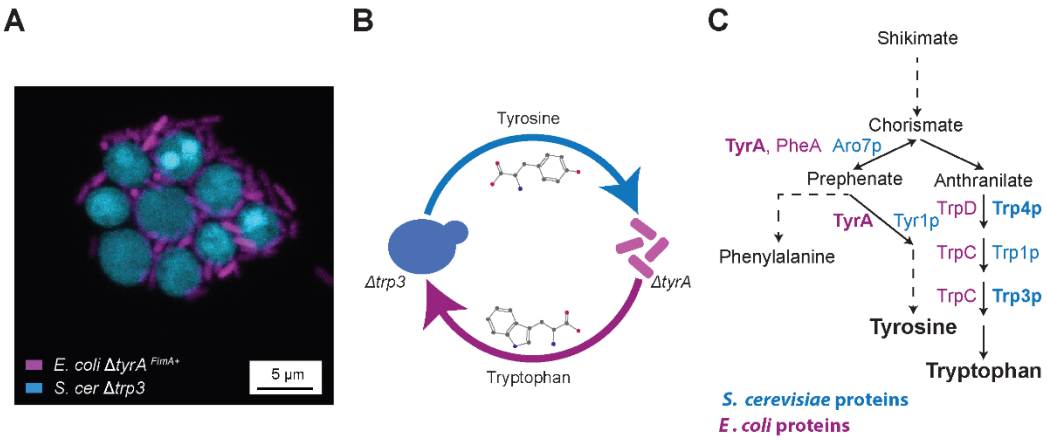

Figure 24 Aggregative and metabolic characteristic of the selected cross-feeding pair

A Confocal image of a cell cluster in the co-culture containing cross-feeding strains of Fim+ *E. coli* (magenta) and *S. cerevisiae* (blue).
B Schematic representation of metabolic dependencies within the engineered community. *E. coli* (magenta) is auxotroph for tyrosine while *S. cerevisiae* (blue) is auxotroph for tryptophan.
C Biosynthetic pathway for aromatic amino acids. Arrows represent individual reactions, with the corresponding enzymes shown both for *E. coli* (magenta) and for (blue).

Since this physical association, and the consequent aggregates formation, was retained by our cross-feeding communities (Fig. 24A), such model system represents the perfect chassis for the investigation of the role of adhesion and aggregation on cross-feeding communities displaying an obligate mutualistic metabolic dependency. Furthermore, the fact that one of the partners, specifically *E. coli,* is able to swim and respond to chemical gradients (chemotaxis) allows the study of the role of these two additional parameters on suspended co-cultures relying on cross-feeding. Therefore, we selected from all the cross-feeding communities generated (Fig. 5) a pair of auxotrophs displaying a strong growth phenotype when in co-culture. Specifically, the selected pair

is constituted by *E. coli* Δ*tyrA,* requiring tyrosine for growth, and the *S. cerevisiae* Δ*trp3* strain, relying on the other partner for tryptophan biosynthesis (Fig. 24B,C, Appendix Fig. S6).

Notably, although the expression of fimbriae in *E. coli* is known to be phase-variable [105], we confirmed that the fraction of fimbria-expressing cells was very high (~90%) under our conditions, ensuring that the majority of genetically Fim+ *E. coli* cells possess the ability to adhere to yeast (Fig. 25).

This specific cross-feeding community showed robust growth in a co-culture without any further genetic enhancement, possibly because the metabolite exchange underlying their growth is

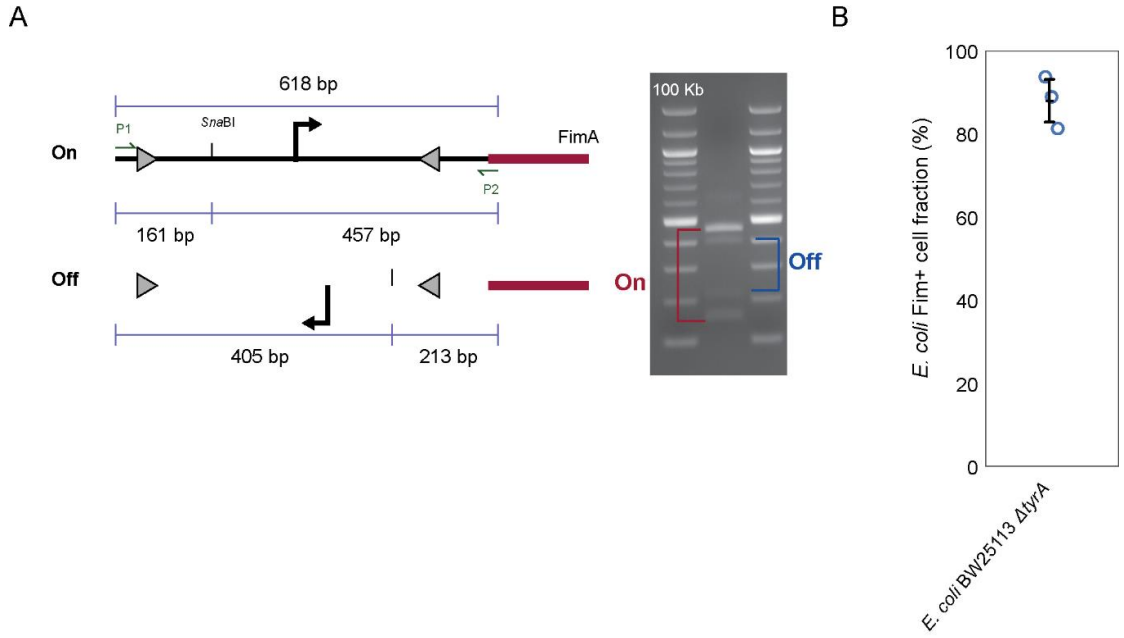

Figure 25 Activation status of the fim operon

A Assay used to determine the promoter orientation. The promoter region (618 bp) of the fim operon was amplified by PCR using primers P1 and P2, as indicated. This region contains a unique *Sna*BI restriction site. The digestion of the PCR fragments with *Sna*BI results in specific fragment pairs according to the state (On/Off) of the promoter, thus displaying a specific pattern of bands once the digestion is run via electrophoresis on a 2% agarose gel. B Quantification of the fim status of the *E. coli* partner based on band intensities as shown in (A), which is comparable to values obtained in LB cultures. Three biological replicates were used and are indicated as circles.

favoured by interruptions of different branches of the same metabolic pathway in *S. cerevisiae* and *E. coli* (Fig. 24C, Fig. 26A). Despite their metabolic interdependence, the two organisms showed differences in their time course of growth, with *S. cerevisiae* reaching the maximal cell density

earlier than *E. coli* (Figure 26B), suggesting a difference in growth limiting factors between the two organisms present in the co-culture.

While comparable growth profiles were observed when this synthetic community was assembled with either fimbriated (Fim$^+$) or fimbrialess (*ΔfimA*) *E. coli*, both the overall density of the co-

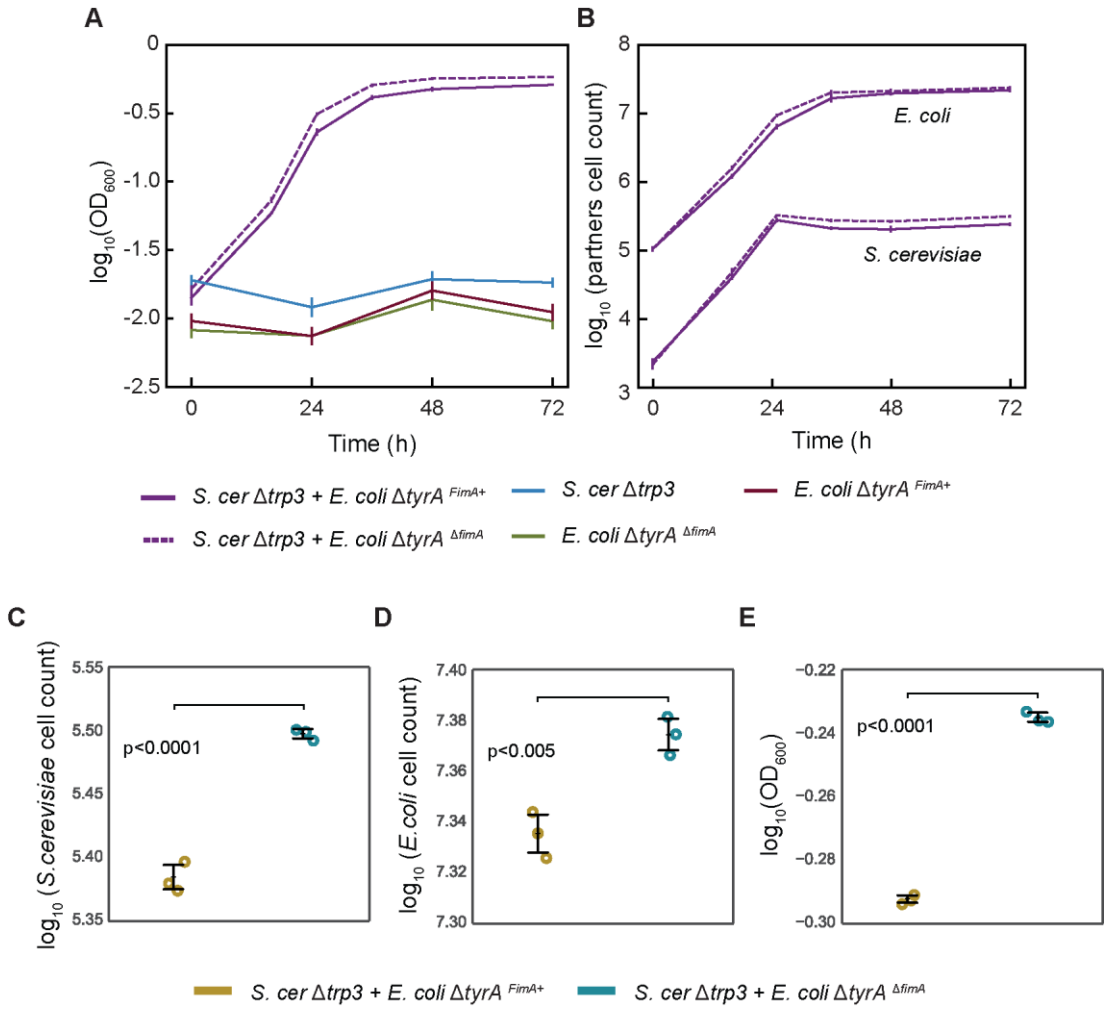

Figure 26 Growth profile of cross-feeding co-cultures

A Growth of the co-cultures and of individual strains incubated in the selective YNB-glucose minimal medium, measured as optical density at 600 nm. Solid and dashed magenta lines indicate communities containing Fim+ or *ΔfimA E. coli*, respectively. Error bars are standard deviations of three biological replicates.
B Numbers of *S. cerevisiae* (labelled with mTurquoise2) and *E. coli* (labelled with mCherry) cells measured by flow cytometry in the same co-cultures as shown in (A).
C,D Final cell counts from co-cultures as in A,B for (C) *S. cerevisiae* and (D) *E. coli*. p values were obtained from a two-tailed t-tests assuming equal variances of the data sets, each with three biological replicates (indicated by circles).
E Final OD from co-cultures in A,B. p values were obtained from a two-tailed t-tests assuming equal variances of the data sets, each with three biological replicates (indicated as circles).

culture and the numbers of *S. cerevisiae* and *E. coli* cells were slightly reduced when *E. coli* was fimbriated (Figure 26C-E).

This reduction was shown to due to the formation of multicellular clumps, which apparently affects growth regardless of cross-feeding since this effect was also observed in the minimal media supplemented with a mixture of amino acids (Fig. 8A,B).

Physical association might nevertheless confer a competitive advantage to fimbriated *E. coli* cells in the cross-feeding community, by ensuring their stable association and efficient intermixing with the yeast partner (**Figure 24A**). In order to test this directly, we co-cultured fimbriated and fimbrialess *E. coli*, each labelled with a different fluorescent marker, with the yeast auxotroph. Although both *E. coli* strains were inoculated in equal amounts, we observed that fimbriated cells were significantly enriched in the final community (**Fig. 27A**), and this enrichment was even more pronounced at lower inoculation density (**Fig. 27B**).

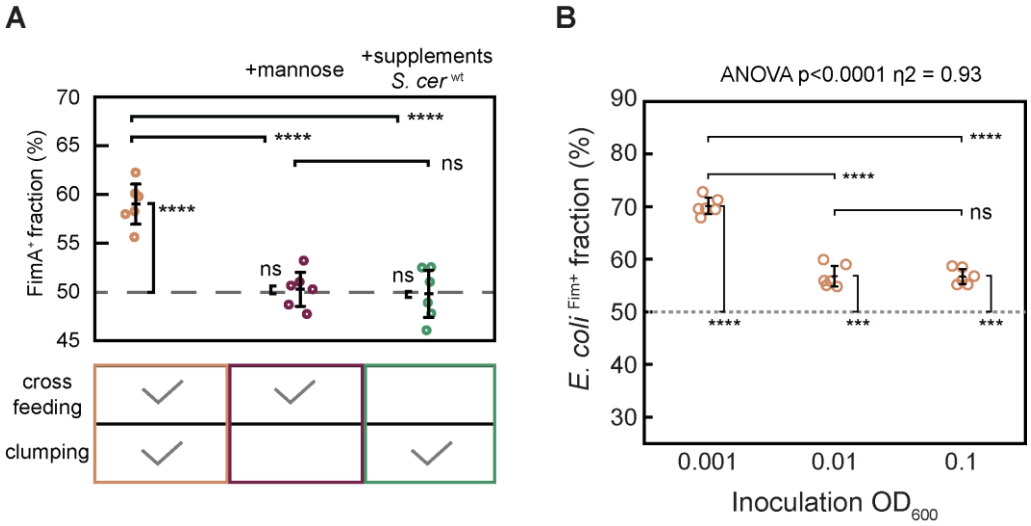

Figure 27. Competition between fimbriated and fimbrialess *E. coli* in co-culture with *S. cerevisiae*

A Fraction of Fim+ cells (labeled with mCherry) in the total *E. coli* population measured by flow cytometry in co-culture with sfGFP-labelled fimbrialess (*ΔfimA*) *E. coli* and *S. cerevisiae* Δtrp3. Co-cultures were inoculated with equal amounts of Fim+ and *ΔfimA* cells and grown for 72 h either in YNB-glucose, in YNB-glucose supplemented with 4 % mannose or YNB-glucose supplemented with CSM (complete supplement mixture). In the latter case the yeast auxotroph was additionally replaced by the parental prototroph. Boxes represent the second and third quartile of the distribution and whiskers show the rest of the distribution for six biological replicates (indicated by circles). ****p ≤0.0001 in a two-tailed t-test assuming equal variances of the data sets.
B Co-cultures were inoculated at different initial cell densities, with initially equal amounts of Fim+ (labelled with mCherry) and *ΔfimA* (labelled with sfGFP) cells and grown for 96 h in YNB-glucose. Error bars represent standard deviations of six biological replicates represented as circles. One-way ANOVA test, followed by an HSD Tukey test as *post hoc* analysis were performed to assess for difference between samples. A one-sample *t*-test was performed to assess difference from an average fraction of 50%.

This competitive advantage of fimbriation depends of the interaction with the yeast partner and on cross-feeding, since it was abolished when the medium was supplemented with mannose or in a co-culture with the yeast prototroph for tryptophan and in a medium supplemented with a mixture of amino acids (**Fig. 27A**). Comparable results were obtained in co-cultures with Δ*trp4* strain of *S. cerevisiae* that is interrupted at a different step in the tryptophan biosynthetic pathway (**Figure 24C** and **Fig. 28**).

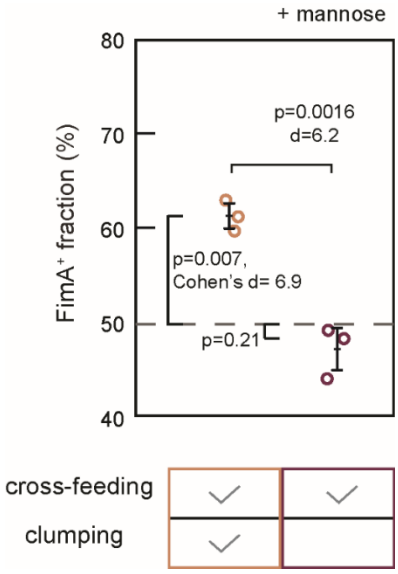

Figure 28 Effects of partner adhesion on fitness for a community with *S. cerevisiae* Δtrp4 strain

Fraction of Fim+ cells (labelled with mCherry) in the total *E. coli* population co-cultured with *ΔfimA E. coli* (labelled with sfGFP) and *S. cerevisiae Δtrp4* (labelled with mTurquoise2). Co-cultures were inoculated with equal amounts of Fim+ and ΔfimA cells and grown for 96 h either in YNB-glucose or in YNB-glucose supplemented with 4% mannose. Scatter plots represent the distribution of three biological replicates (indicated by circles). Whiskers represent the standard deviation. Both two-tailed *t*-test assuming equal variances of the data sets and one sample *t*-test to assess differences from a 50% average were performed. Cohen´s d values were used to quantify the effect size.

In contrast to growth in planktonic culture, no competitive advantage of fimbriation was observed for communities grown on a minimal media plate (Fig. 29A,B). This difference might be due to the observed spatial segregation between fimbriated and fimbrialess *E. coli* strains into different sectors of the colony, which likely prevents their local competition. Such segregation of competing *E. coli* strains into sectors within growing colonies is similar to previous reports [64,68,70,106] . Notably, distribution of yeast cells was uniform under these conditions.

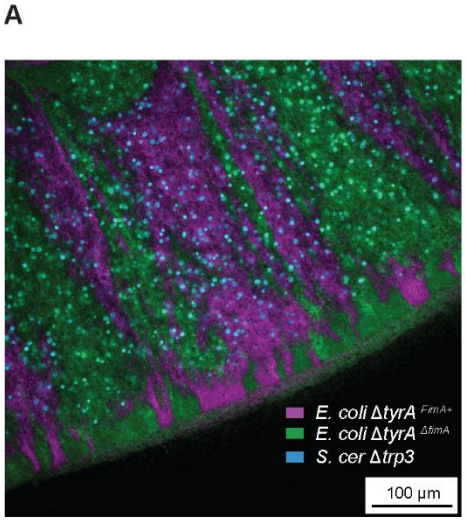

Figure 29 Assessing the role of fimbriation on communities grown on a solid surface

A,B Co-culture of *S. cerevisiae* (blue) with equal amounts of Fim+ (magenta) and *ΔfimA* (green) *E. coli* grown on an agarose plate. Cells were labelled as in Fig. 27. Confocal microscopy image of a colony sector (A) and the fraction of Fim+ cells (B) after 10 days of incubation are shown.

Partner adhesion reduces invasion of community by a cheater

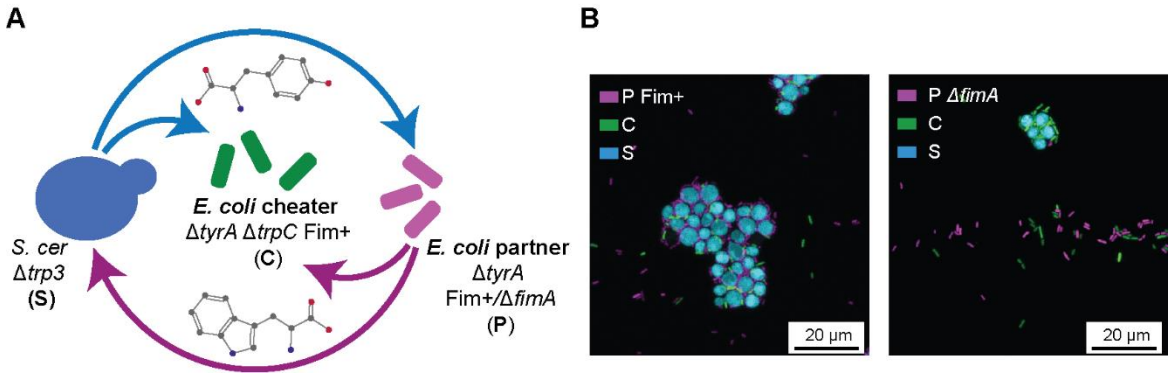

Figure 30 Engineering of a cheater strain

A Schematic representation of metabolic dependencies within the engineered community containing a non-cooperating *E. coli* cheater (green) that is auxotroph for both tyrosine and tryptophan. Partner strains are as in Fig. 24B.
B Confocal microscopy images of cell clusters of *S. cerevisiae* expressing mTurquoise2 (blue) and either Fim+ or *ΔfimA E. coli* partners expressing mCherry (magenta), in presence of an *E. coli* cheater expressing sfGFP (green). Scale bar= 20 μm.

One potential ecological benefit of the physical association between species in planktonic community could reside in protection against the exploitation of shared metabolites by non-cooperators which do not contribute to the consortium. We thus engineered an *E. coli* strain with disruptions in both the tryptophan and tyrosine biosynthetic pathways (Δ*tyrA* Δ*trpC*) (Fig. 30A), which behaves as a cheater exploiting metabolites released by both partners for its own growth without providing any benefits to the community. This strain mimics a plausible scenario how natural cheaters could emerge by gene loss [50,107,108]. When this fimbriated cheater strain was introduced in our community along with the partner (Δ*tyrA*) *E. coli* strain, it showed expected localization to bacteria-yeast aggregates (Figure 30B) and growth within community but not with individual partners (Appendix Fig. S7,8). Introduction of the cheater led to a small but significant reduction of the community growth rate and of final OD, dependent on the dose of the cheater (Fig. 31C; Fig. 32A,B,D,E). The number of yeast cells in the community was also significantly reduced in the presence of the cheater (Fig. 31C; Fig. 32C,F). The community containing the fimbrialess *E. coli* was more strongly affected by the initial dose of the cheater, i.e., showed higher slopes of the regression fits in (Fig. 32A-I). This was apparently due to the reduced final cheater abundance in the presence of partner fimbriation (Fig. 31B), since the regression lines became similar for both communities when plotted against the final cheater abundance, apart from

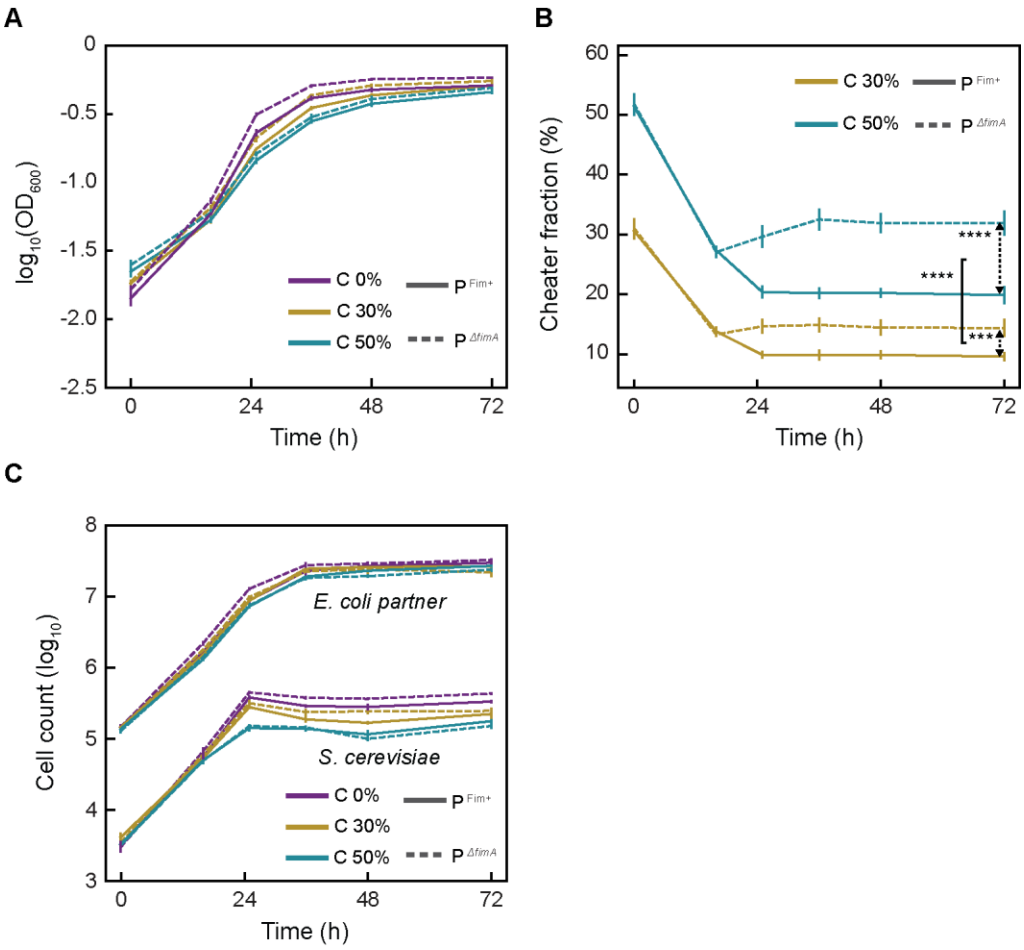

Figure 31 Impact of cheater on cross-feeding communities

A Growth of the co-cultures in the selective YNB-glucose minimal medium in presence of indicated initial levels of cheater. Solid and dashed lines indicate communities containing Fim+ or ΔfimA *E. coli* partner, respectively. Error bars are standard deviations of three biological replicates.
B Fraction of cheater in the total *E. coli* population in the same co-cultures as in (A).
C Numbers of *S. cerevisiae* (labelled with mTurquoise2) and *E. coli* partner (labelled with mCherry) cells measured by flow cytometry in the same co-cultures as in (A).

differences due to the direct reduction of community growth caused by *E. coli* fimbriation (Fig. 32G-I). Thus, physical association with yeast helps the bacterial partner outcompete the cheater, and this beneficial association effect could compensate or, in the presence of a higher number of cheater cells, even outweigh the aggregation-dependent reduction of *S. cerevisiae* growth (Fig. 32C,F).

Consistently, the dependence of cheater fraction and of the total *E. coli* cell count on partner fimbriation was no longer significant in the presence of mannose or in the absence of cross-feeding (Fig. 33).

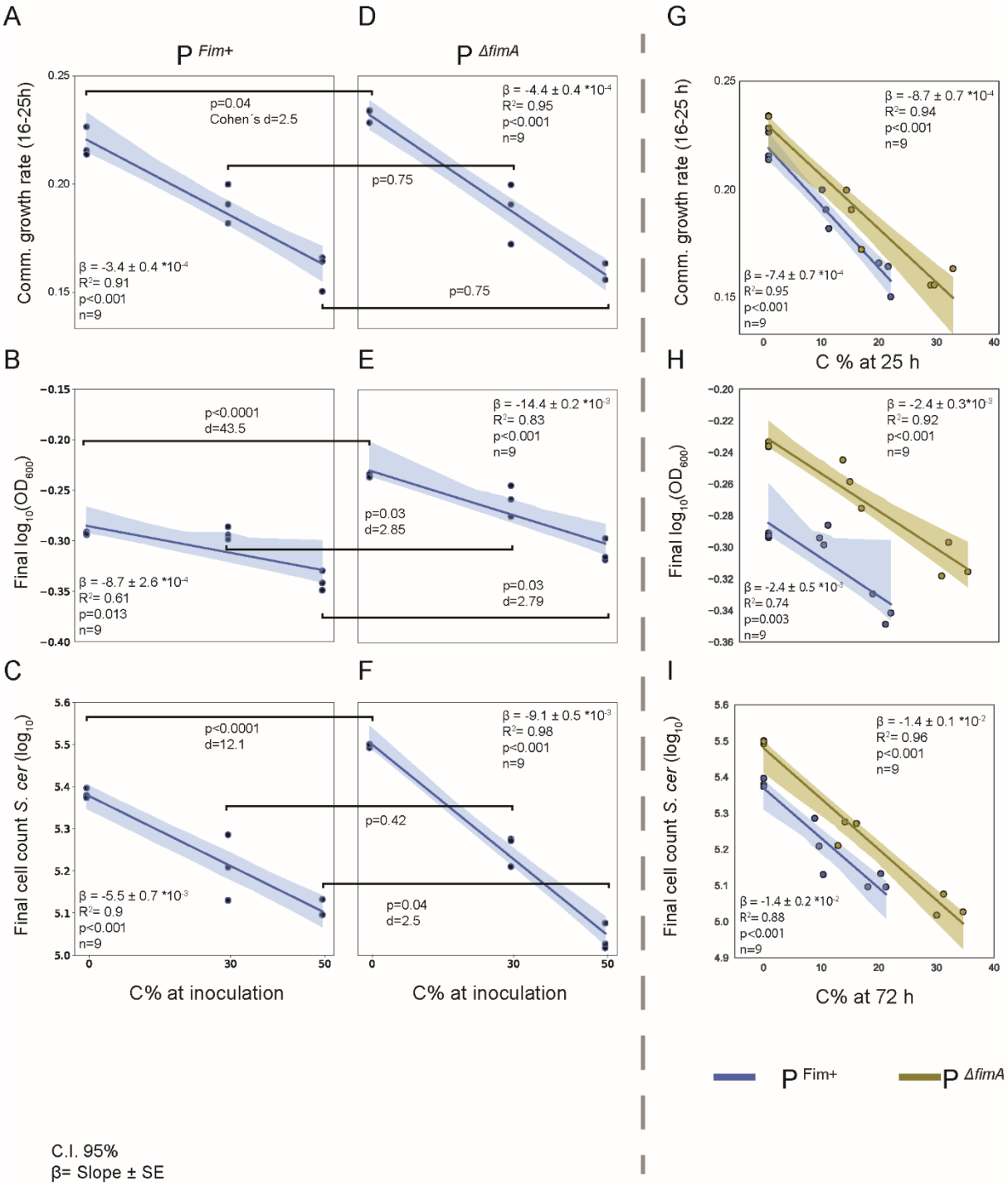

Figure 32 Dependence of the composition and growth of communities on the cheater fraction

A-F Dependence of the growth rate in exponential phase (A,D), of the total final OD600 (B,E) and of the final yeast cell count (C,F) from cocultures as in Figure 31 A,C on the initial fraction of the cheater (labelled "C") at inoculation and either a fimbriated (left) or fimbrialess (right) *E. coli* partner (labelled "P").
G-I Same data but plotted against the final cheater fraction at the time of the measure, 25 h in (G) and 72 h in (H) and (I). Linear regression analysis and two-tailed t-test assuming equal variances of the data sets were performed. Each condition was assessed for three biological replicates, indicated as dots while shadings indicate a confidence interval of 95%. Regression line slopes, indicated as β, have been included along with the standard error.

The final fraction of cheater cells in *E. coli* population in the supplemented medium was below 50% (around 40%), indicating moderately lower fitness of the cheater compared to the partner strain in the absence of cross-feeding, most likely due to imperfect compensation of *trpC* deletion effects by supplementing the medium with tryptophan. Nevertheless, this cheater fraction was further

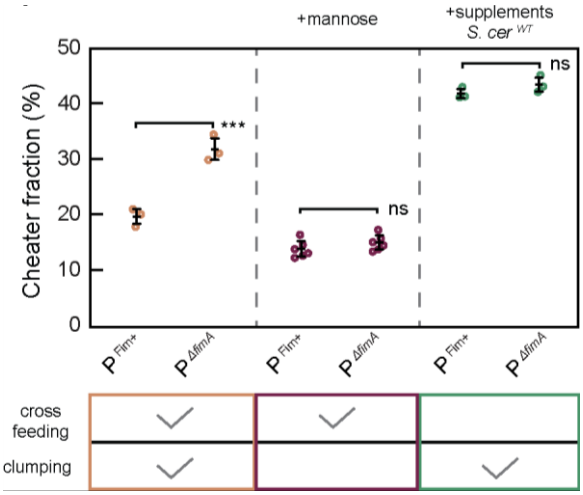

Figure 33 Effects of direct physical association between partners in presence of fimbriated cheater

Fraction of cheater in communities containing either Fim+ or *ΔfimA E. coli* partner at the initial 50% abundance of cheater, grown in YNB-glucose (orange) (Data from C), YNB-glucose supplemented with 4% mannose (red) and in in YNB-glucose supplemented with CSM and with *S. cerevisiae* prototroph (green). ****p<0.0001 from two tailed t-test assuming equal variances of the data sets for three to six biological replicates). ns, non-significant, p>0.15.

significantly reduced in the cross-feeding community, to 30% in the presence of the fimbrialess *E. coli* partner and to 20% in the presence of the fimbriated *E. coli* partner, possibly due to the negative selection on cheater-enriched cell aggregates (see Discussion). Similarly, beneficial impacts of partner fimbriation were observed when using a fimbrialess cheater strain (Fig. 34) as well as for the alternative yeast tryptophan auxotroph *Δtrp4* (Appendix Fig. S9).

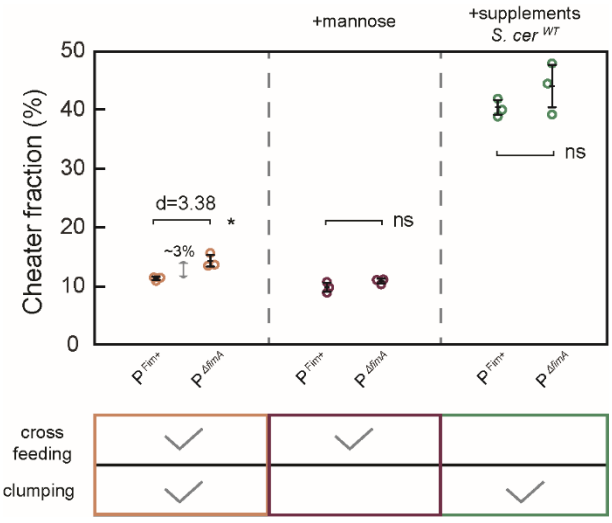

Figure 34 Effects of direct physical association between partners in presence of fimbrialess cheater

Fraction of a fimbrialess cheater (*ΔfimA*) in communities containing either Fim+ or *ΔfimA E. coli* partner at the initial 50% abundance of cheater, grown in YNB-glucose (orange), YNB-glucose supplemented with 4% mannose (red) and in in YNB-glucose supplemented with CSM and with *S. cerevisiae* prototroph (green). *p ≤0.05, ns=not significant in a two tailed t-test assuming equal variances of the data sets for three biological replicates, represented as circles

Such enhancement of partner competitiveness due to its fimbriation was again no longer detectable once the communities containing cheater were grown on a solid surface (Fig. 35). Notably, the fraction of cheater cells in a colony was ~11% and thus generally lower than in the batch culture

with or without partner fimbriation. Such low fitness of the cheater might be the consequence of stable spatial segregation between partner and cheater bacteria within the colony (Fig. 35A). *S. cerevisiae* does not, however, display an apparent segregation from *E. coli* cheaters (Appendix, Fig. S10), most likely because the relatively small size of cheater sectors is below the range of metabolic interactions within the colony [68].

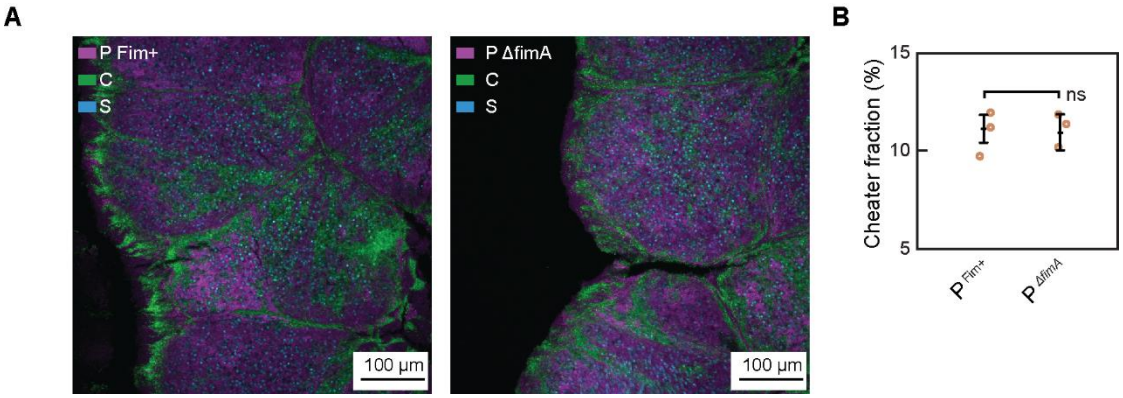

Figure 35 Impact of cheater on cross-feeding communities grown on a solid surface

A,B Confocal microscopy image of a colony sector (A) and the fraction of cheater in the total *E. coli* population (B) from co-cultures of *S. cerevisiae* with either Fim+ or *ΔfimA E. coli* as indicated, and the cheater at the initial 50% abundance, grown on a 1% agarose plate for 10 days.

Beyond a single growth cycle of the community, we studied the longer-term impact of partner fimbriation by culturing our community in a semi-continuous growth mode. This was done by transferring an inoculum from the culture to fresh media every 24 hours (Fig. 36A). In the absence of the cheater, such repeated transfers eventually resulted in the establishment of a relatively stable community (Fig. 36B,C). Consistently with previous experiments, cell density and *S. cerevisiae* and *E. coli* partner cell counts were lower when the *E. coli* partner was fimbriated (Fig. 36B,C). In contrast, in the presence of the cheater, the community was no longer stable and experienced a gradual decline after an initial phase of increased density, with the count of yeast cells eventually dropping to a number of events comparable to that in the blank, even though the relative abundance of the cheater was low (Fig. 36D). In that case, partner fimbriation became again beneficial, resulting not only in largely reduced cheater and increased *E. coli* partner abundance, but also leading to a significantly higher number of yeast cells over most of the experimental time course ($p<0.05$ from day 2 until day 8, t test assuming equal variance between samples) (Fig. 36C,D; Appendix Fig. S11), and consequently significantly delaying community collapse (Fig. 36B). Thus, also under these conditions benefit due to exclusion of the cheater overweighed the immediate

negative impact of fimbriation on yeast growth, although it could not prevent the eventual collapse of the community.

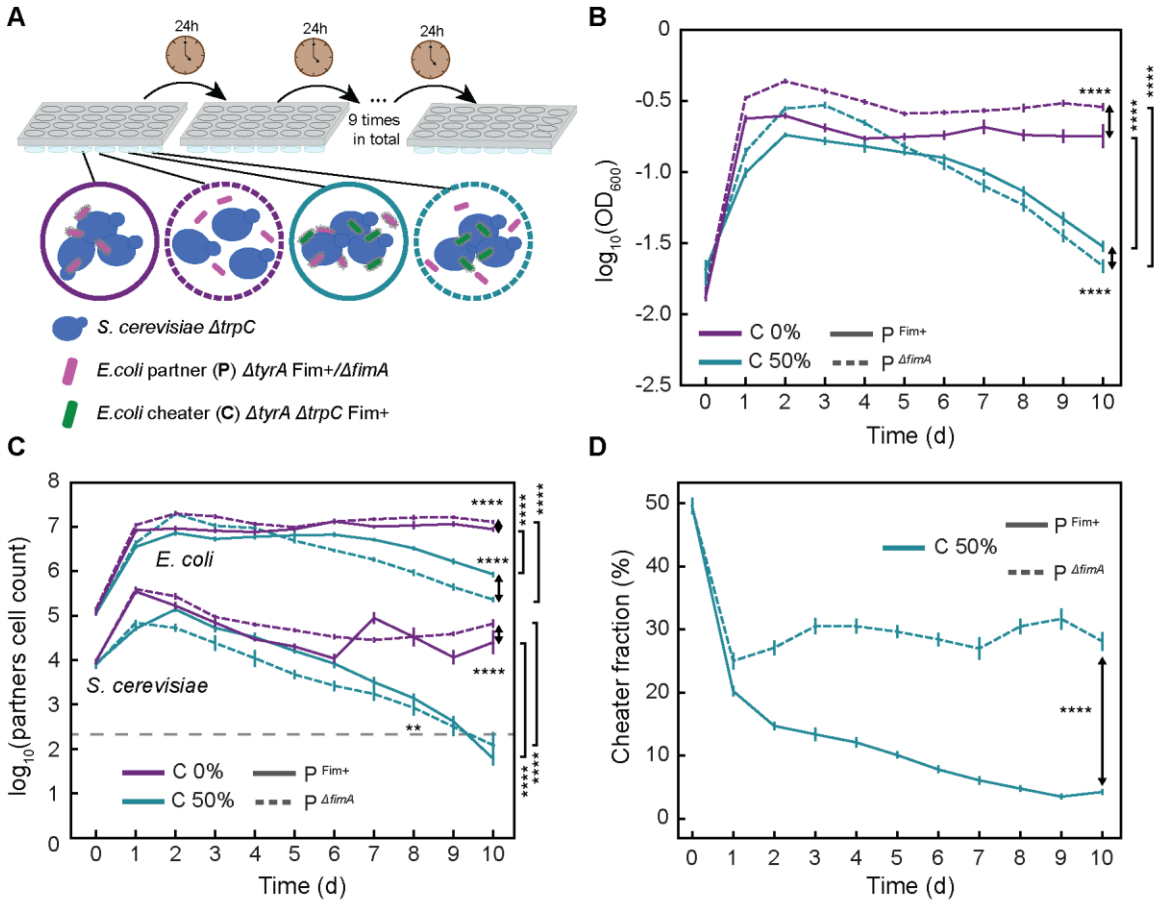

Figure 36. Impact of cheater on communities in a semi-continuous growth mode.

A Schematic representation of the experimental setup for the semi-continuous growth mode, where 500 µL of the co-cultures are repeatedly transferred to 500 µL fresh media every 24 h for a total of 10 days.

B Growth of the co-cultures in the selective YNB-glucose minimal medium either in absence (magenta) or in presence (turquoise) of 50% cheater (labeled "C"), as indicated. Solid and dashed lines indicate communities containing either Fim+ or *ΔfimA E. coli* partner (labeled "P"), respectively. Error bars represent standard deviations of six to twelve biological replicates. ****p<0.0001 from one tailed t-test assuming equal variances of the data sets.

C Numbers of *S. cerevisiae* (labelled with mTurquoise2) and *E. coli* partner (labelled with mCherry) cells measured by flow cytometry in 20 µL of the same co-cultures as in (B). For *S. cerevisiae*, the last two time points were excluded (opaque) since the value obtained is below, or just above the blank control (gray dashed line) ****p<0.0001 and *0.05>p>0.01 from one tailed t-test assuming equal variances of the data sets for each comparison.

D Fraction of cheater in the cheater-containing communities in (B). ****p<0.0001 from one tailed t-test assuming equal variances of the data sets.

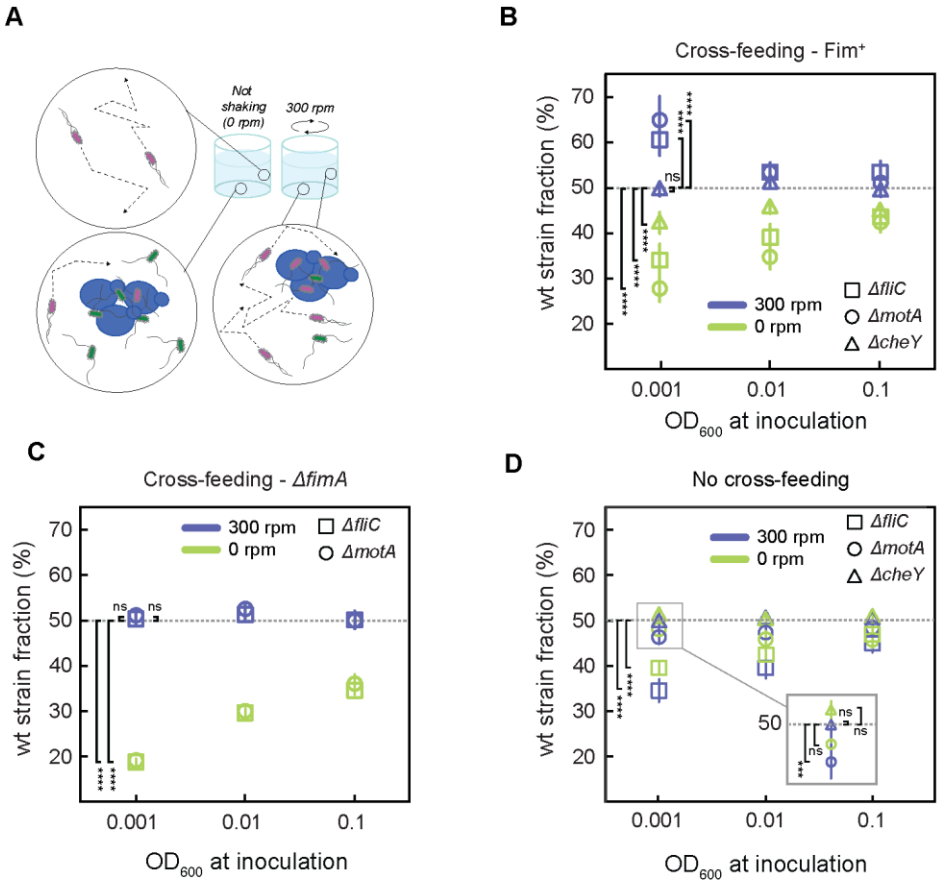

Figure 37. Effects of motility on the bacterial partner fitness in physically interacting community

A Schematic representation of the experimental setup to study effects of motility on the community, with yeast-bacteria co-cultures grown either without shaking or with shaking at 300 r.p.m. While without shaking non-motile *E. coli* (e.g. *ΔmotA*, green) and yeast cells (blue) sediment to the bottom of the well, and the motile *E. coli* (red) is in suspension, under shaking the entire community is maintained in suspension.

B Fraction of motile and chemotactic *E. coli* cells (labeled with mCherry) compared to the total *E. coli* population in co-culture with sfGFP-labeled non-motile (either *ΔfliC*, or *ΔmotA*) or non-chemotactic (*ΔcheY*) *E. coli* cells and with yeast. Communities were inoculated with different initial optical density (OD) as indicated and grown for 96 hours under shaking (blue) or without shaking (light green) in YNB-fructose minimal medium. Error bars represent standard deviations of at least six biological replicates. ****p<0.0001 and ***p<0.001 from one sample *t*-test assessing for difference to a 50% fraction average for each statistically different comparison. ns, non-significant.

C Fraction of motile and chemotactic cells in the total *E. coli* population in the co-cultures grown like in (B) but in *ΔfimA* background. Error bars represent standard deviations of at least six biological replicates. ****p<0.0001 and ***p<0.001 from one sample *t*-test assessing for difference to a 50% fraction average for each statistically different comparison. ns, non-significant.

D Fraction of motile and chemotactic cells in the total *E. coli* population in co-cultures grown like in (B) but supplemented with CSM.

In aquatic environments, the ability of cells to actively move could increase the encounter rate between partners, but it might also enhance cell detachment. To test the impact of motility on the relative fitness of bacteria in our community, we performed competition assays between motile and non-motile *E. coli* partners co-cultured with yeast (Fig. 37A). Two different non-motile strains of *E. coli* were used, either deleted for flagellin gene *fliC* and thus lacking flagellar filaments, or deleted for the flagellar motor gene *motA* and displaying non-functional, yet structurally intact, flagella. Moreover, we further tested a motile but non-chemotactic *E. coli* strain (*ΔcheY*) that is no longer capable of following chemical gradients in the environment. Since the motility of the parental strain *E. coli* BW25113 used in the previous experiments is generally poor, and large spontaneous variability of swimming abilities was reported for its derivatives [109], here we used another common K12-derived strain MG1655, where Δ*tyrA* and the aforementioned motility and chemotaxis mutations were introduced. Furthermore, since motility gene expression in *E. coli* is repressed by glucose [110], fructose was used instead as the carbon source. All knockout strains showed the expected motility phenotypes under these experimental growth conditions (Fig. 38). Moreover, no effects of fimbriation on swimming (Fig. 39) or of motility on the on/off state of the *fim* promoter (Fig. 40) were observed, confirming that motility and fimbriation do not exhibit cross-regulation under our experimental conditions. Motility was observed to provide a significant competitive fitness benefit to *E. coli* at low initial cell densities and under conditions of mixing in an orbital shaker, with over 60% of the final *E. coli* partner population being wildtype for motility at the initial OD of 0.001 (Fig. 37B), which is comparable to typical microbial cell densities in aquatic environments [111]. This was true for competition with either *ΔmotA* or *ΔfliC* strains, suggesting that this effect is purely determined by motility, and not by possible flagella-mediated adhesion [112]. In contrast, chemotaxis does not seem to provide benefit under these conditions, since the fraction of a non-chemotactic but motile *ΔcheY* stain was not statistically different from 50% even at low initial cell density.

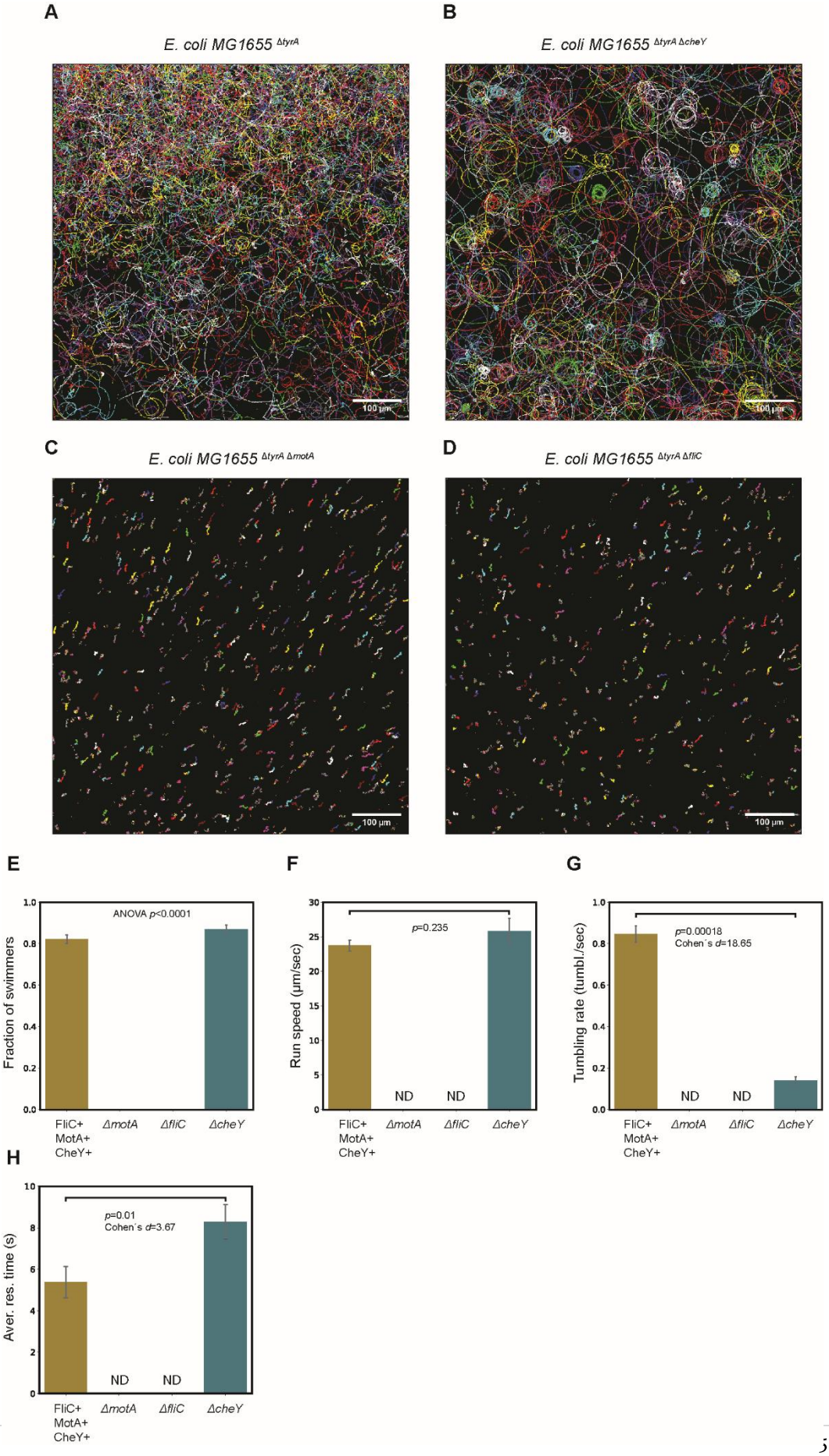
A
E. coli MG1655 ΔtyrA
B
E. coli MG1655 ΔtyrA ΔcheY
C
E. coli MG1655 ΔtyrA ΔmotA
D
E. coli MG1655 ΔtyrA ΔfliC
100 μm
E
Fraction of swimmers
ANOVA p<0.0001
F
Run speed (μm/sec)
p=0.235
G
Tumbling rate (tumbl./sec)
p=0.00018
Cohen´s d=18.65
H
Aver. res. time (s)
p=0.01
Cohen´s d=3.67
ND
FliC+ MotA+ CheY+
ΔmotA
ΔfliC
ΔcheY

Figure 38 Characterization of motility phenotypes

A-D Particle tracking of *E. coli* strains used to assess influence of motility, for motility wildtype (A), *ΔcheY* (B), *ΔmotA* (C), and *ΔfliC* (D). Each color represents the trajectory of a single bacterium.
E-H Quantification of fraction of swimmers (E), swimming speed (F), tumbling rate (G) and average residence time at the surface (H) for each strain. Of note, rare reorientation events in *ΔcheY* strain that are detected as tumbling are rather caused by cell collisions with other cells, surface defects or alike. Error bars represents the standard deviations of three biological replicates, each measuring at least fifty cell trajectories. One-way ANOVA and two-sided t-test assuming equal variance between data sets were performed.

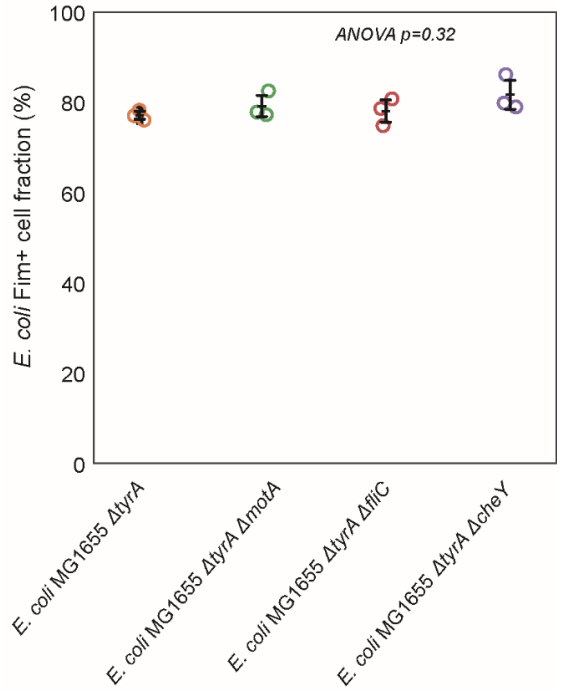

Figure 39 Activation status of the fim operon does not depend on motility

Quantification of the fim status of all the *E. coli* MG1655 partners used in this study, as described in Fig. 26, including the non-motile and non-chemotactic. p value from a one-way ANOVA test with three biological replicates per each strain indicated as circles.

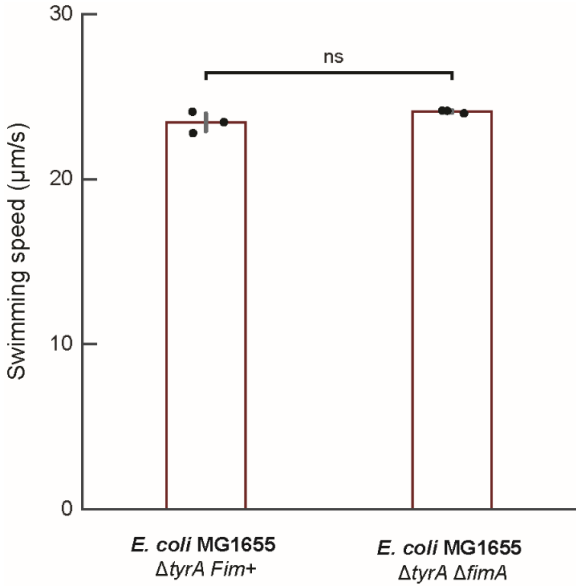

Figure 40 Fimbriation has no impact of motility

Swimming speed, measured as in Fig. S19, of fimbriated or fimbrialess *E. coli* cells grown in YNB fructose supplemented with CSM. ns from a *t*-test assuming equal variances between the samples for three biological replicates, each measuring at least fifty cell trajectories, indicated as dots.

The benefit of *E. coli* motility in the cross-feeding co-culture decreased and eventually inverted at lower shaking rates (Fig. 37B and Fig. 41), and both non-motile strains clearly outcompeted the motile one when the culture was grown in the absence of shaking, possibly as a consequence of co-sedimentation between non-motile *E. coli* and *S. cerevisiae* cells.

The slight but significant increase in fitness of *ΔcheY* compared to the chemotactic strain in the absence of shaking could also be due to its known [113] increased residence time at the surface (Fig. 38B,G,H), and therefore more frequent encounters with sedimented yeast cells.

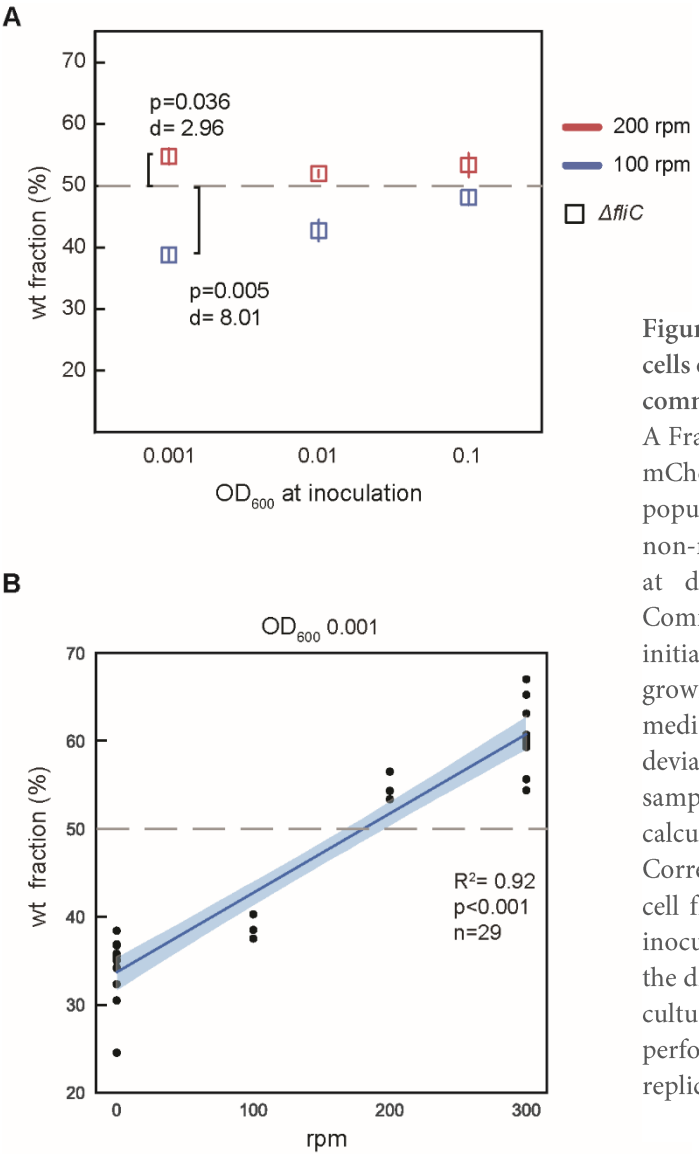

Figure 41 Dependence of fitness of motile cells on shaking rate in physically interacting community

A Fraction of motile *E. coli* cells (labeled with mCherry) compared to the total *E. coli* population in co-culture with sfGFP-labeled non-motile (ΔfliC) *E. coli* cells and with yeast at different shaking rates, as indicated. Communities were inoculated with different initial optical density (OD) as indicated and grown for 96 hours in YNB-glucose minimal medium. Error bars represent standard deviations of three biological replicates. One sample t-test was performed. Cohen´s d was calculated to quantify the effect size. B Correlation analysis between motile strain cell fractions in FliC+ and ΔfliC co-cultures inoculated with an initial OD600 of 0.001 and the different shaking rates at which they were cultured. The linear regression analysis was performed with a sample size of 29 biological replicates.

The beneficial effects of motility at high shaking rates required physical association between partners, since the beneficial effect of motility was no longer present when the competing strains were fimbrialess (Fig. 37C). It was also apparently related to cross-feeding, with the fraction of *ΔmotA* cells showing an average close to 50% once the community was grown in supplemented

medium (Fig. 37D). Cross-feeding was also necessary to observe the beneficial effect of *ΔmotA* sedimentation or of *ΔcheY* surface trapping under static conditions. The motile partner was outcompeted by *ΔfliC* knockout in the absence of cross-feeding, which is consistent with the general growth advantage this strain has due to the absence of burden derived by flagellar biosynthesis [110,114]. However, this fitness cost of motility was not observed in the non-aggregating cross-feeding community, where the wildtype and *ΔfliC* strains maintained an equal ratio, indicating that under these conditions the growth is not limited by protein biosynthesis.

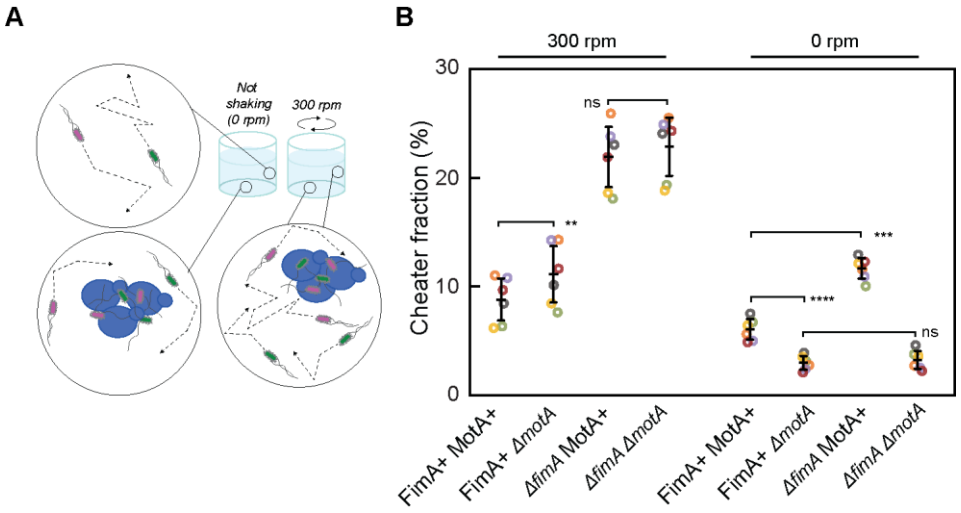

Figure 42 Impact of motility on *E. coli* partner fitness in presence of a cheater
A Schematic representation of the experimental setup to study effects of motility on the community in presence of a cheater.
B Cheater fraction from communities with a motile and fimbriated *E. coli* cheater (labeled with sfGFP) compared to the total *E. coli* population co-cultured with yeast and with an mCherry-labeled *E. coli* partner displaying different status of fimbriation and motility, as indicated. Communities were inoculated with an initial 50% cheater fraction and an initial optical density of 0.001 and grown for 96 hours under shaking (300 r.p.m) or without shaking (0 r.p.m) in YNB-fructose minimal medium. Error bars represent standard deviations of at six biological replicates represented as circles. ****p<0.0001, ***p<0.001, **p<0.01 from paired t-test.

Motility of the *E. coli* partner also increased its competitiveness against a non-cooperator strain in a turbulent environment. When a motile cheater was introduced, in equal amounts with an *E. coli* partner, in co-cultures with yeast (Fig. 42), motility of the partner modestly but significantly reduced cheater abundance when the culture was grown with shaking, but only when the partner was fimbriated. Consistent with the results above (Fig. 37B), non-motile *ΔmotA* strain showed higher fitness in the absence of shaking, again likely due to the co-sedimentation with yeast. Comparable results were also obtained when the cheater was non-motile (Fig. 43A). The positive

effect of partner motility was abolished when the media was supplemented with CSM, corroborating its dependence on cross-feeding (Fig. 43B).

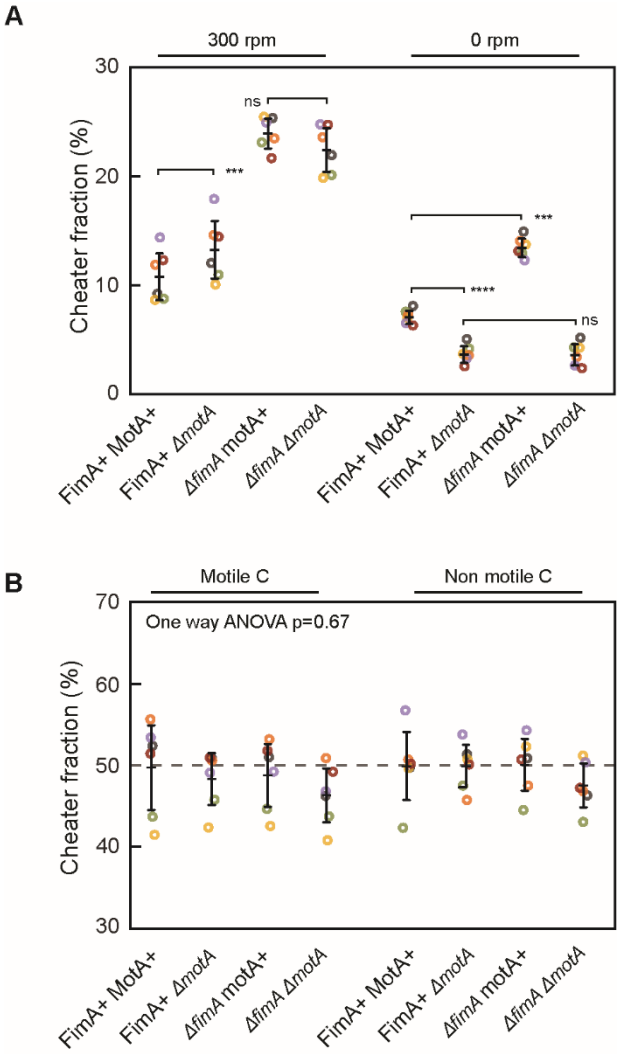

Figure 43 Effects of motility on communities containing cheater with or without cross feeding
A Cheater fraction within the total *E. coli* population in cross-feeding communities containing a non-motile and fimbriated *E. coli* cheater (labeled with sfGFP) co-cultured with yeast and with an mCherry-labeled *E. coli* partner displaying different status of fimbriation and motility, as indicated. Communities were inoculated with an initial 50% cheater fraction and an initial optical density of 0.001, and grown for 96 hours under shaking (300 r.p.m) or without shaking (0 r.p.m) in YNB-fructose minimal medium. Error bars are standard deviations of at six biological replicates represented as circles. ****p<0.0001, ***p<0.001, **p<0.01 from paired t-test.
B Cheater fraction in communities in absence of cross feeding, having either motile or non-motile fimbriated cheater strains (labeled "C"), in combination with indicated *E. coli* partner cells, inoculated with a total initial OD of 0.001 and grown in YNB fructose supplemented with CSM under shaking (300 r.p.m). p value from a one-way ANOVA test.

3. Discussion and outlook

3.1. Evolution of microbial communities

Understanding how metabolic mutualism can emerge within microbial communities represents a key question in microbial ecology. Its relevance derives not only from the fact that cooperation between microbes allows fascinating parallelism with phenomena occurring in animal communities and even those within the human society that can be described by socio-economic models[115] but also because, under an evolutionary perspective, it implies that under certain circumstances, the abandonment of an autonomous lifestyle towards a dependent one is favoured. Furthermore, metabolic mutualistic interactions might have guided the emergence of symbionts and eukaryotic cells[116], thus representing a crucial step leading to the appearance of more complex cellular systems. Consequently, several studies have focused their attention on the initial steps guiding the appearance of such interdependence. These reported the emergence of auxotrophies in microorganisms grown in rich media[50], the development of bidirectional interdependences between organisms originally linked by unidirectional cross-feeding[52] and also the reinforcement of these established interactions by, for example, an active overproduction of the traded building blocks[54], thus providing empirical evidence on how metabolic interdependencies can originate. However, both eco-evolutionary models describing the emergence of mutualism[25,41] and the existence of symbiotic communities relying on the exchange of different metabolites between partners[25] suggest that the appearance and reinforcement of interactions based on a single compound is just the first milestone. Subsequently, it should be followed by the acquisition of additional interdependences, thus strengthening the metabolic entanglement between interacting partners. Nonetheless, for these later stages of the evolution of metabolic dependencies, empirical evidence of such transitions is scarce.

In order to investigate this, we generated mutualistic cross-feeding communities by co-culturing auxotroph pairs of *S. cerevisiae* and *E. coli*. When grown together, prototroph strains of these two organisms were previously described to display a competitive behaviour, thus resulting in unstable communities [117]. Nonetheless, we were able to obtain viable and stable communities by exploiting both the optimization of the growth conditions and media through an adjustment of pH and the introduction of a buffering component but also by forcing cooperation by the use of auxotrophic strains of the two organisms. Several of these communities evolved by repeatedly transferring the

co-cultures into fresh media. In most cases, one of the two partners restored prototrophy, thus leading either to the extinction of the other community member or to partner coexistence, potentially supported by a unidirectional cross-feeding. Such "re-gain" of function could possibly be derived either from a rewiring of metabolic fluxes able to circumvent the catabolic blockade determined by the deletion carried by the strain[118], or the result of an improvement in the activity of promiscuous enzymes[119]. Notably, the reacquisition of metabolic autonomy proves not only the tremendous flexibility of the metabolic network but also the potentially high degree of redundancy that it contains[120,121]. Interestingly, while one of the *E. coli* strain used in our evolutionary experiment (*ΔtyrA*) regained prototrophy in all the evolved lines when co-evolved with the *S. cerevisiae* tryptophan, other studies reported the maintenance of the same auxotrophy when the strain was grown together with an *E. coli* strain auxotroph for tryptophan, thus performing similar metabolic trades but with partners belonging to different species[54]. This might imply that not only the traded metabolite but also the growth conditions influence the tendency to reacquire prototrophy.

Despite such high resilience of the metabolic network, which resulted in the reacquisition of prototrophy in several lines, we observed that in one specific community both members retained their auxotrophy throughout the evolution while the consortium performances drastically increased. This community comprised the *S. cerevisiae Δarg1* and the *E. coli ΔhisG* strains. While NGS analysis performed on these lines revealed the presence of multiple genetic alterations in both organisms, we focused on a small set of genetic regions in the two partners showing mutations at high frequencies among most of the lines. Notably, *S. cerevisiae* presented a higher number of mutations compared to *E. coli*. This could be explained either by a difference in mutation rate[101,102] and genome size between *E. coli* and *S. cerevisiae* but also by a generally higher amount of beneficial mutations affecting the yeast partner.

Some of the most recurrent genetic alterations in *E. coli* were a set of point mutations at the promoter level of *hisJQMP*, an operon encoding for an ABC transporter involved in arginine and histidine import. These mutations were proven to increase transcription and, thus, potentially result in a higher histidine uptake. The second group of recurrent mutations was represented by nonsense mutations or interruptions via transposon-like sequences of *argR*, a gene encoding a transcription factor involved in the repression of different genes, including those belonging to the arginine biosynthetic pathway and the *hisJQMP* operon[99,100]. *argR* interruptions could provide a benefit either by increasing the production of arginine and/or by enhancing the uptake of histidine.

While the potential effect on histidine uptake was suggested by the enhanced transcription of the *hisJQMP* promoter observed for the *argR* deleted mutant, in previous studies, the single deletion of *argR* on an *E. coli* wt background did not lead to arginine overproduction[122]. Nonetheless, since differences both in the growth conditions and the strain used (our ancestral has an additional *ΔhisG* mutation) are present, and these might cause a rewiring of fluxes, direct measurements of metabolite levels are required to assess for any arginine overproduction.

Even though additional mutations were detected from the sequencing analysis and might play a relevant role in metabolite uptake or secretion, such as the point mutations identified on *ompF*, or might have an impact on resistance towards oxidative stress, such as mutations in *rsxC*, additional investigations are required to specifically assess for their impact on *E. coli* fitness.

For what concerns *S. cerevisiae*, the first set of recurrent nonsense mutations was observed on *ecm21*. This encodes for a ubiquitin ligase adaptor regulating the internalization and degradation of diverse amino acids transporters under nitrogen starvation [103], including the arginine permease *can1*. Thus, its interruption should guarantee a higher uptake of amino acids from the extracellular environment. The second highly-frequent and recurrent target of non-sense mutations in yeast was *gdh1*. This encodes for one of the two NADPH-dependent glutamate dehydrogenases present in *S. cerevisiae*[123]. This enzyme plays a key role in direct ammonium assimilation when glucose is the main carbon source[124]. Consequently, its inactivation resulted in a reduced ability of all the evolved lines to assimilate ammonium. Additional passages of one of those evolved lines caused a further reduction in ammonium assimilation. This could be explained by the inactivation of another gene, *glt1,* coding for an enzyme crucial for the GOGAT pathway [125]. This is the second main pathway in *S. cerevisiae* responsible for direct ammonium assimilation. The comparable fitness observed from direct competition between the *S. cerevisiae Δecm21 Δgdh1* double mutant and the ancestral yeast under arginine limiting conditions and the fact that the double mutant outcompetes the ancestral when *E. coli* is introduced in the community indicate that the reduction in direct ammonium assimilation derived by the inactivation of *gdh1,* and potentially also *glt1,* might be compensated by an enhanced scavenging ability of the evolved lines towards arginine and potentially other nitrogen-containing molecules released by *E. coli*. If confirmed, this would prove a rapid and dramatic increase in interdependencies between partners. However, additional experiments are required to confirm this hypothesis and specifically to quantify to which extent direct nitrogen assimilation is lost or, symmetrically, to which extent the evolved yeast relies on the partner for its nitrogen metabolism. This would be done both through direct measurements of metabolites and

nitrogen fluxes and also by confirming the absence of alternative direct nitrogen assimilatory pathways under cross-feeding conditions (e.g. activation *gdh3*). We would also proceed with the identification of the underlying metabolic and molecular processes conferring a fitness advantage from such reduction.

As observed for the evolved *E. coli* partner, additional mutations were also observed in the case of *S. cerevisiae*. Particularly abundant were mutations in *flo1* and *flo9*. These are genes encoding for proteins involved in flocculation, and their modification might alter the aggregation ability of the yeast partner. Furthermore, a possible inactivation of *mtl1* was observed in several lines. This is a membrane protein involved in stress response to various stimuli connected to cell wall integrity. Its inactivation might therefore reduce the stress response of the evolved yeast. However, also for these mutations, additional investigations are required to assess their impact on yeast and, potentially, community fitness.

Eventually, we aimed to recapitulate the temporal dynamics underlying the fixation of these mutations by sequencing the evolved organisms at different evolutionary moments. This revealed that these high-frequency mutations display a specific order of appearance, which was reproducible among all the evolved replicates. The introduction of these four mutations in the ancestral organisms, followed by co-culture experiments, revealed that they account for a good fraction of the growth phenotypes observed in the evolved communities. We further proceed with the analysis of the effect caused by each mutation on growth, either as individual mutations or in combination with the others, and this showed that they have either a positive or negative impact on community growth, and this is caused by either a mutualistic or an exploitative behavior conferred on the respective organism by these mutations. From this screen, an epistatic interaction was observed for the mutations causing increased transcription of the histidine transporters and *argR*. In fact, while the introduction of the *hisJQMP* promoter mutation in the *E. coli* ancestral strain leads to impaired community growth, regardless of the genotype of the *S. cerevisiae* partner, its co-occurrence with the inactivation of the *argR* gene resulted in a neutral effect for the yeast partner but enabled a growth boost to the *E. coli* partner.

The presence of a facultative mutualistic partnership in other bipartite systems was shown to change the extent of the benefit provided by a specific mutation without altering its fitness trade-off (the sign of the impact on fitness)[126]. Conversely, in our community that relies on an obligate interaction, evolution led to the fixation of mutations which are detrimental under monoculture conditions, as shown by direct competition between evolved and ancestral organisms in

supplemented media. This suggests that the presence of an obligate interaction between partners can impact the pool of beneficial mutations available to the community members, thus confirming the crucial role of interactions, and specifically obligate metabolic mutualism, on the evolution of communities.

Besides providing important insights into the evolution of symbiosis, our results might have practical implications in the generation of strains for the bioproduction of value-added compounds. In fact, since the overproduction of metabolites can cause a substantial burden on growth, a boost in their synthesis cannot be easily achieved via direct evolution, while extensive engineering and laborious fine-tuning of fluxes are required to obtain a suitable candidate for bulk production[122]. Conversely, the construction of an obligate mutualistic community relying on the trade of the desired product between interacting partners and its evolution via serial passages has been proven to generate strains with enhanced ability in the production and secretion of the value-added compound[127], thus confirming the use of communities as an appealing alternative to the classic mono strain metabolic engineering strategy.

3.2. Impact of aggregation and motility on fitness

Microbial communities relying on metabolite exchange have been previously studied using different mutants of the same species [38,94,128] or natural isolates [129,130], either in a dispersed liquid culture [94] or under spatial assortment resulting from growth on a surface or in a microfluidic device [63,69]. Here we investigated the impact of the direct physical association and co-aggregation between the cooperating partners and of the partner motility, which are frequently observed in natural suspended communities growing in turbulent aquatic environments [80,131,132], using an engineered mutualistic consortium between *S. cerevisiae* and *E. coli* auxotrophs respectively for tryptophan and tyrosine.

We observed that physical association between partners and the resuting co-aggregation, although moderately reducing the overall community growth, provides competitive fitness benefit to the E. coli partner. This effect is likely explained by the fact that proximity ensures preferential access of associated partners to the exchanged metabolites within co-aggregates. Proximity dependence of cross-feeding has been previously observed for communities grown on solid surfaces [78] or in microfluidic devices[63], where long-range metabolite gradients can be stably maintained. Here we demonstrated that the benefit of physical association can also be observed in a turbulent environment. Since our synthetic community is not likely to rely on a specific matrix that could

retain secreted metabolites[78,133–135] or on direct cytoplasmic channeling of metabolites as nanotubes[77], the efficiency of amino acid uptake by the yeast-associated *E. coli* appears to be sufficiently high to ensure that metabolites are locally consumed by the associated partners before being dispersed into the environment. Physical association and the subsequent formation of mixed aggregates might further enhance partner intermixing, which is crucial for mutualistic interactions because allows an even distribution of exchanged metabolites between partners[71].

Besides its immediate benefit to the bacterial partner, physical association partly protects the community as a whole against invasion by a non-cooperating bacterial cheater strain that consumes but does not share metabolites. Although under our conditions such a cheater establishes itself in the community at a relatively low frequency, it can nevertheless affect community growth and causes community collapse under a semi-continuous growth regime. This is consistent with the theoretically predicted and experimentally observed tragedy of the commons [43,58–60,136,137], and it contrasts with the coexistence between the partner and cheater described in previous studies [43,138–141]. We hypothesize that the decrease in cheater abundance and the delayed community collapse in the presence of the fimbriated bacterial partner result from faster growth of aggregates that contain fewer cheater cells, since the non-cooperating strain makes no contribution to the growth of the aggregate. Such effect, that has been previously theorized [142] and described as analogous to the Simpsons paradox [143], could potentially lead to the overall decrease in the cheater abundance in the community. This beneficial protective effect of co-aggregation on the community in presence of a non-cooperator overweighs the burden imposed on the community growth.

The fitness advantages provided by the co-adhesion mediated by fimbriation in suspended co-culture is no longer observed when communities are grown on a solid surface as an agarose plate. This might be caused by the segregation between *E. coli* strains provided by the spatial structure of the colony [70] which might reduce their direct competition while ensuring that resources are only shared locally even without the need for direct physical association between partners. This segregation may also negatively affect growth of non-cooperating community members, as already reported previously [64], and observed under our experimental conditions where a lower fraction of cheater cells within the colony community was observed compared to the non-aggregating liquid culture.

Under turbulence, partners engaged in metabolic trades further profited from motility, which allowed them to outcompete the non-motile partners and also to reduce invasion by a cheater strain. Consistent with previous studies[110], although flagella biosynthesis showed a pronounced

burden on *E. coli* growth in supplemented medium, we observed that motility has a net benefit under cross-feeding conditions. This advantage provided by motility could be explained by the increased encounter rate and therefore of association between fimbriated bacteria and yeast cells that are kept in suspension by mixing, as previously described for interactions between motile bacteria and suspended particles [144,145]. In aquatic environments swimming remains faster than stirring at the spatial scales below 0.1-1 mm [146], implying that motility can provide an enhancement in local cell-cell encounters even when the liquid is mixed. Consistently, motility provided an advantage only at low initial cell densities, comparable to the ones observed in aquatic environments[111], where locating partners is particularly challenging and motility could indeed represent a key strategy to increase the partners encounter rate. Another source for an enhancement in attachment might derive from the non-homogeneous distribution of motile organisms which can be induced by turbulence[147,148]. In contrast, in the static co-culture non-motile bacteria might have an advantage regardless of the physical association because of their co-sedimentation with yeast which might guarantee a closer proximity to the partner, and therefore the amino acid source, in the sessile community of the sediment.

4. Concluding remarks

Microbial communities are widespread in natural habitats and can establish diverse interactions with other partners, including metabolic trades. Mutualistic cross-feeding of metabolites is a subset of these interactions relying upon the obligate exchange of essential metabolites between partners otherwise unable to produce the traded compounds.

The main goals of this work were three. Firstly, we aimed to design, engineer and build a synthetic consortium based on bidirectional cross-feeding. This was successfully achieved via the co-culture of auxotrophic strains of the bacterium *Escherichia coli* and the budding yeast *Saccharomyces cerevisiae* in a minimal media optimized for the co-culture of these two microorganisms.

We further proceed by evolving them through multiple growth and dilution cycles. This resulted in a substantial enhancement in the growth performances of one of the tested communities. Such improvement was related to the fixation of mutations which appear detrimental under monoculture conditions, thus suggesting that the presence of preexisting interactions can alter the pool of beneficial mutations available for each partner. Furthermore, most indications suggest that the yeast strain strongly reduced or even lost its direct ammonium assimilation, which might be compensated by the supply of assimilated nitrogen from *E. coli*, which would be the source of most of the nitrogen for the yeast partner.

Secondly, we investigated the role of cell adhesion and aggregation, motility and chemotaxis in these engineered communities. We demonstrated that direct physical association and partner motility can provide fitness benefits to one or both partners in the mutualistic community growing in a turbulent environment, which outweigh their costs at a low initial density of the co-culture and in the presence of non-cooperators. Since low cell densities and the presence of competitors are likely to be common in aquatic environments, we propose that these benefits might explain the widespread presence of mechanisms involved in cell-cell adhesion and motility in natural pelagic communities [79,80].

5. Materials and methods

5.1. Growth conditions and main methods

- **Strain construction**

E. coli auxotrophic strains were obtained from the Keio collection[95]. The rest of the *E. coli* mutant strains were derived from BW25113 or, for motility studies, MG1655. Mutant strains were generated via λ-red recombinase using the pSIJ8 plasmid. *E. coli* strains in the co-culture were labelled either with a sfGFP-expressing plasmid (pTrc99A:sfGFP: pNB1) or with an mCherry-expressing plasmid (pTrc99A:mCherry: pOB2), both inducible by isopropyl-β-d-thiogalactopyranoside (IPTG). For co-cultures grown in minimal media, sufficient expression of fluorescent markers was observed even without IPTG induction, but 10 μM IPTG was used for cultures grown in supplemented media. All *S. cerevisiae* strains were obtained from the gene knockout collection (Dharmacon, Lafayette, Colorado, US) derived from the BY4741 strain. The his3Δ1 auxotrophy of this strain was rescued by an insertion restoring histidine prototrophy and introducing either mTurquoise2 or mNeonGreen as a fluorescent marker. Further gene deletions in the yeast strains were obtained via homologous recombination with the protocol described below. Yeast strains carrying either one or the other fluorescent markers were used for competition experiments.

- ***E. coli* KO generation**

Cassettes containing kanR were amplified from the Keio strains carrying the desired KO using the respective primers reported in the primer list. Primers were designed to generate homology arms of approx. 100bp on both sides of the resistance cassette. KO were then generated with the plasmid pSIJ8, a plasmid carrying both the lambda red recombinase system and the flippase required to remove the antibiotic cassette. The protocol followed is the one described in[149]. When required, a concentration of 50 mM rhamnose was used to induce the flippase activity.

- ***E. coli* gene replacement**

(this protocol and the plasmids used were kindly provided by the lab of Prof. John S. Parkinson)

Electrocompetent *E. coli* cells carrying the pKD46 plasmids were transformed with a cassette containing the neo gene and the ccdB gene under the regulation of a rhamnose promoter flanked by 50 bp of homology arm targeting the desired region in the *E. coli* genome. After the

electroporation, cells were recovered for 5h on SOC and subsequently plated on LB+ Amp100+Kan50 plates and incubated overnight at 30 degrees. Positive cells were then transformed via electroporation with the insertion cassette carrying the desired mutation and, after recovery of 5h in SOC, cells were plated on rhamnose minimal plates and incubated for 4 days at 37 degrees. Potential candidates were screened by amplifying the replaced region by Q5 PCR followed by Sanger Sequencing.

- ***S. cerevisiae* KO generation**

Linear recombination fragments were obtained through the amplification of the resistance cassette from the pH3FS and the appropriate plasmids. The amplified fragment is then constituted by the HygB resistance flanked by *loxP* sites and having at both the 5' and 3' terminal regions homology arms 50 bp long.

These cassettes were integrated into the yeast genome via chemical transformation (see protocol above) and transformation products were plated on YPD plates enriched with HygB. After a two days incubation, the correct insertion of the cassette was verified via colony PCR. Colonies were then inoculated in YPD and transformed with the Cre carrying plasmid (pPL5071_TEF1*-Cre_URA3) and transformation products plated on selective plates for Ura (CSM Ura-) and incubated at 30 degrees for 48 h. Successful cassette removal was verified via colony PCR. Positive candidates were inoculated in complete YNB minimal media and grown at 30 degrees for 24h to allow plasmid loss. Grown cultures were then streaked on complete minimal media plates supplemented with 5-FOA to isolate colonies that had lost the plasmid.

- **Growth conditions**

For pre-cultures, *S. cerevisiae* cells were streaked from glycerol stocks on yeast extract peptone dextrose (YPD) plates supplemented with the appropriate antibiotic and incubated at 30°C for 48 h. Four to six colonies were inoculated from each plate in 5 mL YPD supplemented with the appropriate antibiotic, and cells were grown at 30°C for 16-18 h with shaking at 200r.p.m. *E. coli* pre-cultures were inoculated directly from glycerol stocks in 5 mL lysogeny broth (LB) with the appropriate antibiotic and grown at 37°C for 16-18 h with shaking at 200r.p.m.

For both organisms, cells from 2 mL pre-culture were washed twice with phosphate-buffered saline (PBS), resuspended in 1 mL PBS and incubated for 5 h, at 30°C degrees for *S. cerevisiae* and 37°C for *E. coli.* Unless indicated otherwise, cells were diluted to a total OD600 of 0.05 for *S. cerevisiae*

and a total of 0.025 (or 0.05 for the evolutionary experiments) for *E. coli* partner strain(s), values referring to a 1 cm cuvette. When the *E. coli* cheater was introduced into the community, an initial inoculum of 0.025 (for 50% inoculation) or 0.011 (for 30% inoculation) of this strain was further added to the culture. Growth and competition assays were performed at 30°C with shaking at 200r.p.m. in 24-well microtiter plates (Greiner Bio-One, Frickenhausen, Germany) in 1 mL low fluorescence (LoFlo) yeast nitrogen base (YNB) minimal media (Formedium, Swaffham, UK) buffered with 100 mM 2-(N-morpholino) ethanesulfonic acid (MES) (Roth, Karlsruhe, Germany) at pH 6.15 and with 2% D-glucose, or 1% D-fructose for the motility assay, as carbon source. For the cross-feeding experiments the media was supplemented with a mixture of 100 mg/L L-leucine, 20 mg/L L-methionine and 20 mg/L uracil to complement the auxotrophies present in the *S. cerevisiae* background strain. For the controls experiments with fully supplemented media two mixtures were used: either the complete supplement mixture (CSM, a mixture of diverse amino acids, Foremedium) enriched with 20 mg/L L-serine or a mixture of all the twenty amino together with alanine and uracil (see protocols). Concentrations used are indicated in the figures. Where indicated, 4% D-(+)-mannose was introduced into the media. For the co-cultures grown in a semi-continuous mode, 500 µL of each culture were transferred to a new well containing 500 µL of fresh media every 24 h for 10 days. For all the experiments, growth was measured using a plate reader (m200 Infinite Pro, Tecan, Männedorf, Switzerland). When present, clumps were disrupted prior to measurements or culture transfer by pipetting the sample up and down 10 times with a 1 mL pipette.

For the evolutionary experiments, 100 µL of each culture were transferred to a new well containing 900 µL of fresh media every seven days (one transfer was done after 8 days of culture). In order to measure growth, 100 µL from each well were transferred to a well from a 96 wells plate containing 100 µL of PBS enriched with 4% mannose. Samples were pipetted up and down 10 times with a 300 µL multipipette prior to plate reader measurements (m200 Infinite Pro, Tecan, Männedorf, Switzerland) to disrupt clumps.

For plate reader growth experiments, 48 wells plates were used. Plates were filled with 300 µL of culture and subsequently 300 µL of light mineral oil were gently added on top to prevent evaporation. The OD600 was measured every 20 minutes and, between measurements, plates were shaken with a speed set to 2.5 alternating 5 minutes of linear and 5 minutes of orbital shaking.

Colony assays were performed on minimal media plates containing 1% agarose where 2 µL of cell mixture with the same initial concentration as for liquid cultures were deposited. Plates were incubated at 30°C for ten days to reach the maximal colony size.

- **Competition experiment**

For the competition experiments, the organisms tested were grown as described in in the previous section. According to the specific experiment, the inoculum for each competing organism was set to half compared to the one used for growth experiments (*S. cerevisiae* OD= 0.025 for each competing strain, *E. coli* 0.0125 (impact of adhesion and motility) and 0.025 (evolutionary experiment). Each competing organism was labelled with a different fluorescent marker (mCherry or sfGFP for *E. coli* and mNeonGreen or mTurquoise2 for *S. cerevisiae*) and strain abundance was measured via flow cytometry exploiting both the difference in scattering properties between the two organisms and the different fluorescent markers expressed by the competing organisms.

- ***his* reporter plasmid generation**

Reporter plasmids aimed to assess the transcriptional activity of the promoter of the hisJMPQ operon in both its ancestral and mutated versions were obtained via Gibson assembly using pUA66 as vector. The promoter regions were amplified from colonies carrying the desired version of the promoter with primers Fw: CCTTTCGTCTTCACCTCGAGacggcacctacgacaagatg and rv: TCTCCTTCTTAAATCTAGAGGATCCttaaaccagagagagcgatagcac while the backbone was obtained via amplification from pU66A with primers: Fw GGATCCTCTAGATTTAAGAAGGAGA and Rv CCTTTCGTCTTCACCTCGAG

- **Partners isolation from co-culture**

In order to isolate each organism from the consortium, co cultures were streaked on selective plates. These were YPD supplemented with 100 mg/l streptomycin or LB supplemented with 25 mg/l nystatin to isolate *S. cerevisiae* and *E. coli* respectively. All the colonies obtained from each plate were then pooled together to start a mono-organism culture that was used to prepare cryo-stocks. This was done in order to maintain the population variability of the isolated lines as close as possible to the one present in the community.

- **Aggregation assay**

E. coli and *S. cerevisiae* cultures were grown as described in materials and methods. Cells were washed twice with PBS and resuspended in 1 mL PBS. After that, bacterial and yeast cells were mixed at a final OD_{600} 0.5 for *S. cerevisiae* and 0.2 for *E. coli* and incubated for 1 h at room temperature in a 24-well plate with shaking (200 r.p.m.) before microscopy imaging.

- ***fim* promoter orientation assay**

In order to verify the orientation of the fimbriae operon (*fim*), a procedure similar to the one described in [150] was followed. Specifically, co-cultures were grown as described in the growth conditions section for 72 h, followed by genome extraction using the DNeasy Blood & Tissue Kit (Quiagen, Hilden, Germany). From this, 1 µL was used as PCR template using the Q5 polymerase (New England Biolabs, Frankfurt am Main, Germany) and with primers P1 (5'-AGTAATGCTGCTCGTTTTGC-3') and P2 (5'-GCTGTAGAACTGAGGGACAG-3'). PCR products were then purified (Zymo research Europe GMBH, Freiburg, Germany) and digested for 2 h with *Sna*BI (New England Biolabs, Frankfurt am Main, Germany). Subsequently, samples were separated using gel electrophoresis in a 2% agarose. Band intensity analyses were performed using ImageJ [151].

- **Cell tracking**

E. coli cells were inoculated in YNB+ 1% fructose supplemented with CSM and incubated for 12 h at 30 degrees. Cells were then diluted to an OD between 0.01 and 0.005, and a drop of 5 µL was enclosed between two coverslips in a compartment created with grease. Movies were acquired with a phase contrast microscope at 10x magnification (NA = 0.3) and a Mikrotron Eosens camera (1 px = 0.7 µm) running at 50 frames per second (fps) for 2000 frames. Image analysis, Z-stack projections, particle tracking and image correlation analysis, were performed using ImageJ [151] and custom-made algorithms run as plugins in ImageJ. As previously described[113], the radius of gyration $R_i = \langle\left(\left(r_i(t)\right) - \left(r_i(t)\right)_t\right)^2\rangle_t / T$ was used to sort swimmers from non-swimmers setting a threshold to 0.2px²/fr and determine the fraction of motile cells. T represent the trajectory duration. For these, velocity was calculated as $\vec{v} = \frac{1}{\Delta t}\sum_{t-\Delta t/2}^{t+\Delta t/2}\Delta\vec{r}$ and divided by the average displacement $\vec{v} = \frac{1}{\Delta t}\sum_{t-\Delta t/2}^{t+\Delta t/2}|\overrightarrow{\Delta r}|$ with Δt set to 0.2s. A threshold was then used to distinguish putative runs from tumbles. Each tumble must follow the follow $\sum_t (r - r_{th})^2 > 3v_{run}\, t^2/2$, with

v_{run} defined as the variance of r during the run. Tracking data from swimmer cells were then analyzed to calculate tumbling rate, average swimming speed and average residence time.

- **Statistical analysis**

Both the statistical tests used and sample size (n) are specified in the figure legends. In all cases, n refers to the number of independent co-cultures derived from independent precultures of single strains. Technical replicates are defined as independent co-cultures derived from the same precultures of single strains. For pairwise comparisons asterisks indicates statistical difference (*p<0.05, **p<0.01, ***p<0.001, ****p<0.0001). For boxplots, the internal line indicates the median of values, while the regions of the box below and above indicate respectively the 25th and 75th percentiles. Whiskers extend up to 1.5x the interquartile range from the 25th to the 75th percentile. For line plots, data is displayed as mean values ± S.D. confidence interval. For scatter plots, the central black bars represent the mean value and the whiskers extend to ± S.D as confidential interval, while circles indicate the biological replicates. Statistical analyses (*t*-test one-way ANOVA) were performed using either JupyterLab (ANACONDA) or Microsoft Excel. Correlation analysis were performed using the data analysis add-in of Microsoft Excel and plotted using the regplot function of the seaborn package JupyterLab (ANACONDA). The shadow part represents 95% confidence interval while the lines represent the linear regression fit.

- **Calculations of growth parameters**

Mean growth rate values for the specific time interval from growth curves obtained as single point measurements were calculated as the difference between the ln(OD600) measured respectively at 25 h and 16 h divided by the time interval expressed in hours for growth curves. For growth curved obtained directly from plated incubated in the plate reader, the max growth rates are calculated as the max of the all the slopes calculated as described before but for time intervals of 2h and calculated per each point of the curve. Doubling times are simply the reciprocal of it multiplied by ln(2).

The relative fitness was calculated as the difference between the ln() of the cell count of the mutant at the end of the experiment and the inoculation all divided by the ln() of the same difference calculated for the ancestral strain.

- **Sequencing data analysis**

Sequence analysis was performed with BRESEQ. While for *E. coli* the program was run in polymorphism mode, for yeast the frequency cut off was initially adjusted to 0.8 for the first analysis and subsequently relaxed to 0.05.

- **Flow cytometry**

Flow cytometry was performed with BD LSR Fortessa SORP cell analyzer (BD Biosciences, Heidelberg, Germany). GFP fluorescence was detected using a 488 nm laser line combined with a 510/20 BP filter. mTurquoise2 fluorescence was measured using a 447 nm laser line combined with a 470/15BP filter. mCherry fluorescence was measured using a 561 nm laser line combined with 632/22 BP filter. *S. cerevisiae* and *E. coli* populations were distinguished using forward scatter (FSC) and side scatter (SSC). *E. coli* strains were further distinguished according to their respective fluorescent labelling (mCherry or GFP). Before the measurements, cell aggregates were disrupted by pipetting as described above, followed by a dilution in a ratio 1:10 in PBS supplemented with 4% mannose (1 mL final volume). Measurements were performed using the BD High Throughput Sampler (HTS) with a fixed flow rate set at 1 µL/s for an acquisition time of 20 s with samples diluted to a concentration typically of 10^3–10^4 events per second in PBS supplemented with 4% mannose. Dilution rates, flow rate and sampling time were then used to infer the abundance of cells in the defined volume (20 µL). Flow cytometry results were analyzed using FlowJo (BD Biosciences). An example of the gating strategy used can be found in Appendix Fig. S12. Furthermore, both imaging and flow cytometry data show the effectiveness of the pipetting strategy adopted to desegregate yeast-bacteria aggregates.

5.2. Media, antibiotics and inducers

- **Luria broth (LB) medium and plates**

10 g Tryptone
5 g Yeast extract
5 g NaCl
800 ml ddH2O

The pH was adjusted to 7 and ddH2O was added up to a final total volume of 1 L. The media was then autoclaved at 120 degrees for 20 min. For LB agar plates, 15 g of agar were added to 1 L of LB liquid medium before the autoclavation step.

- **Yeast peptone dextrose (YPD) medium and plates**

50g YPD powder

ddH2O was added up to a final total volume of 1 L. The media was then autoclaved at 120 degrees for 20 min. For YPD agar plates, 15 g of agar were added to 1 L of YPD liquid medium before the autoclavation step.

- **Super optimal broth (SOB) medium**

20 g Bacto tryptone
5 g Bacto yeast extract
10 mM NaCl
2.5 mM KCl

800 ml ddH2O

the pH was adjusted to 7 and ddH2O was added up to a final total volume of 1 L. The media was then autoclaved at 120 degrees for 20 min. After the autoclavation step, the following components were added:

10 mM $MgCl_2$
10 mM $MgSO_4$

- **Super optimal broth with catabolite repression (SOC) medium**

20 mM glucose in SOB media.

- **M9 salts (5X)**

34 g Na_2HPO_4 (64 g Na_2HPO_4 x 7 H_2O)
15 g KH_2PO_4
2.5 g NaCl
5 g NH_4Cl

dissolve in 1 l ddH_2O and autoclave

- **100X Trace elements**

5 g EDTA
0.83 g $FeCl_3$-$6H_2O$
84 mg $ZnCl_2$
13 mg $CuCl_2$-$2H_2O$
10 mg $CoCl_2$-$2H_2O$
10 mg H_3BO_3
1.6 mg $MnCl_2$-$4H_2O$
Up to 1L ddH_2O

Dissolve EDTA in 850 ml ddH_2O and adjust the pH to 7.5 with NaOH. After that add all the other components and bring to a final volume of 1l. Subsequently, proceed with filtration.

- **M9 medium for growth experiments**

50 ml 5x M9 salts (autoclaved)
500 µl 1 M $MgSO_4$ (autoclaved)
250 µl 0.1 M $CaCl_2$ (autoclaved)
250 µl 1 mg/ml biotin
250 µl 1 mg/ml thiamin
2.5 ml 100x trace elements
X ml required carbon source
Up to 250 ml ddH_2O

- **Yeast Nitrogen Base (YNB)**

6.9 g Yeast Nitrogen Base w/o Amino acids LoFlo
20 g Glucose
100 ml 1M MES pH 6.15 (for cross-feeding experiments)
100 ml Drop out solution (mixture of amino acids required to complement yeast auxotrophies)
Adjust to pH 6.15 with NaOH
Up to 1l ddH_2O

When necessary, the media was supplemented with CSM, Complete amino acid mix, or Mannose.

- **Selective YNB minimal media plates**

6.9 g Yeast Nitrogen Base w/o Amino acids LoFlo
15 g Agar
Fill up to 800 ml with ddH2O and autoclave

Add the following solutions

100 ml 20% w/v Glucose solution
100 ml Drop out solution (either CSM Ura^- or CSM complete+5-FoA)

- **Complete amino acid mix (1000X)**

1g/l each amino acid, 200 mg/l Adenine, 200 mg/l Uracil.
Add ddH2O up to 1L. Adjust pH to 11.5 with NaOH.

- **1X TSS**

5g PEG 3350
1.5 mL 1M MgCl2 (or 0.30g MgCl2*6H20)
2.5 mL DMSO
Add LB to 50 mL

Filter sterilize (0.22 µm filter)

- **Rhamnose minimal plates**

A) 15g agar in 500 ml H2O (2L flask)

B) Combine in 500 ml H2O (1L flask)

K2HPO4 . 3H2O 14.7g

KH2PO4 4.8g

(NH4)2SO4 2.0g

Autoclave A and B

When cool enough, add to B

thiamine HCl 1 ml from 10 mg/ml stock

$MgCl_2$	1 ml from 1M stock
Amino acids	10 ml from 100 mM stock
Rhamnose	10 ml from 20% stock

Combine A+B, mix and pour plates.

- **Antibiotic and inducers stock solutions**

Ampicillin (Amp): 100 mg/mL in ddH_2O (1000X)

Kanamycin (Kan): 50 mg/mL in ddH_2O (1000X)

Nystatin (Nys): 25 mg/mL in DMSO (500X)

Geneticin (G418): 300 mg/ml in ddH_2O (1000X)

Hygromycin (HygB): 240 mg/ml in ddH_2O (1000X)

0.1 M IPTG in ddH_2O

10 % L-Arabinose in ddH_2O

1.5 M Rhamnose in ddH_2O

5.3. Buffers

- **Tris-Acetate-EDTA buffer (TAE– 50 x)**

242 g Tris base
57.1g Glacial acetic acid
100 mL 0.5 M EDTA, pH 8
0.1 mL 10 mM Methionine
1 mL 90% lactic acid
ddH_2O was added up to a total volume of 1 L.

- **10x Phosphate-buffered saline (PBS)**

80 g NaCl

2 g KCl

2 g KH_2PO_4

11.5 g Na_2HPO_4

Adjust with HCl to pH 7.4

Add ddH2O to 1 l

Sterilization via autoclavation

- **High-density-solution (Glycerol-Mannitol-Solution)**

200 g Glycerol
15 g Mannitol
ddH2O was added to 200 g glycerol and filled up to a total volume of 1 L. 15 g mannitol were dissolved in the solution and sterile-filtered prior usage.

- **PLAG solution**

40 mL PEG4000
10 mL LiAc solution 1 M
10 mL Tris-HCl 100 mM
10 mL EDTA 10 mM
15 mL Glycerol
15 mL ddH2O

5.4. Chemicals

Chemicals	SOURCE
Lysogeny broth (LB)	Roth
LB-Agar	Roth
Yeast extract Peptone Dextrose (YPD)	Roth
YPD-Agar	Roth
Agar-Agar Kobe	Roth
L(+)-Arabinose	Roth
IPTG (Isopropylb-D-1-thiogalactopyranoside)	Roth
Kanamycin sulphate	Roth
Ampicillin sodium salt	Roth
L(+)-Rhamnose monohydrate	Roth
Complete Supplement Mixture (CSM)	Formedium
Yeast Nitrogen Base (YNB) Loflo	Formedium
D-mannose	Sigma-Aldrich
D-(+)-Glucose	Roth
D-(-)-Fructose	Sigma-Aldrich
L-leucine	Sigma-Aldrich
L-Methionine	Roth
Uracil	Formedium
G418 disulfate salt (Geneticin)	Sigma-Aldrich
2-(N-morpholino)ethanesulfonic acid (MES)	Roth
Agarose, low gelling temperature	Sigma-Aldrich

L-Serine	Roth
Hygromicin	Formedium
Glycerol	Roth
EDTA	Merck
Lithium Acetate	Sigma-Aldrich
PEG 3350	Roth
Amino acids	Roth
Adenine	Roth
Mannitol	Sigma-Aldrich
DMSO	Roth
G418	Sigma-Aldrich
Glass Beads 0.5 mm	Sigma-Aldrich

5.5. Strains and plasmids

- ***E. coli***

Strains used in this study	
Escherichia coli BW25113	[152]
Escherichia coli BW25113 PhisJ(E4) *ΔfimA*::FRT *ΔhisG*::kanR	This study
Escherichia coli BW25113 PhisJ(E4) *ΔfimA*::FRT *ΔargR*::FRT ΔhisG::kanR	This study
Escherichia coli BW25113 *ΔargA*::kanR	This study
Escherichia coli BW25113 *ΔargG*::kanR	This study
Escherichia coli BW25113 *ΔargH*::kanR	This study
Escherichia coli BW25113 Δ*cheY*::kan^R	[95]
Escherichia coli BW25113 *ΔcysG*::kan^R	This study
Escherichia coli BW25113 *ΔfimA*::FRT *ΔargA*::kan$_R$	This study
Escherichia coli BW25113 *ΔfimA*::FRT *ΔargR*::FRT *ΔhisG*::kan^R	This study
Escherichia coli BW25113 *ΔfimA*::FRT Δ*tyrA*::kan^R	This study
Escherichia coli BW25113 *ΔfimA*::kan^R	[95]
Escherichia coli BW25113 Δ*fliC*::kan^R	[95]
Escherichia coli BW25113 *ΔglnA*:: kan^R	[95]
Escherichia coli BW25113 *ΔglyA*:: kan^R	[95]
Escherichia coli BW25113 *ΔhisB*:: kan^R	[95]
Escherichia coli BW25113 *ΔhisG*:: kan^R	[95]
Escherichia coli BW25113 *ΔilvA*:: kan^R	[95]
Escherichia coli BW25113 *ΔilvC*:: kan^R	[95]
Escherichia coli BW25113 *ΔlysA*:: kan^R	[95]
Escherichia coli BW25113 *ΔpdxH*:: kan^R	[95]
Escherichia coli BW25113 *ΔproC*:: kan^R	[95]
Escherichia coli BW25113 *ΔserA*:: kan^R	[95]
Escherichia coli BW25113 *ΔserB*:: kan^R	[95]
Escherichia coli BW25113 *ΔthrC*:: kan^R	[95]
Escherichia coli BW25113 *ΔtrpC*::FRT Δ*tyrA*::kan^R	This study
Escherichia coli BW25113 *ΔtrpC*::kan^R	[95]
Escherichia coli BW25113 ΔtyrA::kan^R	[95]
Escherichia coli MG1655	[153]
Escherichia coli MG1655 Δ*cheY*::FRT Δ*tyrA*::kan^R	This study

Escherichia coli MG1655 Δ*fimA*::FRT Δ*fliC*::FRT Δ*tyrA*::kan^R	This study
Escherichia coli MG1655 Δ*fimA*::FRT Δ*tyrA*::kan^R	This study
Escherichia coli MG1655 Δ*fliC*::FRT Δ*tyrA*::kan^R	This study
Escherichia coli MG1655 Δ*motA*::FRT	[154]
Escherichia coli MG1655 Δ*motA*::FRT Δ*tyrA*::kan^R	This study
Escherichia coli MG1655 Δ*motAA*::FRT Δ*fliC*::FRT Δ*tyrA*::kan^R	This study
Escherichia coli MG1655 Δ*tyrA*::kan^R	This study

- ***S. cerevisiae***

Strains used in this study	
S. cerevisiae BY4741 (MATa his3Δ1 leu2Δ0 met15Δ0 ura3Δ0)	[155]
S. cerevisiae BY4741 *Δade1*::kanMX^R	[96]
S. cerevisiae BY4741 *Δade4*:: kanMX^R	[96]
S. cerevisiae BY4741 *Δade5,7*:: kanMX^R	[96]
S. cerevisiae BY4741 *Δade6*:: kanMX^R	[96]
S. cerevisiae BY4741 *Δade8*:: kanMX^R	[96]
S. cerevisiae BY4741 *Δarg1*:: kanMX^R	[96]
S. cerevisiae BY4741 *Δarg4*:: kanMX^R	[96]
S. cerevisiae BY4741 *Δlys1*:: kanMX^R	[96]
S. cerevisiae BY4741 *Δlys4*:: kanMX^R	[96]
S. cerevisiae BY4741 *Δlys9*:: kanMX^R	[96]
S. cerevisiae BY4741 *Δser1*:: kanMX^R	[96]
S. cerevisiae BY4741 *Δthr1*:: kanMX^R	[96]
S. cerevisiae BY4741 *Δtrp3*:: kanMX^R	[96]
S. cerevisiae BY4741 *Δtrp4*:: kanMX^R	[96]
S. cerevisiae BY4741 *Δhis3*::HIS3-Pglk1-mNeonGreen-Tglk1 *Δarg1*:: kanMX^R	This study
S. cerevisiae BY4741 *Δhis3*::HIS3-Pglk1-mNeonGreen-Tglk1 *Δarg1*:: kanMX^R *Δgdh1*::loxP *Δecm21*::loxP	This study
S. cerevisiae BY4741 *Δhis3::HIS3-Pglk1-mTurquoise2-Tglk1*	This study
S. cerevisiae BY4741 *Δhis3*::HIS3-Pglk1-mTurquoise2-Tglk1 *Δade1*:: kanMX^R	This study
S. cerevisiae BY4741 *Δhis3*::HIS3-Pglk1-mTurquoise2-Tglk1 *Δade4*::kanMX^R	This study
S. cerevisiae BY4741 *Δhis3*::HIS3-Pglk1-mTurquoise2-Tglk1 *Δade5,7*::kanMXR	This study
S. cerevisiae BY4741 *Δhis3*::HIS3-Pglk1-mTurquoise2-Tglk1 *Δade6*:: kanMX^R	This study
S. cerevisiae BY4741 *Δhis3*::HIS3-Pglk1-mTurquoise2-Tglk1 *Δade8*:: kanMX^R	This study
S. cerevisiae BY4741 *Δhis3*::HIS3-Pglk1-mTurquoise2-Tglk1 *Δarg1*:: kanMX^R	This study
S. cerevisiae BY4741 *Δhis3*::HIS3-Pglk1-mTurquoise2-Tglk1 *Δarg1*:: kanMX^R *Δecm21*::loxP	This study
S. cerevisiae BY4741 *Δhis3*::HIS3-Pglk1-mTurquoise2-Tglk1 *Δarg1*:: kanMX^R Δgdh1::loxP	This study
S. cerevisiae BY4741 *Δhis3*::HIS3-Pglk1-mTurquoise2-Tglk1 *Δarg1*:: kanMX^R *Δgdh1*::loxP Δecm21::loxP	This study

S. cerevisiae BY4741 *Δhis3*::HIS3-Pglk1-mTurquoise2-Tglk1 *Δarg4*:: kanMX^R	This study
S. cerevisiae BY4741 *Δhis3*::HIS3-Pglk1-mTurquoise2-Tglk1 Δlys1::kanMXR	This study
S. cerevisiae BY4741 *Δhis3*::HIS3-Pglk1-mTurquoise2-Tglk1 *Δlys4*:: kanMX^R	This study
S. cerevisiae BY4741 *Δhis3*::HIS3-Pglk1-mTurquoise2-Tglk1 *Δlys9*:: kanMX^R	This study
S. cerevisiae BY4741 *Δhis3*::HIS3-Pglk1-mTurquoise2-Tglk1 *Δser1*:: kanMX^R	This study
S. cerevisiae BY4741 *Δhis3*::HIS3-Pglk1-mTurquoise2-Tglk1 *Δthr1*:: kanMX^R	This study
S. cerevisiae BY4741 *Δhis3*::HIS3-Pglk1-mTurquoise2-Tglk1 *Δtrp3*:: kanMX^R	This study
S. cerevisiae BY4741 *Δhis3*::HIS3-Pglk1-mTurquoise2-Tglk1 *Δtrp4*:: kanMX^R	This study

- **Plasmids**

Plasmid Name	Source	Description
pGS5 (HIS3-Pglk1-mTurquoise2-Tglk1)	this work	plasmid carryong the integrative cassette for yeast with mTurquoise2 as fluorescent marker
pSIJ8	[149]	plasmid containing the λ-red recombineering system and the flippase
pH3FS	[156]	plasmid containing the loxP-HygB-loxP cassette
pPL5071_TEF1*-Cre_URA3	[157]	plasmid expressing the Cre recombinase
pMFM073 (HIS3-Pglk1-mNeongreen-Tglk1)	[158]	plasmid carryong the integrative cassette for yeast with mNeonGreen as fluorescent marker
pOB2	[159]	plasmid expressing mCherry
pNB1	[160]	plasmid expressing sfGFP
pUA66-PhisJQMP_E4	this work	plasmid expressing sfGFP under the regulation of a mutant version of the hisJqmp promoter
pUA66-PhisJQMP_E6	this work	plasmid expressing sfGFP under the regulation of a mutant version of the hisJQMP promoter
pUA66-PhisJQMP_H4	this work	plasmid expressing sfGFP under the regulation of a mutant version of the hisJQMP promoter
pUA66-PhisJQMP_H5	this work	plasmid expressing sfGFP under the regulation of a mutant version of the hisJQMP promoter
pUA66-PhisJQMP_wt	this work	plasmid expressing sfGFP under the regulation of the wt version of the hisJQMP promoter
pUA66-no promoter	[161]	original plasmid
pKD45	Parkinson's lab	plasmid containing the KanR-ccdb cassette
pKD 46	Parkinson's lab	plasmid containing the λ-red recombineering system

pH3FS was a gift from Scott Briggs (Addgene plasmid # 85780 ; http://n2t.net/addgene:85780 ; RRID:Addgene_85780)

5.6. Molecular cloning, sequencing and relevant kits

- **Polymerase chain reaction (PCR)**

PCR reactions were performed in TPersonal (Biometra) and peqSTAR (PEQLAB) thermocyclers. Products were run in a 1% TAE-agarose gel at 120 volts and, when necessary, purified with the DNA Clean & Concentrator-5 (Capped) from, Zymo Research or the GeneJET Gel Extraction Kit from Thermo Fisher Scientific.

- ***E. coli* PCR from single colonies**

A single colony was resuspended in 20 ul ddH2O. One ul was then used as template.

Reaction mix

25 µL DreamTaq Green PCR Master Mix (2x)
1 µL forward primer (10 pmol/ µL)
1 µL reverse primer (10 pmol/ µL)
1 µL fron the resuspended colony
up to 50 µL ddH2O

Thermocycler setting

95°C	5 min	
95°C	30 sec	x 30-35 cycles
Ta°C	30 sec	
72°C	1 min/Kb	
72°C	10 min	

- ***S. cerevisiae* PCR from single colonies**

A single colony was resuspended in 20 ul ddH2O. One ul was then used as template.

Reaction mix

25 µL 2X Phire Tissue Direct PCR Master Mix
1 µL forward primer (10 pmol/ µL)
1 µL reverse primer (10 pmol/ µL)
1 µL fron the resuspended colony
up to 50 µL ddH2O

Thermocycler setting

98°C	5 min	
98°C	5 sec	x 40 cycles
Ta°C	5 sec	
72°C	20 sec/Kb	
72°C	1 min	

- **PCR with Q5 polymerase**

Reaction mix

10 µl Q5 reaction buffer (5X)
2.5 µl forward primer (10 pmol/ µl)
2.5 µl reverse primer (10 pmol/ µl)
1 µl dNTPs (10 mM)
0.5 µl Q5 high fidelity DNA polymerase
1 µl template DNA
up to 50 µl ddH2O

Thermocycler setting

98°C	5 min	
98°C	5 sec	x 40 cycles
Ta°C	5 sec	
72°C	20 sec/Kb	
72°C	1 min	

- **Gibson assembly**

10 µl Gibson Assembly Mastermix 2x
100 ng backbone
3:1 molar amount of inserts
ddH2O to 20 µl

once mixed, samples were incubated for fifteen minutes at 50 degrees. After dialysis, performed by pipetting the mix on top of a membrane filter (0.025µm MCE membrane-Millipore-Merck) deposited over 25 ml of ddH2O and incubating it for 15 minutes, 5 ul were used to transform electrocompetent cells.

- **One step *E. coli* chemical competent cells**

Low competence chemically competent *E. coli* cells were prepared as in [162] with minor adjustments.

- Inoculate in 5ml LB the *E. coli* strain that need to be transformed and let it grow overnight at 37°C 200rpm
- the next day inoculate 1/100 of the preculture in fresh LB and let it grow under the same conditions until the OD 600 reaches a value between 0.3 and 0.4
- Transfer the culture in a 50 ml falcon tube and chill on ice for 10 min.
- **All subsequent steps should be carried out at 4°C and the cells should be kept on ice wherever possible**
- Centrifuge for 10 min at 3000 rpm and 4°C.
- Remove supernatant.
- Resuspend cells in cold TSS buffer (4°C). The volume of TSS to use is 5% of the culture volume used. Pipette gently to fully resuspend the culture.
- Transfer 100 µL aliquots to 1.5 ml eppendorfs and add the plasmid you desire to transform the cells with.
- Store at 4°C for 20-60min
- Incubate for 45 seconds at 42 degrees. Immediately afterwards incubate on ice for 5-10 min.
- Add 900 ml SOC and let cell recovery for the time required by the antibiotic used (1-2h)

- ***E. coli* electrocompetent cells**

E. coli electrocompetent cells were prepared as in[163]

- Inoculate in 5ml LB the *E. coli* strain that need to be transformed and let it grow overnight at 37°C 200rpm
- Day culture in 50 ml SOB-Medium to OD600=0,4-0,6
- Chill for 10 min on ice
- Spin down for 15 min at 3000 g with the centrifuge set at 4 °C
- Resuspend the pellets from a 50 mL cell culture in 20 mL cold (4 °C) ddH2O
- Underlay with 10 mL of high-density-solution without disturbing the interface
- Spin down for 15 min at 2600 g with the centrifuge set at 4 °C and a slow acceleration/deceleration
- gently remove the supernatant
- Resuspend in 100 µl high-density-solution

- Freeze aliquots of 50 µl in liquid nitrogen

Transformation

- Mix the desalted DNA, the 50ul cell aliquot and 50 µl cold ddH2O and transfer 100 µl in a pre-chilled 1mm cuvettes
- dry the cuvettes carefully
- pulse settings (*E. coli*)
- After the pulse transfer the cells into pre-warmed Eppendorf tubes with SOC
- incubate in the shaker at 37° for the time required by the antibiotic used (1-2h)

- ***S. cerevisiae*** **competent cells preparation and transformation**

Heat shock competent *S. cerevisiae* cells were prepared as follow:

- Inoculate a colony from strain that need to be transformed in 5 ml YPD and let it grow overnight at 30°C 200rpm
- Day culture in 25 ml YPD (inoculum 1:50) to a final OD600=0,7-1 under the same growth conditions
- Transfer the culture in a 50 ml falcon and spin down for 1 min at 4000 g at room temperature
- Discard the supernatant and resuspend the pellet in 1 ml PLAG solution. Add 125 µl denatured salmon sperm DNA and transfer 200 µl aliquots in 1.5 ml Eppendorf tubes.
- Aliquots can be either immediately used for transformation or frozen slowly at -80 °C.

All *S. cerevisiae* genomic integrations were based on the same principle: linear fragments, either generated via PCR or by plasmid digestion, carrying homologous regions (>50bp each) for the delivered integration region were mixed (concentrations ranging from 500ng to 1 µg of DNA) with an aliquot of competent cells. For plasmids, 250-300 ng of plasmid were mixed with an aliquot of competent cells

- Incubate the mix for 1-2h at 32°C at 500 rpm.
- Heat shock the cells at 42°C for 15 min and, if the marker is a metabolic marker, plate on the appropriate plates, otherwise, for antibiotic markers
- Add 1 ml YPD and incubate for 3-5 h at 30 degrees.
- Spin down, remove the supernatant, plate on appropriate plates and incubate at 30°C.

- ***S. cerevisiae*** **genome extraction**

The desired strain was streaked on YPD plates supplemented with the appropriate antibiotic and incubated for 48h at 30 degrees.

In order to sample the vast majority of the genotypes, an inoculation loop was used to scoop from a region of high colony density on the plate and the sample was then inoculated in 5 ml YPD and grown overnight at 30 degrees 200 rpm.

The next day, 2 ml from the overnight culture were harvested and transferred to a 2ml Eppendorf tube, cells were pelleted by spinning the tubes down at 8000 g for 3 minutes. The media was removed and the samples were resuspended in 100 µl of Elution buffer from the genomic DNA extraction kit (Macherey-Nagel). Resuspended cells were transferred to a new tube containing 500 ul of glass beads and 40 µl of Buffer MG and 10 ul of proteinase K were added. Tubes were fixed on a Vortex Genie 2 Mixer and vortexed at max. speed for 5 minutes. The rest of the procedure was as decribed from point 3 of the protocol provided by the manufacturer of the kit.

- ***E. coli* genome extraction**

The extraction of *E. coli* genome was done by harvesting 2 ml of cell culture from an overnight in LB. Extraction was performed using the genome extraction kit from Macherey-Nagel and according to the manufacturer's protocol.

- **Sequencing library preparation and verification**

Libraries from the extracted genomes were prepared according to the protocol of the Nextera XT DNA Library Preparation Kit. Library fragment size quantification was performed with a Bioanalyzer (Agilent) and samples were prepared according to the manufacturer's protocol.

- **Relevant kits used in this study**

Kits were used according to the guidelines provided by the manufacturers.

- GeneJET Gel Extraction Kit, ThermoFisher Scientific, Dreieich
- GeneJET Plasmid Miniprep Kit, ThermoFisher Scientific, Dreieich
- Q5 Site-Directed Mutagenesis Kit, New England BioLabs GmbH, Frankfurt a.M.
- DNA Clean & Concentrator-5 (Capped), Zymo Research, Freiburg
- Qubit™ dsDNA HS Assay Kit, Thermo Fisher Scientific, Dreieich
- Nextera XT DNA Library Preparation Kit (24 samples), Berlin
- Nextera XT Index Kit (24 indexes, 96 samples), Berlin
- MiniSeq Reagent Kit, Illumina, Berlin
- NucleoSpin Microbial DNA Mini kit for DNA from microorganisms, Macherey-Nagel, Düren
- Agilent High Sensitivity DNA Reagents, Agilent, Waldbronn

- **Primers**

Name	Sequence 5'->3'	function
55_GS_ADE5,7_cnt	GCGTTAAGAAATCGTCTAATCTTCA	primers to verify mutant strains in yeast (fw)
56_GS_ADE6_cnt	GATTTATCCTTACCAACGATGAGTG	
57_GS_ADE8_cnt	GATTTCAGCATAAAGACTAAAAGCG	
58_GS_ARG4_cnt	TTTTCTTTACTCTTCCAAACCCTCT	
59_GS_CYS3_cnt	ACCCCATACCACTTCTTTTTGTTAT	
60_GS_ILV1_cnt	TGCAGATACTTCATTATCAGCTTTG	
61_GS_LYS4_cnt	TAATCGATGAGTCTATACCAGAGGC	
62_GS_LYS9_cnt	TCTTTTGATATTCACCACAACAGAA	
63_GS_SER1_cnt	CAAAAGAAAAGCCATAATAAGGACA	
64_GS_THR1_cnt	GTTATTAATCAGCTCTCTGCTTTGC	
65_GS_TRP3_cnt	AGGCCTTTTTGAACTATTTTCTGTT	
66_GS_ADE1_cnt	TTCTTTGAGGTAAGACGGTTGGGTT	
67_GS_ADE4_cnt	GGACAGAGTTAGAACGAACATGAAT	
68_GS_TRP4_cnt	ATGACTAATATTATTGCTGCGCTTC	
69_GS_SER2_cnt	ACCCTTTTCACCGGAACTAATATAC	
70_GS_AAT2_cnt	ATACACAATTACTCCAGTAGCTGCC	
71_GS_PHA2_cnt	AGAAACTCCAGTTGCTAAACAGAGA	
72_GS_PRO2_cnt	AAGGTCACTTTACAAAAATGGTACG	
73_GS_ARG1_cnt	GCTCTCCAGTCATTTATGTGATTTT	
74_GS_ADH3_cnt	GTCCGTACACTGTCCTTTTGTTACT	
75_GS_LYS14_cnt	TATTTGATAACACAAGGAAACGATG	
76_GS_GLY1_cnt	GTTCACCGGTTTTTCTTTTTATTTC	
77_GS_SHM2_cnt	GTCACCATCTTCATCTACCTCATCT	
78_GS_LYS1_cnt	AGTACTTGAGCTATAATGACCCTGC	
79_GS_KanB_cnt	CTGCAGCGAGGAGCCGTAAT	primers to verify mutant strains in yeast (rv)
ERI122	CGGTGCCCTGAATGAACTGC	primers to verify mutant strains in *E. coli*(fw)
175_GS_argG_cnt_rv	gcacactataaaggagactcacg	primers to verify mutant strains in *E. coli*(rv)
176_GS_cysG_cnt_rv	ttgtaagtcgctgtaacggtg	
177_GS_hisG_cnt_rv	caaacttcgcgctgtattcc	
178_GS_argA_cnt_rv	cagagcacgaaactacgtg	
179_GS_argH_cnt_rv	aacttttgcggatctccagg	
180_GS_glnA_cnt_rv	aacaatttgcgggagctttggg	
181_GS_glyA_cnt_rv	tgatggcgcgataacgtagaaagg	
182_GS_hisB_cnt_rv	tgggtacaggctttgatgag	
183_GS_ilvA_cnt_rv	gaagtggtgctggaaaacag	
184_GS_ilvC_cnt_rv	ggttttctcttgtccggtactg	
185_GS_lysA_cnt_rv	gaaatttcactgcggtagcctg	
186_GS_pdxH_cnt_rv	ttacgctcggcagctttgaag	
187_GS_proC_cnt_rv	attaccgccatgttacgg	
188_GS_serA_cnt_rv	tagtgagtaagggtaagggagg	

189_GS_serB_cnt_rv	aaaaacgcggcagctcttcaag	
190_GS_thrC_cnt_rv	gttatgggtcgatatccgg	
191_GS_trpC_cnt_rv	tggttagttttatgcgcgccg	
192_GS_tyrA_cnt_rv	gcgaaaaccacgttgttaatggcg	
197_GS_fliC_KO_fw	aagcacgttgctgacaaattgcg	Amplify Kan cassette from Keio strain
198_GS_fliC_KO_rv	cagggttgacggcgattgagc	
199_GS_cheY_KO_fw	gatgcgcgcaatgatatcgccag	Amplify Kan cassette from Keio strain
200_GS_cheY_KO_rv	tagtgccggacaggcgatacg	
243_GS_argR_kass_fw	aatgttgtatcaaccaccatatcgggtgacttatgcgaagctcggctaagtggtgtcc ctgttgataccg	primers used to generate the KO of *argR*
244_GS_argR_kass_rv	accttatgtattcattgtgtgaatgacatgtcgcagtaaaacgcactattgactgaggt atgtgctctctc	
245_GS_argR_amp_fw	cagaatttgcatgccgtgac	Sequencing/ verification primers
246_GS_argR_amp_rv	ccttatgtattcattgtgtgaatgac	
249_GS_hisJ_amp_fw	tcaatacgtccggcagtcag	Sequencing/ verification primers
250_GS_hisJ_amp_rv	gaagcttacgctaacgagacc	
259_GS_ECM21_KO_fw	AAATAGAGAAGAACAAGCAAGATTTTTCCCTACCC CTATTGGGCATGCCGgtcgacggatctgatatcacc	primers used to generate thr KO of *ecm21*
260_GS_ECM21_KO_rv	ATTCATTCTTCATCACTCATCAAAGGCACTATTTC GTCATAACGCGGAGGatggtgtcgacaacccttaat	
261_GS_GDH1_KO_fw	GCATTATTCTAATATAACAGTTAGGAGACCAAAAA GAAAAAGAAATGTCAgtcgacggatctgatatcacc	primers used to generate thr KO of *gdh1*
262_GS_GDH1_KO_rv	AGACTATTTAAAATACATCACCTTGGTCAAACATA GCATCAGAGACCTTGatggtgtcgacaacccttaat	
263_GS_GDH1_cnt_fw	AATTGCGGAAGAAGAAAGCG	Sequencing/ verification primers
264_GS_GDH1_cnt_rv	TCTGTCTCTGTTATATTTCCACATGTC	
265_GS_ECM21_cnt_fw	TTTGAAGGTCCATCGGAAAGGTG	Sequencing/ verification primers
266_GS_ECM21_cnt_rv	TCGCCACATGCTTCATGACG	
288_GS_hisJ_ccdB_KO_fw	cgatctggctgcaggacgtctggatgctgcgttacaagatgaagttgctggagcctg acatttatattcc	gene replacement promoter *hisJQMP* (amplification neo-ccdB cassette)
289_GS_hisJ_ccdB_KO_rv	atggcgtcaatcttcttcgcttttaaggacgggattaacgcatccagcgggtcccgct cagaagaactc	

6. Appendix

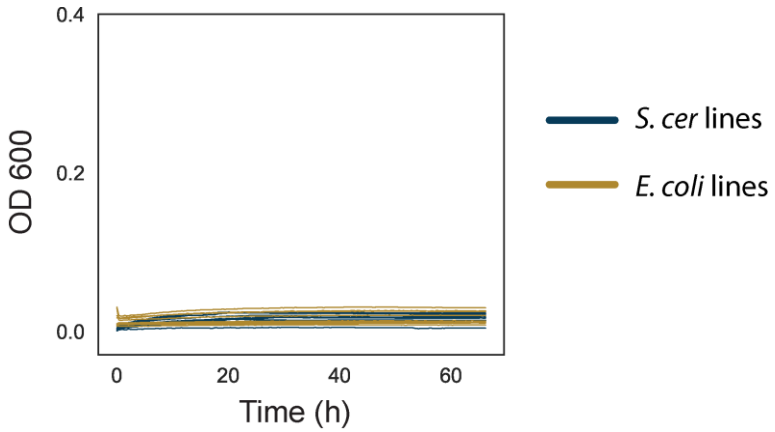

S1 Test for auxotrophy.

Culture of isolated community members from evolved co-cultures #3 and #4 (Table1). *E. coli* (yellow) *S. cerevisiae* (blue) isolates were inoculated in YNB minimal media without supplements in monocultures

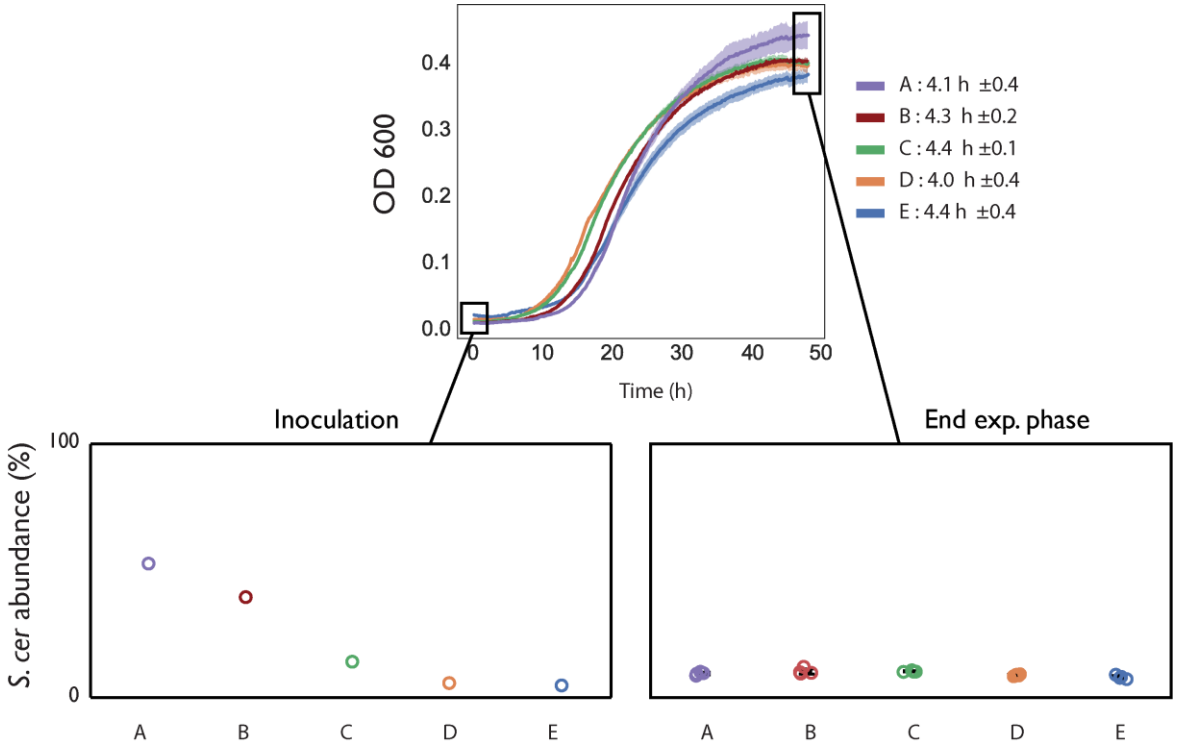

S2 Effects of partners ratio on community growth.

Growth curves, initial and final *S. cerevisiae* cell abundance expressed as the fraction from the total cell count from *E. coli ΔargR -S. cerevisiae Δecm21* co-cultures with different initial ratios between *E. coli* and *S. cerevisiae*. Different colors indicate different initial ratios. Doubling times are reported in the legend

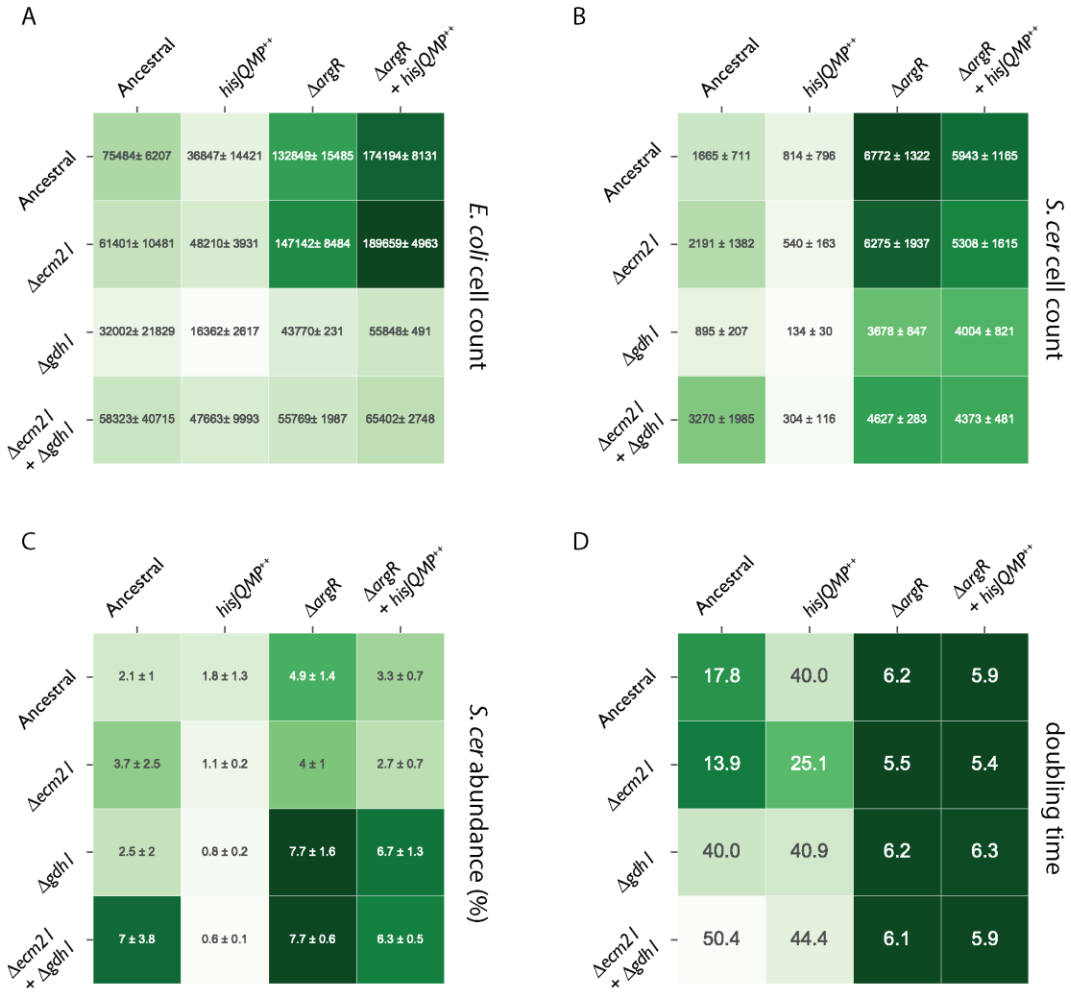

S3 Effects of mutations on growth

A-C Heatmap indicating the average *E. coli* cell count (A), *S. cerevisiae* cell count (B) and the *S. cerevisiae* abundance (C) calculated as fraction of the total cell measured after five days of growth from co-cultures between all the pairwise combinations between ancestral, single mutant and double mutant *E. coli* and *S. cerevisiae* as in Fig. 14. The standard deviation calculated from 3 biological replicates is indicated.
D Doubling time from growth curves presented in Fig. 14.

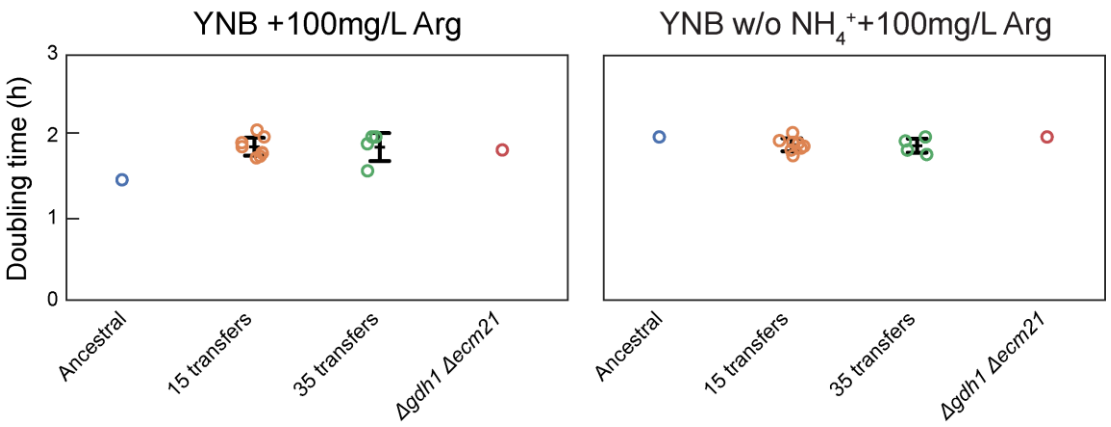

S4 Impact of ammonium on doubling time

Plots representing the average doubling times calculated from growth curves presented in Fig. 17 and 18. Ancestral, evolved for 15 transfers, evolved for 35 transfers, and double mutant yeast strains were grown in YNB supplemented with arginine either in presence (left) or absence (right) of ammonium. Circles represent the average from two technical replicates per each strain tested.

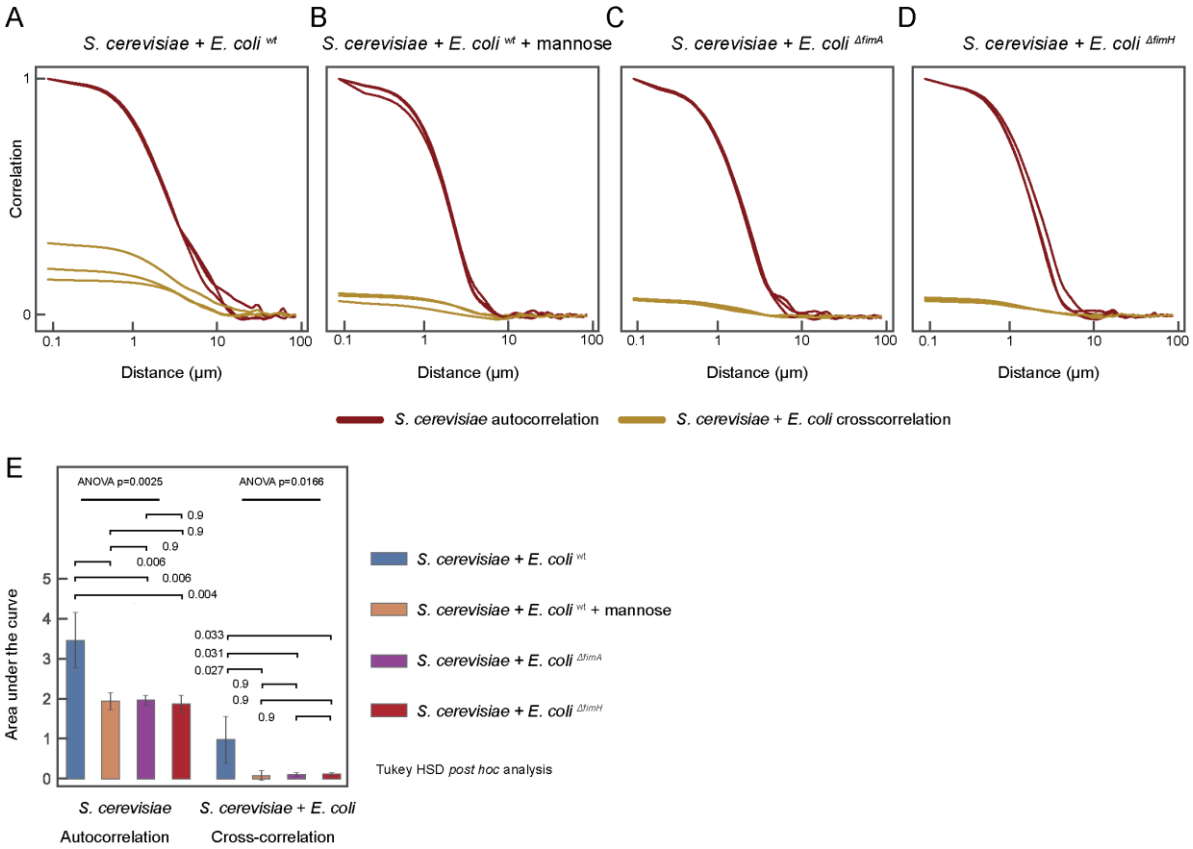

S5 Characterization of *S. cerevisiae* and *E. coli* co-aggregation

A-D Auto- and cross-correlation analysis of co-aggregation between *S. cerevisiae* and (A) *E. coli* Fim+, (B) *E. coli* Fim+ in presence of mannose, (C) *E. coli ΔfimA* and (D) *E. coli* ΔfimH, each with three biological replicates (represented by different lines). Autocorrelation analysis between neighboring pixels in one fluorescent channel (mTurquoise2) reflects the characteristic size of yeast cells or/and aggregates, whereas the cross-correlation analysis between two different channels (mCherry and mTurquoise2) reflects the characteristic size and number of mixed bacteria-yeast aggregates. These analyses were performed for the entire images, with each image contained at least twenty yeast cells and one hundred bacterial cells. E Quantification of aggregation, calculated as area under the curve for auto- and cross-correlations analysis from the plots shown in A-D. One-way ANOVA tests, followed by an HSD Tukey test as post hoc analysis were performed from three biological replicates.

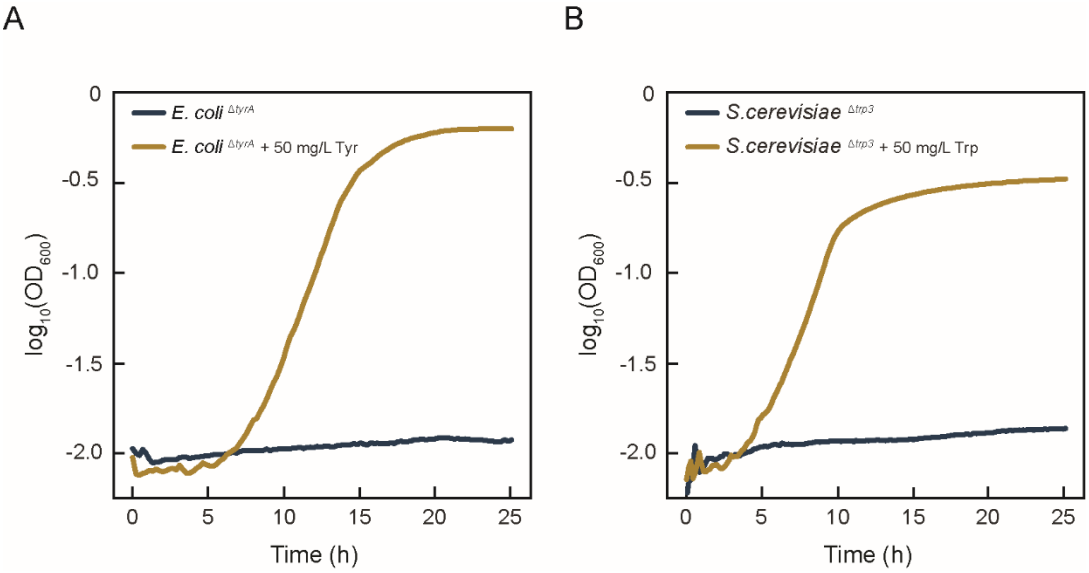

S6 Verification of auxotrophies

A,B Growth curves of monocultures of (A) *E. coli ΔtyrA* and (B) *S. cerevisiae Δtrp3* in minimal media either not supplemented (blue lines) or supplemented with the required amino acid (yellow lines).

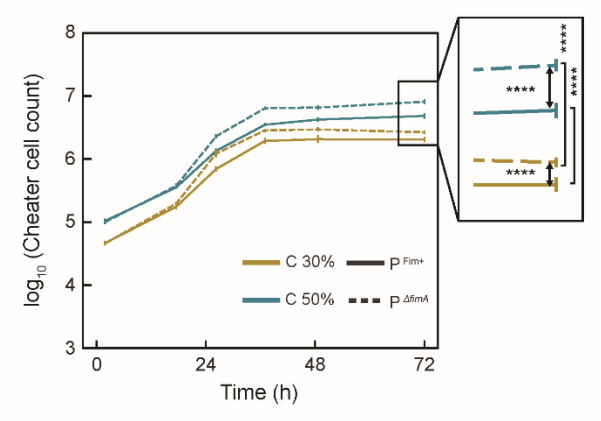

S7 Cell count of cheater *E. coli* in the cross-feeding community

Number of cheater (labeled "C") *E. coli* cells measured by flow cytometry in the cross-feeding co-cultures with yeast and an *E. coli* partner (labeled "P") that is either fimbriated (straight lines) or fimbrialess (dotted line. Error bars represent standard deviations of three biological replicates. ****p ≤0.0001 from a two-tailed t-test assuming equal variances of the data sets.

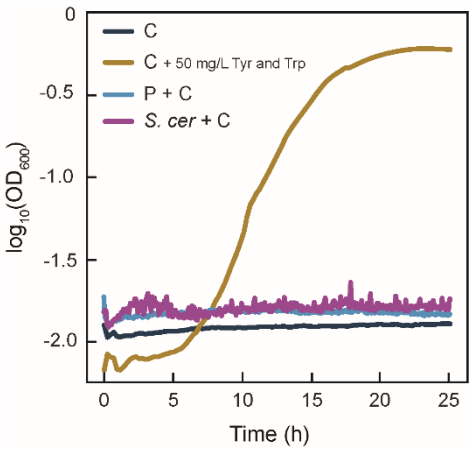

S8 Verification of the auxotrophies

Growth curves from cultures of the *E. coli ΔtyrA ΔtrpC* cheater strain (labeled "C") both in mono culture in YNB + glucose, either with no supplements or supplemented with tyrosine and tryptophan, and in co culture in YNB + glucose with either *S. cerevisiae Δtrp3* or *E. coli ΔtyrA (labeled "P").*

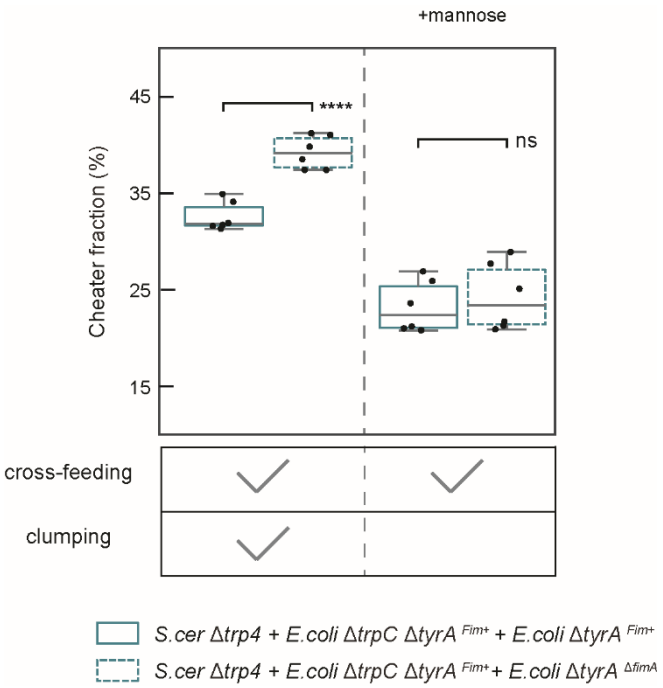

S9 Protective effects of fimbriation against cheater in community with *Δtrp4* yeast strain

Fraction of fimbriated cheater in communities containing either Fim+ (solid line boxes) or *ΔfimA* (dashed line boxes) *E. coli* partner at the initial 50% abundance of the cheater, grown either in YNB-glucose or YNB-glucose supplemented with 4% mannose, as indicated. ****p ≤0.0001, ns=not significant in a two tailed t-test assuming equal variances of the data sets for six biological replicates represented as dots.

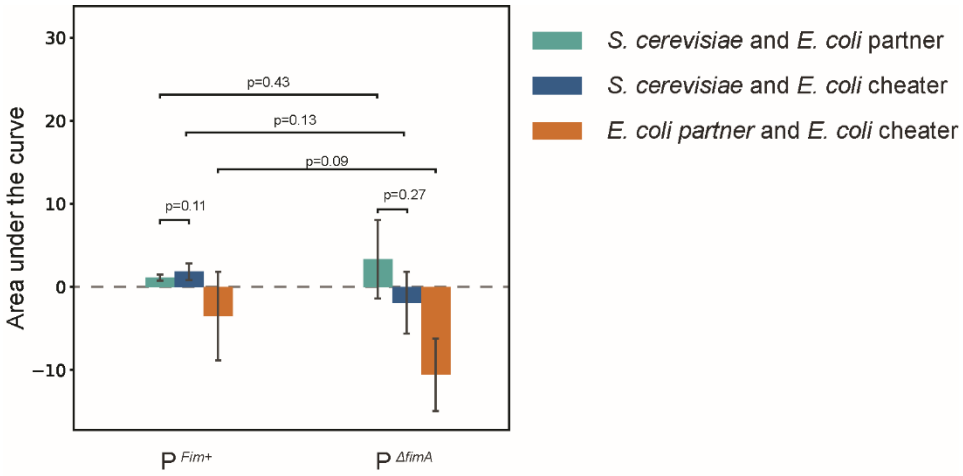

S10 Cross-correlation between spatial arrangement of community members in presence of cheater strain

Area under the curve from cross correlations analysis (see Fig. S1) between different community members in sessile communities grown as in Figure 29A. Two-sided t-test assuming equal variance between data sets were performed. Each data set included four biological replicates.

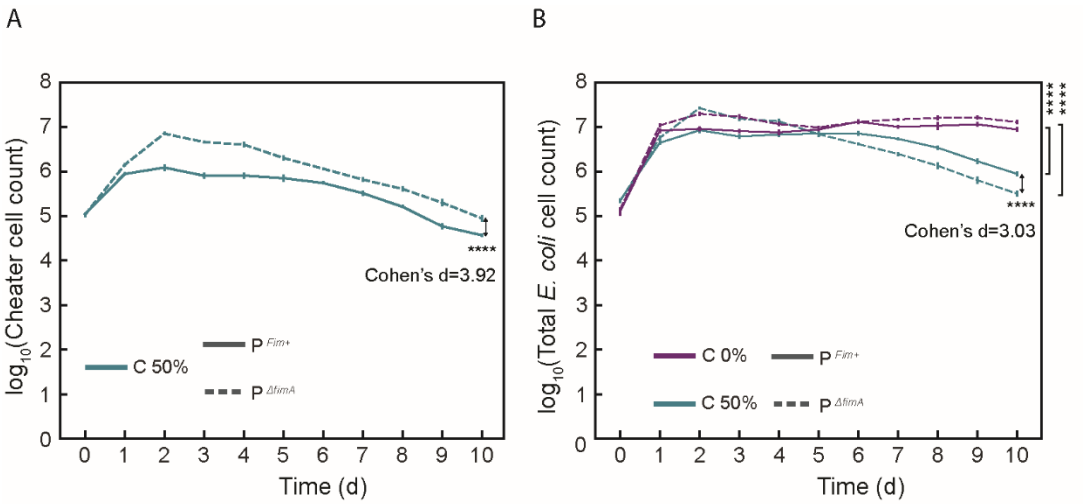

S11 Cell count of cheater and of total *E. coli* population in semi-continuous co-culture

A,B Numbers of cheater (A) and total (B) *E. coli* cells measured by flow cytometry in in 20 µL of the same cross-feeding semi-continuous co-cultures as in Figure 36B. Error bars represent standard deviations of six to twelve biological replicates. ****p ≤0.0001 in a two tailed t-test assuming equal variances of the data sets. Cohen´s d was calculated to quantify the effect size.

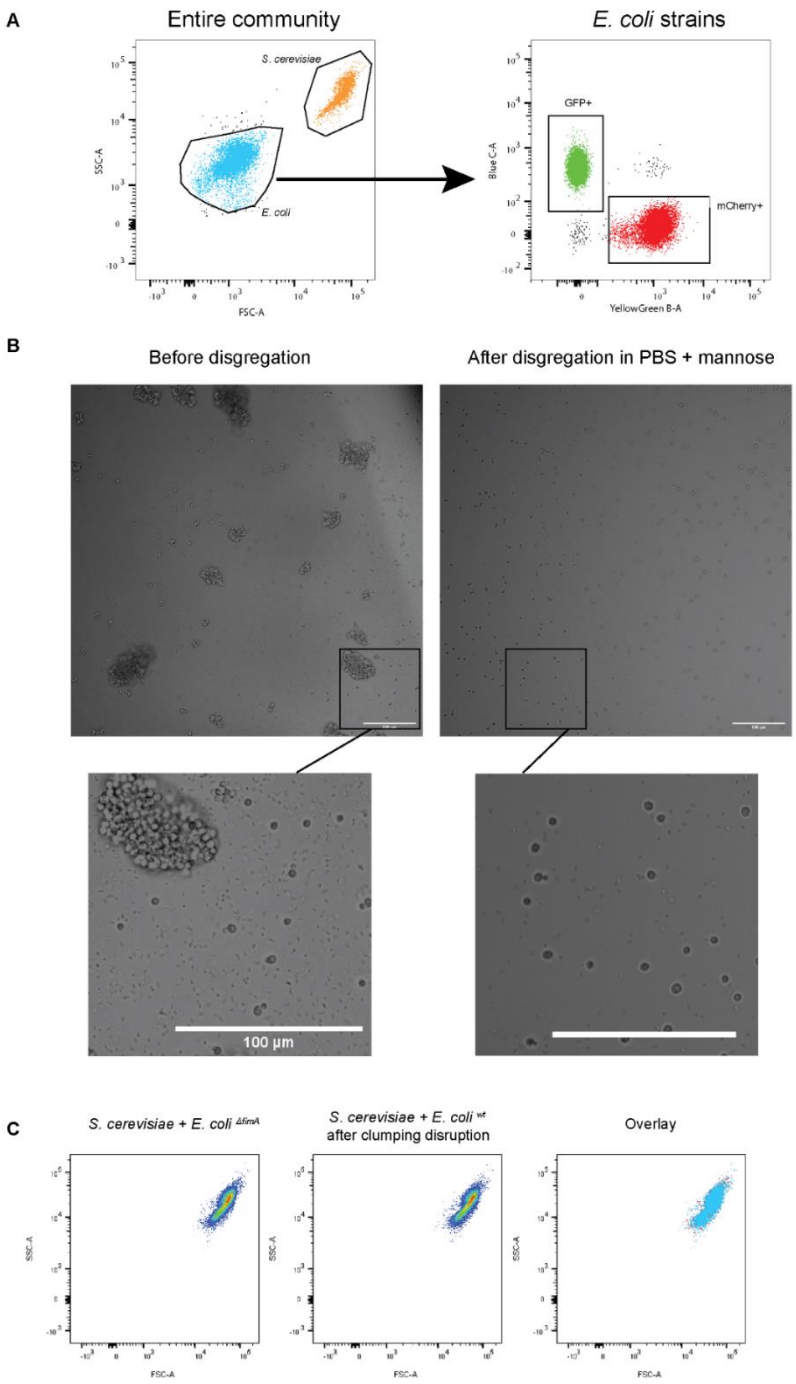

S12 Flow cytometry measurements after cell aggregate disruption.

A Illustration of the gating strategy performed on flow cytometry data for *S. cerevisiae-E. coli* co-cultures. *E. coli* and *S. cerevisiae* were distinguished according to their different scatter properties (SSC and FSC). When applicable, individual *E. coli* strains were further distinguished according to their respective fluorescent markers (Blue positive cells express GFP, YellowGreen positive cells express mCherry).
B Microscopy images showing the complete disruption of aggregates after vigorous mixing in PBS + mannose. **C** Flow cytometry analysis performed on the gated *S. cerevisiae* subpopulation showing the overlap between a yeast population obtained after clump disruptions from an aggregative community and a population of *S. cerevisiae* grown with a fimbrialess bacterial partner, confirming complete disruption of the aggregates.

Appendix Table 1

Heatmap showing the OD measured at the end of every growth cycle (day from inoculation on top of each column) from all the evolved lines during the evolutionary experiment. The genotype of community members present in each line are reported in the first column for *S. cerevisiae* and in the second for *E. coli*. Presence (+) or absence (-) of fimbriae on the *E. coli* strain is reported in the third column. The last two columns report the presence of growth of strains from the last growth cycle (day 113) streaked on selective plates respectively for yeast (S) or the bacterium (E). Dark green indicates the presence of more than 10 colonies on the selective plates, light green between 1 and 10, white indicates absence of colonies. Lines E4, E6 and G5 were proven both via PCR analysis and sequencing to derive from a contamination from lines containing the fimbriated partner of community #4. Notably, while the original *E. coli* partner is the same for both communities, the *S. cerevisiae* partner is different. Nonetheless, the yeast partner was not detected in the final communities and we therefore proceed by including these lines as additional replicates from community #4.

Community members				Days from inoculation																	
S. cer	*E. coli*	Fim	Line	7	14	21	29	36	43	50	57	64	71	78	85	92	99	106	113	S	E
TRP3	tyrA	+	E1	0.68	0.68	0.47	0.47	0.36	0.27	0.78	0.72	0.86	1.04	1.1	1.34	1.04	1.13	0.74	0.87		
			E2	0.69	0.66	0.45	0.5	0.38	0.31	0.24	0.34	0.31	0.36	0.54	0.51	0.52	0.56	0.48	0.45		
			E3	0.66	0.62	0.39	0.43	0.39	0.89	0.9	0.96	0.82	1.09	1.09	1.26	1	1.27	0.77	0.9		
TRP3	tyrA	-	G1	1.11	0.76	1.04	0.62	0.6	0.72	0.65	0.59	0.7	1.23	0.5	0.94	0.79	0.99	1.06	0.92		
			G2	1.11	0.75	1.06	0.56	0.54	0.62	0.8	1.01	0.94	1.25	1.41	0.81	1.1	1.2	1.2	1.08		
			G3	1.09	0.76	1.03	0.74	0.58	0.7	0.57	0.66	0.74	0.5	0.43	0.43	0.46	0.45	0.43	0.38		
TRP3	serA	+	F1	0.31	0.34	0.37	0.34	0.42	0.35	0.29	0.3	0.23	0.21	0.3	0.71	0.63	1.02	0.64	1.13		
			F2	0.31	0.34	0.36	0.33	0.35	0.99	0.69	0.78	0.6	0.56	0.53	0.94	1.03	0.71	0.92	0.5		
			F3	0.28	0.36	0.33	0.36	0.44	0.4	0.14	0.28	0.25	0.48	0.8	0.67	0.59	0.79	0.69	0.53		
TRP3	serA	-	H1	0.31	0.32	0.32	0.12	0.02	0	0	0	0	0	0	0	0	0	0	0		
			H2	0.29	0.35	0.34	0.37	0.37	0.39	0.32	0.24	0.9	0.4	0.28	0.39	0.47	0.41	0.35	0.33		
			H3	0.32	0.31	0.32	0.32	0.28	0.2	0.04	0.01	0	0	-0.01	0	0	-0.01	0	0		
ADE4	hisG	+	E4	0.34	0.14	0.09	0.09	0.14	0.19	0.13	0.08	0.03	0.55	0.43	0.36	0.54	0.49	0.38	0.3		
			E5	0.32	0.15	0.14	0.11	0.2	0.27	0.26	0.25	0.17	0.15	0.05	0.03	0.01	0.01	0	0.01		
			E6	0.29	0.12	0.06	0.04	0.05	0.13	0.35	0.3	0.15	0.15	0.12	0.09	0.12	0.54	0.76	0.54		
ADE4	hisG	-	G4	0.54	0.28	0.12	0.05	0.03	0.03	0.02	0.02	0.02	0.01	0.01	0.01	0.02	0.02	0.02	0.04		
			G5	0.57	0.22	0.08	0.04	0.05	0.04	0.39	0.35	0.25	0.36	0.54	0.72	0.83	0.87	0.73	0.58		
			G6	0.5	0.31	0.34	0.25	0.27	0.27	0.32	0.44	0.42	0.43	0.38	0.18	0.05	0.03	0.01	0.01		
ARG1	hisG	+	F4	0.42	0.38	0.4	0.6	0.45	0.4	0.52	0.43	0.32	0.45	0.41	0.67	0.82	0.93	0.65	0.54		
			F5	0.44	0.52	0.38	0.64	0.46	0.41	0.43	0.44	0.29	0.57	0.46	0.89	1.01	1.13	1.01	0.8		
			F6	0.45	0.47	0.34	0.51	0.45	0.36	0.4	0.35	0.25	0.4	0.44	0.63	1.04	0.98	0.95	0.83		
ARG1	hisG	-	H4	1.03	0.92	0.91	0.88	0.75	0.85	0.81	0.77	0.7	1.13	0.9	1.05	1.04	1.21	1.02	0.94		
			H5	0.99	0.98	0.97	0.94	0.86	0.96	0.89	0.84	0.76	1.22	0.83	1.03	1.07	1.16	0.99	0.97		
			H6	1	0.95	0.96	0.9	0.84	0.9	0.67	0.91	0.71	1.18	0.9	1.05	1.15	1.2	1.05	0.97		
LYS1	argA	+	E7	0.4	0.34	0.3	0.51	0.4	0.42	0.54	0.67	0.65	1.01	0.94	0.84	0.96	0.78	0.77	0.77		
			E8	0.41	0.36	0.32	0.51	0.35	0.36	0.4	0.48	0.46	0.72	0.74	0.72	0.75	0.73	0.64	0.64		

			E9	0.4	0.31	0.33	0.49	0.35	0.36	0.4	0.56	0.55	0.73	0.76	0.7	0.74	0.71	0.68	0.68		
LYS1	argA	-	G7	0.79	0.66	0.72	0.59	0.59	0.55	0.58	0.59	0.58	0.81	0.65	0.69	0.73	0.69	0.71	0.67		
			G8	0.8	0.67	0.72	0.63	0.51	0.54	0.5	0.49	0.54	0.73	0.7	0.67	0.73	0.72	0.7	0.67		
			G9	0.8	0.66	0.72	0.57	0.53	0.57	0.56	0.56	0.56	0.81	0.71	0.7	0.75	0.74	0.7	0.7		
LYS1	argG	+	F7	0.18	0.15	0.18	0.15	0.17	0.21	0.23	0.25	0.21	0.09	0.85	0.68	0.72	0.79	0.69	0.65		
			F8	0.19	0.14	0.23	0.23	0.31	0.31	0.26	0.28	0.3	0.23	0.14	0.15	0.12	0.08	0.07	0.05		
			F9	0.18	0.12	0.25	0.33	0.32	0.28	0.24	0.33	0.29	0.16	0.13	0.17	0.14	0.09	0.08	0.06		
LYS1	argG	-	H7	0.25	0.32	0.39	0.32	0.38	0.84	0.49	0.32	0.59	0.48	0.63	0.66	0.71	0.66	0.76	0.71		
			H8	0.25	0.29	0.27	0.27	0.29	0.35	0.73	0.34	0.44	0.73	0.73	0.6	0.71	0.57	0.68	0.61		
			H9	0.25	0.3	0.24	0.23	0.23	0.13	0.04	0	0	0	0	0	0	0	0	0		
LYS4	argA	+	E10	0.2	0.53	0.37	0.52	0.32	0.43	0.48	0.56	0.55	0.62	1	0.71	1.04	0.78	0.75	0.65		
			E11	0.22	0.49	0.36	0.51	0.31	0.39	0.5	0.62	0.62	0.77	0.77	0.83	0.92	0.82	0.77	0.7		
			E12	0.21	0.51	0.36	0.52	0.3	0.39	0.46	0.55	0.56	1.12	0.9	0.97	1.18	1.06	0.9	0.83		
LYS4	argA	-	G10	0.21	0.15	0.14	0.2	0.74	0.35	0.36	0.38	0.38	0.42	0.96	0.74	0.85	0.72	0.7	0.64		
			G11	0.23	0.71	0.4	0.44	0.37	0.36	0.61	0.63	0.58	0.72	0.77	0.73	0.77	0.75	0.75	0.68		
			G12	0.23	0.68	0.37	0.48	0.37	0.37	0.55	0.59	0.56	0.69	0.72	0.71	0.76	0.68	0.69	0.61		
LYS4	argG	+	F10	0.12	0.18	0.21	0.11	0.07	0.12	0.14	0.1	0.11	0.08	0.07	0.04	0.02	0.01	0	0		
			F11	0.13	0.09	0.08	0.07	0.04	0.05	0.06	0.06	0.09	0.08	0.06	0.05	0.05	0.04	0.02	0		
			F12	0.14	0.07	0.07	0.04	0.03	0.04	0.05	0.06	0.16	0.28	0.33	0.31	0.26	0.17	0.19	0.13		
LYS4	argG	-	H10	0.17	0.24	0.13	0.1	0.06	0.07	0.02	0.01	0	0	0	0	0	0	0	0		
			H11	0.2	0.34	0.42	0.27	0.32	0.4	0.27	0.19	0.12	0.06	0.03	0.01	0	0	0	0		
			H12	0.21	0.19	0.21	0.09	0.02	0	0	0	0	0	0	0	0	0	0	0		

Appendix Table 2 Table summarizing mutations detected in *E. coli* isolates from lines retaining mutualism after 15 transfers. The fraction of the population carrying the specific mutation is indicated. **The threshold for mutation call was set to 0.15**

mutation	E4	E6	F4	F5	F6	G5	H4	H5	H6	Relative position	gene
G→T									0.16	R104L (CGA→CTA)	pdhR →
G→C		0.17								intergenic (-8/+27)	glnW ← / ← glnU
T→G	0.14	0.18								intergenic (-21/+14)	
Δ111 bp			0.16							coding (1967-2077/2685 nt)	kdpD ←
T→A								1.00		intergenic (-122/+481)	ompF ← / ← asnS
T→C							0.38			intergenic (-122/+481)	
A→C									0.15	intergenic (+651/+85)	ycdU → / ← serX
IS5 (+) +4 bp								0.45		coding (442-445/2868 nt)	ycgV ←
A→G									0.24	intergenic (+267/+273)	narI → / ← rttR
T→G		0.16								intergenic (+305/+235)	
A→C		0.20	0.27							intergenic (+439/+101)	
C→G	0.16								0.19	pseudogene (945/2513 nt)	ydbA →
T→A								0.34		R597R (CGT→CGA)	rsxC →
G→C		0.18			0.19					E614Q (GAA→CAA)	
T→A						0.33				R629R (CGT→CGA)	
A→C	0.21									A632A (GCA→GCC)	
A→C	0.16		0.15	0.24	0.24	0.18	0.20	0.30	0.21	R661R (CGA→CGC)	
A→C							0.19			K666N (AAA→AAC)	
A→G								0.15		K666K (AAA→AAG)	
C→A					0.20	0.18	0.20		0.24	P671Q (CCG→CAG)	
+TTTA				0.25					0.65	coding (34/699 nt)	proQ ←
C→T							0.60	0.63	0.51	G8R (GGA→AGA)	insH1 ←

Δ1 bp			1.00								intergenic (-66/+155)	hisJ ← / ← argT
Δ1 bp	1.00										intergenic (-78/+143)	
A→T							1.00				intergenic (-86/+135)	
A→T								0.42			intergenic (-87/+134)	
A→C	0.19	0.21									noncoding (55/77 nt)	argY ←
C→A				0.86	0.79						E414* (GAA→TAA)	pepP ←
A→C	0.21										intergenic (+367/+247)	yhaC → / ← rnpB
IS5 (+) +4 bp					0.56						coding (14-17/471 nt)	argR →
IS5 (+) +4 bp								1.00			coding (28-31/471 nt)	
IS5 (+) Δ17 bp									0.63		coding (32-48/471 nt)	
IS5 (–) +4 bp			0.22								coding (53-56/471 nt)	
C→T	1.00										Q26* (CAG→TAG)	
A→C			0.17								Q34P (CAG→CCG)	
C→T			0.64								Q43* (CAG→TAG)	
C→T		1.00				1.00					A109V (GCT→GTT)	
IS5 (–) +4 bp									0.17		coding (445-448/471 nt)	
IS evidence				X			X					
T→G	0.35										E51A (GAG→GCG)	yhdE ←
C→A		1.00									D73Y (GAC→TAC)	rplN ←
G→A								0.17			G153G (GGC→GGT)	aslA ←

Appendix Table 3 Table summarizing mutations detected in *S. cerevisiae* isolated from lines retaining mutualism after 15 transfers. For this analysis, only mutations with a frequency >0.8 are reported.

mutation	E4	E6	F4	F5	F6	G5	H4	H5	H6	annotation	gene
Δ3 bp	1				1			1	1	intergenic (–/-491)	– / → YOL166W-A
Δ3 bp		1	1							intergenic (–/-492)	– / → YOL166W-A
Δ1 bp		1								intergenic (–/+351)	– / ← YHL050C
Δ3 bp									1	intergenic (-223/-425)	ADH2 ← / → UBP15
+T		1								intergenic (-209/-456)	AMD1 ← / → SRC1
Δ3 bp				1						intergenic (+91/+264)	AOS1 → / ← SEC23
Δ3 bp								1		intergenic (+440/-16)	ATP3 → / → FIG1
Δ1 bp									1	intergenic (-75/+219)	BUB2 ← / ← AAC1
+GTT				1						coding (310/2514 nt)	CCR4 ←
Δ1 bp			1							intergenic (+260/+115)	CCZ1 → / ← AGP2
Δ1 bp	1									intergenic (+32/+36)	CHL4 → / ← RMD5
C→T	1								1	intergenic (+531/+1120)	COS9 → / ← SRY1
A→T	1								1	intergenic (+540/+1111)	COS9 → / ← SRY1
Δ3 bp							1			coding (1545-1547/1587 nt)	CTK1 →
T→A								1		T203T (ACA→ACT)	DAN4 ←
C→A									1	S96* (TCA→TAA)	DAS1 →
G→A								1		P131P (CCC→CCT)	DRS2 ← HRA1 →
C→A			1					1		E680* (GAG→TAG)	ECM21 ←
Δ1 bp									1	coding (2435/3354 nt)	ECM21 ←
G→C									1	S550* (TCA→TGA)	ECM21 ←
T→A								1		R204* (AGA→TGA)	ECM21 ←
A→C						1				Y591D (TAC→GAC)	ECM21 ←
G→A									1	T73M (ACG→ATG)	EFM6 ←
C→T								1		D326N (GAT→AAT)	ENT5 ←
Δ3 bp								1		coding (1724-1726/6837 nt)	FAB1 →
C→T	1	1	1			1		1	1	T803T (ACC→ACT)	FLO1 →
T→C			1					1	1	T809T (ACT→ACC)	FLO1 →
T→C		1			1	1		1		T795T (ACT→ACC)	FLO1 →
C→T	1	1	1							T811T (ACC→ACT)	FLO1 →
T→C									1	T828T (ACT→ACC)	FLO1 →
2 bp→TG								1		coding (987-988/4614 nt)	FLO1 →
C→T								1		T333T (ACC→ACT)	FLO1 →

3 bp→ CTG			1							coding (986-988/ 4614 nt)	FLO1 →
T→C			1							F332F (TTT→T TC)	FLO1 →
A→T							1			intergenic (+113 15/-867)	FLO1 → / → YAR06 4W
C→T					1					intergenic (+361/ -2854)	FLO10 → / → NFT1
3 bp→ CAG	1	1	1	1			1	1		coding (986-988/ 3969 nt)	FLO9 ←
G→C	1	1	1	1	1		1			I519M (ATC→A TG)	FLO9 ←
G→A	1		1	1			1	1		T811T (ACC→A CT)	FLO9 ←
A→G	1		1	1			1	1		T809T (ACT→A CC)	FLO9 ←
A→G	1		1	1		1	1			F332F (TTT→T TC)	FLO9 ←
G→C		1	1	1				1		I699M (ATC→A TG)	FLO9 ←
G→A		1	1					1		T333T (ACC→A CT)	FLO9 ←
2 bp→ GG		1						1		coding (995-996/ 3969 nt)	FLO9 ←
G→A		1	1							T296T (ACC→A CT)	FLO9 ←
+135 bp		1	1							coding (877/396 9 nt)	FLO9 ←
T→C						1				S330G (AGC→G GC)	FLO9 ←
T→G						1				N329T (AAC→ ACC)	FLO9 ←
T→G								1		Q86H (CAA→C AC)	FRS2 ←
Δ1 bp	1						1	1		intergenic (+107/ -250)	GAD1 → / → GTO3
+TTT		1	1	1			1	1	1	intergenic (+366/ +1367)	GAT1 → / ← PAU5
+TT	1				1	1				intergenic (+366/ +1367)	GAT1 → / ← PAU5
C→G			1			1				A435P (GCT→C CT)	GDH1 ←
A→T									1	C414* (TGT→T GA)	GDH1 ←
C→T								1		W366* (TGG→ TGA)	GDH1 ←
G→A							1			S186F (TCT→T TT)	GDH1 ←
C→T					1					G338D (GGT→ GAT)	GDH1 ←
Δ1 bp		1								coding (152/136 5 nt)	GDH1 ←
C→T								1		A149A (GCC→ GCT)	GLK1 →
C→G								1		R580P (CGT→C CT)	GLT1 ←
+T						1				intergenic (+1/-4 95)	HCM1 → / → RAD1 8
Δ1 bp						1				intergenic (+184/ +200)	HOR7 → / ← MLO1
Δ3 bp									1	coding (1941-19 43/2280 nt)	HRK1 ←
G→A				1						intergenic (-577/ -2267)	HXT15 ← / → THI1 3
Δ4 bp		1								intergenic (-431/ -540)	IFH1 ← / → UCC1
Δ3 bp	1									intergenic (-206/ +195)	KCS1 ← / ← YDR01 8C
Δ3 bp					1			1	1	intergenic (+18/ +97)	LSM8 → / ← MDE1
Δ1 bp				1						intergenic (+19/ +98)	LSM8 → / ← MDE1
C→T								1		intergenic (-748/ +1186)	LYS14 ← / ← YDR0 34C-D

+TTT				1	1		1	1	1	intergenic (-41/+192)	MDJ1 ← / ← YFL015C
+TT	1	1	1			1				intergenic (-41/+192)	MDJ1 ← / ← YFL015C
Δ1 bp					1	1				intergenic (-183/-302)	MEP1 ← / → YGR121W-A
+T				1						intergenic (+256/+1501)	MGA1 → / ← RIE1
C→A	1									intergenic (-342/+460)	MHF2 ← / ← DHH1
LTR (+) +5 bp						1				intergenic (-77/+5)	MMS2 ← / ← MMS2
Δ3 bp	1									intergenic (+151/+189)	MNR2 → / ← YKL063C
Δ4 bp					1					intergenic (-386/+292)	MPC54 ← / ← GAC1
G→C					1					D129H (GAC→CAC)	MSB3 →
+G	1	1				1	1		1	intergenic (+131/-948)	MST27 → / → tR(UCU)G1
Δ1 bp					1					intergenic (+472/-607)	MST27 → / → tR(UCU)G1
2 bp→ GC				1						intergenic (+544/-534)	MST27 → / → tR(UCU)G1
Δ1 bp			1							coding (311/420 nt)	MTC7 →
1 bp→ 13 bp								1		coding (771/1656 nt)	MTL1 →
+84 bp								1		coding (793/1656 nt)	MTL1 →
+81 bp						1				coding (793/1656 nt)	MTL1 →
A→C				1						S251S (TCA→TCC)	MTL1 →
+TTT			1							intergenic (+126/+206)	NCL1 → / ← MCM2
+TGT			1							coding (336/1665 nt)	NDD1 ←

Δ3 bp						1				coding (46-48/2181 nt)	NFI1 ←
A→T	1									intergenic (-1381/-1892)	NRG1 ← / → HEM13
Δ1 bp				1				1		intergenic (+33/+23)	NSE4 → / ← QRI7
Δ4 bp						1				intergenic (+33/+20)	NSE4 → / ← QRI7
Δ3 bp		1								intergenic (+33/+21)	NSE4 → / ← QRI7
G→T					1					P371T (CCA→ACA)	OCH1 ←
G→A									1	S318L (TCG→TTG)	ORC4 ←
C→G		1	1					1	1	intergenic (+1759/-951)	PAU10 → / → YRF1-1
+T	1									intergenic (+1761/-949)	PAU10 → / → YRF1-1
Δ98 bp				1		1				intergenic (+1778/-800)	PAU4 → / → YLR462W
Δ1 bp					1					coding (259/1242 nt)	PBP2 →
G→A								1		V53V (GTC→GTT)	PDR17 ←
C→A					1					K175N (AAG→AAT)	PGM2 ←
T→G	1									intergenic (-654/-99)	PHO91 ← / → YNR014W
Δ1 bp	1				1					intergenic (+199/+336)	PRP39 → / ← YNCM0007C
T→A	1				1					intergenic (+206/+329)	PRP39 → / ← YNCM0007C
G→A	1									intergenic (+228/+307)	PRP39 → / ← YNCM0007C
2 bp→ TC	1									intergenic (+237/+297)	PRP39 → / ← YNCM0007C
+TATA	1									intergenic (+224/+195)	PRY2 → / ← YPT52

Δ5 bp				1						intergenic (+33/+690)	PSP2 → / ← PPZ1
A→C	1									N207H (AAT→CAT)	PTI1 →
+AAA		1	1			1	1			intergenic (+206/+921)	RDN5-1 → / ← RDN25-2
+AAA			1				1		1	intergenic (+587/+540)	RDN5-1 → / ← RDN25-2
C→T		1				1		1		intergenic (+7/+1120)	RDN5-1 → / ← RDN25-2
+A								1	1	intergenic (-324/+276)	RNR3 ← / ← FIS1
+T								1		intergenic (-236/+216)	RPC11 ← / ← BAP3
C→T							1			K72K (AAG→AAA)	RPS15 ←
G→T					1					intergenic (-108/+325)	RPS16B ← / ← RPS16B
T→C									1	T276T (ACT→ACC)	RPT5 →
Δ3 bp		1								coding (2227-2229/3117 nt)	RQC2 ←
G→C						1				V364V (GTG→GTC)	SCC2 →
Δ3 bp	1								1	intergenic (-217/-791)	SDS23 ← / → OLE1
Δ1 bp							1	1		intergenic (-217/-793)	SDS23 ← / → OLE1
Δ3 bp			1					1		coding (540-542/6030 nt)	SEC7 ←
Δ1 bp					1					intergenic (-287/-305)	SKG6 ← / → PEX28
+TTT				1						intergenic (-99/-292)	SNO2 ← / → SNZ2
Δ1 bp						1	1			intergenic (-100/-294)	SNO3 ← / → SNZ3
+A									1	intergenic (-514/-319)	SNP1 ← / → YIL060W
+A									1	intergenic (-530/-303)	SNP1 ← / → YIL060W
A→G								1		K16R (AAA→AGA)	SNX4 →
T→A		1					1			intergenic (+157/-513)	SNZ3 → / → THI5
Δ1 bp								1		intergenic (-562/+37)	SRB7 ← / ← GIC2
Δ36 bp									1	coding (79-114/1221 nt)	SRP40 ←
Δ3 bp	1									coding (192-194/1221 nt)	SRP40 ←
G→C					1					Y102* (TAC→TAG)	SSD1 ←
G→C		1	1				1			P165A (CCA→GCA)	SUB1 ←
Δ3 bp				1		1				coding (3033-3035/3285 nt)	TBS1 ←
Δ3 bp	1									coding (2883-2885/3285 nt)	TBS1 ←
Δ1 bp			1							intergenic (-2160/-101)	TOS3 ← / → MPT5
+TT	1	1					1	1	1	intergenic (+94/+23)	TPD3 → / ← NTG1
+TTT			1	1		1				intergenic (+94/+23)	TPD3 → / ← NTG1
+T					1					intergenic (+94/+23)	TPD3 → / ← NTG1
+T			1							intergenic (+94/+23)	TPD3 → / ← NTG1
G→T						1				noncoding (64/74 nt)	tV(AAC)G2 →
A→G								1		D375G (GAC→GGC)	UBP1 →
T→C		1								D115G (GAC→GGC)	UPS1 ←
Δ3 bp					1					intergenic (-157/+90)	VAN1 ← / ← TAF8

Δ3 bp					1			1	intergenic (-129/+128)	VMA2 ← / ← ATG14
Δ4 bp		1							intergenic (-71/+379)	VPS55 ← / ← SSC1
+A				1	1			1	intergenic (+4029/+499)	YAL067W-A → / ← SEO1
+AAA			1				1		intergenic (+4029/+499)	YAL067W-A → / ← SEO1
+AAAA		1							intergenic (+4029/+499)	YAL067W-A → / ← SEO1
C→T						1			intergenic (+237/-913)	YBL100W-B → / → YNCB0002W
G→A						1			intergenic (-2501/+95)	YBL111C ← / ← PAU9
2 bp→AA			1						intergenic (-2501/+94)	YBL111C ← / ← PAU9
A→G								1	A328A (GCT→GCC)	YBL113C ←
+108 bp			1						coding (501/2379 nt)	YBL113C ←
C→G			1	1		1			A9G (GCG→GGG)	YCL042W →
C→G				1					A10G (GCG→GGG)	YCL042W →
+T					1				intergenic (-395/–)	YCR108C ← / –
G→A				1		1			intergenic (+469/+290)	YDR261W-B → / ← YDR261C-D
+A	1		1	1		1			intergenic (-418/+588)	YER053C-A ← / ← GIP2
G→C								1	intergenic (-383/-7038)	YGR038C-A ← / → YGR039W
T→C								1	intergenic (-391/-7030)	YGR038C-A ← / → YGR039W
A→T	1								intergenic (-410/-7011)	YGR038C-A ← / → YGR039W
A→G	1			1		1			T231T (ACT→ACC)	YHL050C ←
+C					1				intergenic (-395/+379)	YHL050C ← / ← YHL050C
G→A		1			1				intergenic (+327/–)	YHR219W → / –
Δ1 bp		1			1				intergenic (+339/–)	YHR219W → / –
T→C		1			1	1	1	1	intergenic (+301/+578)	YML039W → / ← YMD8
A→G		1	1		1	1		1	S274S (TCA→TCG)	YMR317W →
A→G					1		1		S346S (TCA→TCG)	YMR317W →
A→T					1				T363S (ACA→TCA)	YMR317W →
C→T	1								P349S (CCA→TCA)	YMR317W →
Δ2 bp			1			1	1		intergenic (-154/+66)	YNCH0016C ← / ← KOG1
Δ1 bp					1				intergenic (-155/+66)	YNCH0016C ← / ← KOG1
C→T						1			intergenic (-756/+770)	YNCJ0019C ← / ← NOP9
Δ1 bp		1							intergenic (-968/-187)	YOR062C ← / → RPL3
A→T							1		intergenic (+121/+303)	YOX1 → / ← RPS18B
Δ3 bp	1								intergenic (-124/+241)	YPK3 ← / ← CDS1
C→A						1			A569A (GCC→GCA)	YPR204W →
Δ1 bp								1	intergenic (-542/-1690)	YRF1-6 ← / → COS1

Appendix Table 4 Table summarizing mutations and the respective frequency observed in *gdh1* and *glt1* genes detected from *S. cerevisiae* strains isolated from lines retaining mutualism after 15 transfers. For this analysis, the frequency cut-off was set to 0.05.

mutation	E4	E6	F4	F5	F6	G5	H4	H5	H6	annotation	gene
Δ1 bp									1	coding (2435/3354 nt)	ECM21 ←
A→T									0.18	L612* (TTG→TAG)	ECM21 ←
Δ50 bp									0.17	coding (1249-1298/3354 nt)	ECM21 ←
G→C								0.73		S550* (TCA→TGA)	ECM21 ←
+A								0.14		coding (1906/3354 nt)	ECM21 ←
T→G								0.13		T633T (ACA→ACC)	ECM21 ←
T→A							0.65			R204* (AGA→TGA)	ECM21 ←
Δ1 bp							0.13			coding (2363/3354 nt)	ECM21 ←
C→A							0.13			E460* (GAG→TAG)	ECM21 ←
C→A	0.39	0.23	0.57			0.91				E680* (GAG→TAG)	ECM21 ←
Δ1 bp	0.39	0.26	0.32			0.11				coding (2474/3354 nt)	ECM21 ←
A→C					0.89					Y591D (TAC→GAC)	ECM21 ←
A→C				0.47						Y658* (TAT→TAG)	ECM21 ←
G→T				0.35						S372* (TCA→TAA)	ECM21 ←
C→A				0.17						E415* (GAG→TAG)	ECM21 ←
A→T									0.83	C414* (TGT→TGA)	GDH1 ←
G→T									0.2	T193N (ACT→AAT)	GDH1 ←
C→T								0.8		W366* (TGG→TGA)	GDH1 ←
G→A								0.28		R78C (CGT→TGT)	GDH1 ←
G→A								1		S186F (TCT→TTT)	GDH1 ←
G→A								0.07		S339F (TCC→TTC)	GDH1 ←
C→G			0.67			0.89				A435P (GCT→CCT)	GDH1 ←
C→T					1					G338D (GGT→GAT)	GDH1 ←
C→G				0.56						G434R (GGT→CGT)	GDH1 ←
A→C				0.37						L33W (TTG→TGG)	GDH1 ←
Δ1 bp				0.37						coding (101/1365 nt)	GDH1 ←
Δ1 bp		1								coding (152/1365 nt)	GDH1 ←
C→T									0.26	W617* (TGG→TGA) ‡	GLT1 ←
C→T									0.26	W617* (TGG→TAG) ‡	GLT1 ←
C→G								0.67	0.22	R580P (CGT→CCT)	GLT1 ←
A→G			0.1							S1094P (TCT→CCT)	GLT1 ←

Bibliography

1. Bachmann, H. *et al.* Availability of public goods shapes the evolution of competing metabolic strategies. **110**, 14302–14307 (2013).
2. Foster, K. R. & Bell, T. Competition, not cooperation, dominates interactions among culturable microbial species. *Curr. Biol.* **22**, 1845–1850 (2012).
3. Kehe, J. *et al.* Positive interactions are common among culturable bacteria. *Sci. Adv.* **7**, 7159 (2021).
4. Huttenhower, C. *et al.* Structure, function and diversity of the healthy human microbiome. *Nature* **486**, 207–214 (2012).
5. Trivedi, P., Leach, J. E., Tringe, S. G., Sa, T. & Singh, B. K. Plant–microbiome interactions: from community assembly to plant health. *Nat. Rev. Microbiol. 2020 1811* **18**, 607–621 (2020).
6. Wang, M., Ma, Y., Feng, C., Cai, L. & Li, W. Diversity of Pelagic and Benthic Bacterial Assemblages in the Western Pacific Ocean. *Front. Microbiol.* **11**, 1730 (2020).
7. Bader, J., Mast-Gerlach, E., Popović, M. K., Bajpai, R. & Stahl, U. Relevance of microbial coculture fermentations in biotechnology. *J. Appl. Microbiol.* **109**, 371–387 (2010).
8. Zhou, K., Qiao, K., Edgar, S. & Stephanopoulos, G. Distributing a metabolic pathway among a microbial consortium enhances production of natural products. *Nat. Biotechnol.* **33**, 377–383 (2015).
9. Derosa, L. & Zitvogel, L. Fecal microbiota transplantation: can it circumvent resistance to PD-1 blockade in melanoma? *Signal Transduct. Target. Ther. 2021 61* **6**, 1–2 (2021).
10. Gilmore, S. P. *et al.* Top-Down Enrichment Guides in Formation of Synthetic Microbial Consortia for Biomass Degradation. *ACS Synth. Biol.* **8**, 2174–2185 (2019).
11. Chang, C. Y. *et al.* Engineering complex communities by directed evolution. *Nat. Ecol. Evol.* **5**, 1011–1023 (2021).
12. Rodríguez Amor, D. & Dal Bello, M. Bottom-Up Approaches to Synthetic Cooperation in Microbial Communities. *Life (Basel, Switzerland)* **9**, (2019).
13. Großkopf, T. & Soyer, O. S. Synthetic microbial communities. *Curr. Opin. Microbiol.* **18**, 72–77 (2014).
14. Muok, A. R. & Briegel, A. Intermicrobial Hitchhiking: How Nonmotile Microbes Leverage Communal Motility. *Trends Microbiol.* **29**, 542–550 (2021).
15. Monteil, C. L. *et al.* Ectosymbiotic bacteria at the origin of magnetoreception in a marine protist. *Nat. Microbiol.* **4**, 1088–1095 (2019).
16. Blair, E. M., Dickson, K. L. & O'Malley, M. A. Microbial communities and their enzymes facilitate degradation of recalcitrant polymers in anaerobic digestion. *Curr. Opin. Microbiol.* **64**, 100–108 (2021).
17. Chiu, H. C., Levy, R. & Borenstein, E. Emergent Biosynthetic Capacity in Simple Microbial Communities. *PLOS Comput. Biol.* **10**, e1003695 (2014).
18. Mee, M. T., Collins, J. J., Church, G. M. & Wang, H. H. Syntrophic exchange in synthetic microbial communities. *Proc. Natl. Acad. Sci.* **111**, E2149–E2156 (2014).
19. D'Souza, G. *et al.* Ecology and evolution of metabolic cross-feeding interactions in bacteria. *Nat. Prod. Rep.* **35**, 455–488 (2018).
20. Pande, S. & Kost, C. Bacterial Unculturability and the Formation of Intercellular Metabolic

Networks. *Trends in Microbiology* **25**, 349–361 (2017).

21. Stewart, E. J. Growing Unculturable Bacteria. *J. Bacteriol.* **194**, 4151 (2012).

22. Karkar, S., Facchinelli, F., Price, D. C., Weber, A. P. M. & Bhattacharya, D. Metabolic connectivity as a driver of host and endosymbiont integration. *Proc. Natl. Acad. Sci. U. S. A.* **112**, 10208–10215 (2015).

23. Garcia, S. L. *et al.* Auxotrophy and intrapopulation complementary in the 'interactome' of a cultivated freshwater model community. *Mol. Ecol.* **24**, 4449–4459 (2015).

24. Johnson, W. M. *et al.* Auxotrophic interactions: a stabilizing attribute of aquatic microbial communities? *FEMS Microbiol. Ecol.* **96**, 115 (2020).

25. Sachs, J. L., Skophammer, R. G. & Regus, J. U. Evolutionary transitions in bacterial symbiosis. *Proc. Natl. Acad. Sci. U. S. A.* **108**, 10800–10807 (2011).

26. López-García, P. & Moreira, D. The Syntrophy hypothesis for the origin of eukaryotes revisited. *Nat. Microbiol.* **5**, 655–667 (2020).

27. McCutcheon, J. P. & Moran, N. A. Extreme genome reduction in symbiotic bacteria. *Nat. Rev. Microbiol. 2011 101* **10**, 13–26 (2011).

28. Giovannoni, S. J., Cameron Thrash, J. & Temperton, B. Implications of streamlining theory for microbial ecology. *ISME J.* **8**, 1553–1565 (2014).

29. Noor, E. *et al.* The Protein Cost of Metabolic Fluxes: Prediction from Enzymatic Rate Laws and Cost Minimization. (2016). doi:10.1371/journal.pcbi.1005167

30. Flamholz, A., Noor, E., Bar-Even, A., Liebermeister, W. & Milo, R. Glycolytic strategy as a tradeoff between energy yield and protein cost. *Proc. Natl. Acad. Sci. U. S. A.* **110**, 10039–44 (2013).

31. Waschina, S., D'Souza, G., Kost, C. & Kaleta, C. Metabolic network architecture and carbon source determine metabolite production costs. *FEBS J.* **283**, 2149–2163 (2016).

32. Yu, Q. *et al.* Biogas Production and Microbial Community Dynamics during the Anaerobic Digestion of Rice Straw at 39-50 °c: A Pilot Study. *Energy and Fuels* **32**, 5157–5163 (2018).

33. Du, B., Zielinski, D. C., Monk, J. M. & Palsson, B. O. Thermodynamic favorability and pathway yield as evolutionary tradeoffs in biosynthetic pathway choice. *Proc. Natl. Acad. Sci. U. S. A.* **115**, 11339–11344 (2018).

34. Goldberg, I., Nadler, V. & Hochman, A. Mechanism of nitrogenase switch-off by oxygen. *J. Bacteriol.* **169**, 874–879 (1987).

35. Ku, S.-B. & Edwards, G. E. Oxygen Inhibition of Photosynthesis. *Plant Physiol.* **59**, 986–990 (1977).

36. Berman-Frank, I. *et al.* Segregation of nitrogen fixation and oxygenic photosynthesis in the marine cyanobacterium Trichodesmium. *Science (80-.).* **294**, 1534–1537 (2001).

37. Rae, B. D. *et al.* Cyanobacterial carboxysomes: microcompartments that facilitate CO2 fixation. *J. Mol. Microbiol. Biotechnol.* **23**, 300–7 (2013).

38. Pande, S. *et al.* Fitness and stability of obligate cross-feeding interactions that emerge upon gene loss in bacteria. *ISME J.* **8**, 953 (2014).

39. Yu, J. S. L. *et al.* Microbial communities form rich extracellular metabolomes that foster metabolic interactions and promote drug tolerance. **7**, 542–555 (2022).

40. Correia-Melo, C. *et al.* Cell-cell metabolite exchange creates a pro-survival metabolic environment that extends lifespan. *Cell* **186**, 63-79.e21 (2023).

41. Morris, J. J. Black Queen evolution: The role of leakiness in structuring microbial communities.

Trends in Genetics **31**, 475–482 (2015).

42. Morris, J. J., Lenski, R. E. & Zinser, E. R. The black queen hypothesis: Evolution of dependencies through adaptive gene loss. *MBio* **3**, (2012).

43. Gore, J., Youk, H. & Van Oudenaarden, A. Snowdrift game dynamics and facultative cheating in yeast. *Nature* **459**, 253–256 (2009).

44. Gjonbalaj, M. *et al.* Antibiotic degradation by commensal microbes shields pathogens. *Infect. Immun.* **88**, (2020).

45. Butaite, E., Baumgartner, M., Wyder, S. & Kümmerli, R. Siderophore cheating and cheating resistance shape competition for iron in soil and freshwater Pseudomonas communities. *Nat. Commun.* **8**, 1–12 (2017).

46. Douglas, A. E. The microbial exometabolome: ecological resource and architect of microbial communities. *Philos Trans R Soc B Biol. Sci* **375**, 20190250 (2020).

47. Basan, M. *et al.* Overflow metabolism in Escherichia coli results from efficient proteome allocation. *Nature* (2015). doi:10.1038/nature15765

48. Seth, E. C. & Taga, M. E. Nutrient cross-feeding in the microbial world. *Front. Microbiol* **5**, 350 (2014).

49. Paczia, N. *et al.* Extensive exometabolome analysis reveals extended overflow metabolism in various microorganisms. *Microb. Cell Fact.* **11**, 1 (2012).

50. D'Souza, G. *et al.* Less is more: selective advantages can explain the prevalent loss of biosynthetic genes in bacteria. *Evolution (N. Y).* **68**, 2559–2570 (2014).

51. D'Souza, G. & Kost, C. Experimental Evolution of Metabolic Dependency in Bacteria. *PLOS Genet.* **12**, e1006364 (2016).

52. Harcombe, W. Novel cooperation experimentally evolved between species. *Evolution (N. Y).* **64**, 2166–2172 (2010).

53. Giri, S., Yousif, G., Shitut, S., Oña, L. & Kost, C. Prevalent emergence of reciprocity among cross-feeding bacteria. *ISME Commun. 2022 21* **2**, 1–7 (2022).

54. Preussger, D., Giri, S., Muhsal, L. K., Oña, L. & Kost, C. Reciprocal Fitness Feedbacks Promote the Evolution of Mutualistic Cooperation. *Curr. Biol.* **30**, 3580–3590 (2020).

55. Gleizer, S. *et al.* Conversion of Escherichia coli to Generate All Biomass Carbon from CO2. *Cell* **179**, 1255-1263.e12 (2019).

56. Arnold, F. H. Directed Evolution: Bringing New Chemistry to Life. *Angew. Chem. Int. Ed. Engl.* **57**, 4143 (2018).

57. Phelan, V. V., Liu, W.-T., Pogliano, K. & Dorrestein, P. C. Microbial metabolic exchange—the chemotype-to-phenotype link. *Nat. Chem. Biol.* **8**, 26–35 (2012).

58. Smith, P. & Schuster, M. Public goods and cheating in microbes. *Curr. Biol.* **29**, 442–447 (2019).

59. Özkaya, Ö., Balbontín, R., Gordo, I. & Xavier, K. B. Cheating on cheaters stabilizes cooperation in *Pseudomonas aeruginosa*. *Curr. Biol.* **28**, 752–755 (2018).

60. Schuster, M., Foxall, E., Finch, D., Smith, H. & De Leenheer, P. Tragedy of the commons in the chemostat. *PLoS One* **12**, e0186119 (2017).

61. Welch, J. L. M., Rossetti, B. J., Rieken, C. W., Dewhirst, F. E. & Borisy, G. G. Biogeography of a human oral microbiome at the micron scale. *Proc. Natl. Acad. Sci. U. S. A.* **113**, E791–E800 (2016).

62. Pernthaler, A. *et al.* Diverse syntrophic partnerships from deep-sea methane vents revealed by

direct cell capture and metagenomics. *Proc. Natl. Acad. Sci. U. S. A.* **105**, 7052–7057 (2008).

63. Dal Co, A., van Vliet, S., Kiviet, D. J., Schlegel, S. & Ackermann, M. Short-range interactions govern the dynamics and functions of microbial communities. *Nat. Ecol. Evol.* **4**, 366–375 (2020).

64. Pande, S. *et al.* Privatization of cooperative benefits stabilizes mutualistic cross-feeding interactions in spatially structured environments. *ISME J.* **10**, 1413–1423 (2016).

65. Momeni, B., Waite, A. J. & Shou, W. Spatial self-organization favors heterotypic cooperation over cheating. *Elife* **2**, e00960 (2013).

66. Campbell, K. *et al.* Self-establishing communities enable cooperative metabolite exchange in a eukaryote. *Elife* **4**, e09943 (2015).

67. Chen, F. & Wegner, S. V. Blue-light-switchable bacterial cell-cell adhesions enable the control of multicellular bacterial communities. *ACS Synth. Biol.* **9**, 1169–1180 (2020).

68. Müller, M. J. I., Neugeboren, B. I., Nelson, D. R. & Murray, A. W. Genetic drift opposes mutualism during spatial population expansion. *Proc. Natl. Acad. Sci. U. S. A.* **111**, 1037–1042 (2014).

69. Momeni, B., Brileya, K. A., Fields, M. W. & Shou, W. Strong inter-population cooperation leads to partner intermixing in microbial communities. *Elife* **2**, e00230 (2013).

70. Blanchard, A. E. & Lu, T. Bacterial social interactions drive the emergence of differential spatial colony structures. *BMC Syst. Biol.* **9**, 59 (2015).

71. Kovács, Á. T. Impact of spatial distribution on the development of mutualism in microbes. *Front. Microbiol.* **5**, 649 (2014).

72. Harcombe, W. R., Chacón, J. M., Adamowicz, E. M., Chubiz, L. M. & Marx, C. J. Evolution of bidirectional costly mutualism from byproduct consumption. *Proc. Natl. Acad. Sci. U. S. A.* **115**, 12000–12004 (2018).

73. Marchal, M. *et al.* A passive mutualistic interaction promotes the evolution of spatial structure within microbial populations. *BMC Evol. Biol.* **17**, 106 (2017).

74. Mehta, A. P. *et al.* Engineering yeast endosymbionts as a step toward the evolution of mitochondria. *Proc. Natl. Acad. Sci.* **115**, 11796–11801 (2018).

75. Mergaert, P., Kikuchi, Y., Shigenobu, S. & Nowack, E. C. M. Metabolic integration of bacterial endosymbionts through antimicrobial peptides. *Trends Microbiol.* **25**, 703–712 (2017).

76. Pande, S. *et al.* Metabolic cross-feeding via intercellular nanotubes among bacteria. *Nat. Commun.* **6**, 6238 (2015).

77. Shitut, S., Ahsendorf, T., Pande, S., Egbert, M. & Kost, C. Nanotube-mediated cross-feeding couples the metabolism of interacting bacterial cells. *Environ. Microbiol.* **21**, 1306–1320 (2019).

78. Nadell, C. D., Drescher, K. & Foster, K. R. Spatial structure, cooperation and competition in biofilms. *Nat. Rev. Microbiol.* **14**, 589–600 (2016).

79. Rickard, A. H., Gilbert, P., High, N. J., Kolenbrander, P. E. & Handley, P. S. Bacterial coaggregation: an integral process in the development of multi-species biofilms. *Trends Microbiol.* **11**, 94–100 (2003).

80. Steffan, B. N., Venkatesh, N. & Keller, N. P. Let's Get Physical: Bacterial-Fungal Interactions and Their Consequences in Agriculture and Health. *J. Fungi* **6**, 243 (2020).

81. Schweitzer-Natan, O., Ofek-Lalzar, M., Sher, D. & Sukenik, A. Particle-Associated Microbial Community in a Subtropical Lake During Thermal Mixing and Phytoplankton Succession. *Front. Microbiol.* **10**, 2142 (2019).

82. Cai, Y. M. Non-surface attached bacterial aggregates: a ubiquitous third lifestyle. *Front. Microbiol.*

11, 3106 (2020).

83. Husnik, F. *et al.* Bacterial and archaeal symbioses with protists. *Curr. Biol.* **31**, R862–R877 (2021).

84. Müller, J. & Overmann, J. Close Interspecies Interactions between Prokaryotes from Sulfureous Environments. *Front. Microbiol.* **2**, 146 (2011).

85. Overmann, J. & van Gemerden, H. Microbial interactions involving sulfur bacteria: implications for the ecology and evolution of bacterial communities. *FEMS Microbiol. Rev.* **24**, 591–599 (2000).

86. Raina, J.-B. *et al.* Chemotaxis shapes the microscale organization of the ocean's microbiome. | *Nat.* | **605**, (2022).

87. Colin, R., Ni, B., Laganenka, L. & Sourjik, V. Multiple functions of flagellar motility and chemotaxis in bacterial physiology. *FEMS Microbiol. Rev.* **45**, 1–19 (2021).

88. Raina, J.-B., Fernandez, V., Lambert, B., Stocker, R. & Seymour, J. R. The role of microbial motility and chemotaxis in symbiosis. *Nat. Rev. Microbiol.* **17**, 284–294 (2019).

89. Robinson, C. D. *et al.* Host-emitted amino acid cues regulate bacterial chemokinesis to enhance colonization. *Cell Host Microbe* **29**, 1221–1234 (2021).

90. Konopka, A. What is microbial community ecology? *ISME J.* **3**, 1223–1230 (2009).

91. Turner, C. B., Blount, Z. D., Mitchell, D. H. & Lenski, R. E. Evolution and coexistence in response to a key innovation in a long-term evolution experiment with Escherichia coli. *bioRxiv* 020958 (2015). doi:10.1101/020958

92. Eshdat, Y., Speth, V. & Jann2, K. *Participation of Pili and Cell Wall Adhesin in the Yeast Agglutination Activity of Escherichia coli. INFECTION AND IMMUNITY* **34**, (1981).

93. Good, N. E. *et al.* Hydrogen Ion Buffers for Biological Research. *Biochemistry* **5**, 467–477 (1966).

94. Wintermute, E. H. & Silver, P. A. Emergent cooperation in microbial metabolism. *Mol. Syst. Biol* **6**, 407 (2010).

95. Baba, T. *et al.* Construction of *Escherichia coli* K-12 in-frame, single-gene knockout mutants: the Keio collection. *Mol. Syst. Biol.* **2**, 2006.0008 (2006).

96. Giaever, G. *et al.* Functional profiling of the Saccharomyces cerevisiae genome. *Nature* **418**, 387–391 (2002).

97. Jann, K., Schmidt, G., Blumenstock, E. & Vosbeck, K. *Escherichia coli* adhesion to *Saccharomyces cerevisiae* and mammalian cells: role of piliation and surface hydrophobicity. *Infect. Immun.* **32**, 484–489 (1981).

98. Rigaud, J.-L. & Lé, D. *[4] Reconstitution of Membrane Proteins into Liposomes.* (2003).

99. Cho, B. K., Federowicz, S., Park, Y. S., Zengler, K. & Palsson, B. Deciphering the transcriptional regulatory logic of amino acid metabolism. *Nat. Chem. Biol.* **8**, 65–71 (2012).

100. Caldara, M., Minh, P. N. Le, Bostoen, S., Massant, J. & Charlier, D. ArgR-dependent Repression of Arginine and Histidine Transport Genes in Escherichia coli K-12. *J. Mol. Biol.* **373**, 251–267 (2007).

101. Drake, J. W., Charlesworth, B., Charlesworth, D. & Crow, J. F. Rates of Spontaneous Mutation. *Genetics* **148**, 1667–1686 (1998).

102. Liu, H. & Zhang, J. Yeast Spontaneous Mutation Rate and Spectrum Vary with Environment. *Curr. Biol.* **29**, 1584-1591.e3 (2019).

103. Ivashov, V. *et al.* Complementary a-arrestin-ubiquitin ligase complexes control nutrient transporter endocytosis in response to amino acids. *Elife* **9**, 1–39 (2020).

104. Ahmad, M. & Bussey, H. Yeast arginine permease: nucleotide sequence of the CAN1 gene. *Curr. Genet.* **10**, 587–592 (1986).

105. Abraham, J. M., Freitag, C. S., Clements, J. R. & Eisenstein, B. I. An invertible element of DNA controls phase variation of type 1 fimbriae of *Escherichia coli*. *Proc. Natl. Acad. Sci.* **82**, 5724–5727 (1985).

106. Hallatschek, O., Hersen, P., Ramanathan, S. & Nelson, D. R. Genetic drift at expanding frontiers promotes gene segregation. *Proc. Natl. Acad. Sci.* **104**, 19926–19930 (2007).

107. Wang, M., Schaefer, A. L., Dandekar, A. A. & Greenberg, E. P. Quorum sensing and policing of Pseudomonas aeruginosa social cheaters. *Proc. Natl. Acad. Sci. U. S. A.* **112**, 2187 (2015).

108. Greig, D. & Travisano, M. The Prisoner's Dilemma and polymorphism in yeast SUC genes. *Proc. R. Soc. London. Ser. B Biol. Sci.* **271**, S25–S26 (2004).

109. Parker, D. J., Demetci, P. & Li, G. W. Rapid Accumulation of Motility-Activating Mutations in Resting Liquid Culture of Escherichia coli. *J. Bacteriol.* **201**, (2019).

110. Ni, B., Colin, R., Link, H., Endres, R. G. & Sourjik, V. Growth-rate dependent resource investment in bacterial motile behavior quantitatively follows potential benefit of chemotaxis. *Proc. Natl. Acad. Sci. U. S. A.* **117**, 595–601 (2020).

111. Whitman, W. B., Coleman, D. C. & Wiebe, W. J. Prokaryotes: the unseen majority. *Proc. Natl. Acad. Sci. U. S. A.* **95**, 6578–6583 (1998).

112. Friedlander, R. S., Vogel, N. & Aizenberg, J. Role of flagella in adhesion of *Escherichia coli* to abiotic surfaces. *Langmuir* **31**, 6137–6144 (2015).

113. Suchanek, V. M. *et al.* Chemotaxis and cyclic-di-GMP signalling control surface attachment of *Escherichia coli*. *Mol. Microbiol.* **113**, 728–739 (2020).

114. Ni, B. *et al.* Evolutionary remodeling of bacterial motility checkpoint control. *Cell Rep.* **18**, 866–877 (2017).

115. Werner, G. D. A. *et al.* Evolution of microbial markets. *Proc. Natl. Acad. Sci.* **111**, 1237–1244 (2014).

116. López-García, P. & Moreira, D. Eukaryogenesis, a syntrophy affair. *Nat. Microbiol.* **4**, 1068–1070 (2019).

117. Barber, J. N. *et al.* The evolution of coexistence from competition in experimental co-cultures of Escherichia coli and Saccharomyces cerevisiae. *ISME J. 2020 153* **15**, 746–761 (2020).

118. Mishima, H. *et al.* L-Alanine Prototrophic Suppressors Emerge from L-Alanine Auxotroph through Stress-Induced Mutagenesis in Escherichia coli. *Microorganisms* **9**, 472 (2021).

119. Copley, S. D. An evolutionary biochemist's perspective on promiscuity. *Trends in Biochemical Sciences* **40**, 72–78 (2015).

120. Allison, S. D. & Martiny, J. B. H. *Resistance, resilience, and redundancy in microbial communities.* (2008).

121. Min, Y. *et al.* Pathway knockout and redundancy in metabolic networks. *J. Theor. Biol.* **270**, 63–69 (2011).

122. Sander, T., Wang, C. Y., Glatter, T. & Link, H. CRISPRi-Based Downregulation of Transcriptional Feedback Improves Growth and Metabolism of Arginine Overproducing E. coli. *ACS Synth. Biol.* **8**, 1983–1990 (2019).

123. Mara, P., Fragiadakis, G. S., Gkountromichos, F. & Alexandraki, D. The pleiotropic effects of the glutamate dehydrogenase (GDH) pathway in Saccharomyces cerevisiae. *Microbial Cell Factories* **17**,

170 (2018).

124. DeLuna, A., Avendaño, A., Riego, L. & González, A. NADP-glutamate dehydrogenase isoenzymes of Saccharomyces cerevisiae. Purification, kinetic properties, and physiological roles. *J. Biol. Chem.* **276**, 43775–43783 (2001).

125. Guillamón, J. M., Riel, N. A. W., Giuseppin, M. L. F. & Verrips, C. T. The glutamate synthase (GOGAT) of Saccharomyces cerevisiae plays an important role in central nitrogen metabolism. *FEMS Yeast Res.* **1**, 169–175 (2001).

126. Venkataram, S., Kuo, H.-Y., Hom, E. F. Y. & Kryazhimskiy, S. Mutualism-enhancing mutations dominate early adaptation in a two-species microbial community. *Nat. Ecol. Evol.* **7**, 143–154 (2023).

127. Konstantinidis, D. *et al.* Adaptive laboratory evolution of microbial co-cultures for improved metabolite secretion. *Mol. Syst. Biol.* **17**, e10189 (2021).

128. Shou, W., Ram, S. & Vilar, J. M. G. Synthetic cooperation in engineered yeast populations. *Proc. Natl. Acad. Sci.* **104**, 1877–1882 (2007).

129. Koo, H., Andes, D. R. & Krysan, D. J. Candida–streptococcal interactions in biofilm-associated oral diseases. *PLOS Pathog.* **14**, e1007342 (2018).

130. Stadie, J., Gulitz, A., Ehrmann, M. A. & Vogel, R. F. Metabolic activity and symbiotic interactions of lactic acid bacteria and yeasts isolated from water kefir. *Food Microbiol.* **35**, 92–98 (2013).

131. Cordero, O. X. & Datta, M. S. Microbial interactions and community assembly at microscales. *Curr. Opin. Microbiol.* **31**, 227 (2016).

132. Grossart, H. P., Riemann, L. & Azam, F. Bacterial motility in the sea and its ecological implications. *Aquat. Microb. Ecol.* **25**, 247–258 (2001).

133. Emge, P. *et al.* Resilience of bacterial quorum sensing against fluid flow. *Sci. Rep.* **6**, 1–10 (2016).

134. Flemming, H.-C. *et al.* Biofilms: an emergent form of bacterial life. *Nat. Rev. Microbiol.* **14**, 563–575 (2016).

135. Drescher, K., Nadell, C. D., Stone, H. A., Wingreen, N. S. & Bassler, B. L. Solutions to the public goods dilemma in bacterial biofilms. *Curr. Biol.* **24**, 50–55 (2014).

136. Yan, H. *et al.* A metabolic trade-offmodulates policing of social cheaters in populations of Pseudomonas aeruginosa. *Front. Microbiol.* **9**, (2018).

137. Cavaliere, M., Yang, G., Danos, V. & Dakos, V. Detecting the collapse of cooperation in evolving networks. *Sci. Rep.* **6**, 1–11 (2016).

138. Bastiaans, E., Debets, A. J. M. M. & Aanen, D. K. Experimental evolution reveals that high relatedness protects multicellular cooperation from cheaters. *Nat. Commun.* **7**, 11435 (2016).

139. Velicer, G. J., Kroos, L. & Lenski, R. E. Developmental cheating in the social bacterium Myxococcus xanthus. *Nature* **404**, 598–601 (2000).

140. Moreno-Fenoll, C., Cavaliere, M., Martínez-García, E. & Poyatos, J. F. Eco-evolutionary feedbacks can rescue cooperation in microbial populations. *Sci. Rep.* **7**, 42561 (2017).

141. Sanchez, A. & Gore, J. Feedback between Population and Evolutionary Dynamics Determines the Fate of Social Microbial Populations. *PLOS Biol.* **11**, e1001547 (2013).

142. Wilson, D. S. A theory of group selection. *Proc. Natl. Acad. Sci. U. S. A.* **72**, 143–146 (1975).

143. Chuang, J. S., Rivoire, O. & Leibler, S. Simpson's Paradox in a Synthetic Microbial System. *Science (80-.).* **323**, 272–275 (2009).

144. Lambert, B. S., Fernandez, V. I. & Stocker, R. Motility drives bacterial encounter with particles responsible for carbon export throughout the ocean. *Limnol. Oceanogr. Lett.* **4**, 113–118 (2019).

145. Schauer, O. *et al.* Motility and chemotaxis of bacteria-driven microswimmers fabricated using antigen 43-mediated biotin display. *Sci. Rep.* **8**, 9801 (2018).

146. Taylor, J. R. & Stocker, R. Trade-offs of chemotactic foraging in turbulent water. *Science (80-.).* **338**, 675–679 (2012).

147. Rusconi, R., Guasto, J. S. & Stocker, R. Bacterial transport suppressed by fluid shear. *Nat. Phys.* **10**, 212–217 (2014).

148. Durham, W. M. *et al.* Turbulence drives microscale patches of motile phytoplankton. *Nat. Commun. 2013 41* **4**, 1–7 (2013).

149. Jensen, S. I., Lennen, R. M., Herrgård, M. J. & Nielsen, A. T. Seven gene deletions in seven days: Fast generation of *Escherichia coli* strains tolerant to acetate and osmotic stress. *Sci. Rep.* **5**, 17874 (2016).

150. Zhang, H., Susanto, T. T., Wan, Y. & Chen, S. L. Comprehensive mutagenesis of the fimS promoter regulatory switch reveals novel regulation of type 1 pili in uropathogenic Escherichia coli. *Proc. Natl. Acad. Sci. U. S. A.* **113**, 4182–4187 (2016).

151. Schindelin, J. *et al.* Fiji: an open-source platform for biological-image analysis. *Nat. Methods 2012 97* **9**, 676–682 (2012).

152. Datsenko, K. A. & Wanner, B. L. One-step inactivation of chromosomal genes in Escherichia coli K-12 using PCR products. *Proc. Natl. Acad. Sci.* **97**, 6640–6645 (2000).

153. Blattner, F. R. *et al.* The Complete Genome Sequence of *Escherichia coli* K-12. *Science (80-.).* **277**, 1453–1462 (1997).

154. Laganenka, L., López, M. E., Colin, R. & Sourjik, V. Flagellum-mediated mechanosensing and RflP control motility state of pathogenic *Escherichia coli*. *MBio* **11**, e02269-19 (2020).

155. Winston, F., Dollard, C. & Ricupero-Hovasse, S. L. Construction of a set of convenient Saccharomyces cerevisiae strains that are isogenic to S288C. *Yeast* **11**, 53–55 (1995).

156. Zhang, Y., Serratore, N. D. & Briggs, S. D. N-ICE plasmids for generating N-terminal 3 × FLAG tagged genes that allow inducible, constitutive or endogenous expression in Saccharomyces cerevisiae. *Yeast* **34**, 223–235 (2017).

157. Macdonald, C. & Piper, R. C. Puromycin- and methotrexate-resistance cassettes and optimized Cre-recombinase expression plasmids for use in yeast. *Yeast* **32**, 423–438 (2015).

158. Mundt, M., Anders, A., Murray, S. M. & Sourjik, V. A System for Gene Expression Noise Control in Yeast. *ACS Synth. Biol.* **7**, 2618–2626 (2018).

159. Besharova, O., Suchanek, V. M., Hartmann, R., Drescher, K. & Sourjik, V. Diversification of gene expression during formation of static submerged biofilms by Escherichia coli. *Front. Microbiol.* **7**, (2016).

160. Bellotto, N. *et al.* Dependence of diffusion in Escherichia coli cytoplasm on protein size, environmental conditions and cell growth. *bioRxiv* 2022.02.17.480843 (2022). doi:10.1101/2022.02.17.480843

161. Zaslaver, A. *et al.* A comprehensive library of fluorescent transcriptional reporters for Escherichia coli. *Nat. Methods 2006 38* **3**, 623–628 (2006).

162. Chung, C. T., Niemela, S. L. & Miller, R. H. One-step preparation of competent Escherichia coli: transformation and storage of bacterial cells in the same solution. *Proc. Natl. Acad. Sci. U. S. A.* **86**, 2172–2175 (1989).

163. Warren, D. J. Preparation of highly efficient electrocompetent Escherichia coli using glycerol/mannitol density step centrifugation. *Anal. Biochem.* **413**, 206–207 (2011).

Erklärung

Ich versichere, dass ich meine Dissertation mit dem Titel

"**Determinants and evolution of metabolic interactions in synthetic microbial communities**"

selbstständig ohne unerlaubte Hilfe angefertigt und mich dabei keiner anderen als der von mir ausdrücklich bezeichneten Quellen und Hilfsmittel bedient habe.

Diese Dissertation wurde in der jetzigen oder einer ähnlichen Form noch bei keiner anderen Hochschule eingereicht und hat noch keinen sonstigen Prüfungszwecken gedient.

Marburg, den 30.01.2023

Giovanni Scarinci